UNIVERSITÀ DEGLI STUDI DI TORINO

SCUOLA DI DOTTORATO

DOTTORATO IN
SCIENZE AGRARIE, FORESTALI E ALIMENTARI

CICLO: XXXIV

FACTORS LIMITING CARBON ASSIMILATION IN PLANTS: EVIDENCES THROUGH GAS EXCHANGE ANALYZES IN WHOLE ROOT AND SHOOT

Davide Lucien Patono

Docente guida:
Prof. Claudio Lovisolo

Coordinatore del Ciclo:
Prof. Domenico Bosco

ANNI
2019; 2020; 2021

INDEX

1. Introduction

In plants, net CO_2 assimilation (A_{net}) is the result of 3 metabolic processes: the rate of carboxylation (V_c), the rate of photorespiration (V_o) and the rate of respiration (R_d).

$$A_{net} = V_c - 0.5\,V_o - R_d \quad (1)$$

here, the factor 0.5 implies that two event of oxygenation catalyzed by Rubisco are required to release of 1 molecule of CO_2 and formation of 2-Phosphoglycolic acid (C2), following the final equilibrium:

2 (2-Phosphoglycolic acid) + $NADH_2$ + ATP + O_2 = PGA + CO_2

V_o and V_c can be related to the CO_2 compensation point in the absence of mitochondrial respiration (T^*) that corresponds to the CO_2 concentration at which the rate of CO_2 uptake equals the rate of CO_2 release from Rubisco oxygenation activity:

$$\frac{V_o}{V_c} = \frac{2T^*}{C} \quad (2)$$

where C denotes the CO_2 concentration at the site of carboxylation (Bush, 2018).
According to the model of Farqhuar et al. (1980), 3 different bottlenecks can limit the carboxylation rate: the rate of Ribulose 1,5- bisphosphate (RuBP) consumption by Rubisco (W_c), the rate of production of NADPH (W_j) and the rate of production of ATP (W_p). The first limitation occurs under saturated RuBP availability while W_j and W_i limit the RuBP regeneration of the Calvin Benson Cycle (CBC). A_{net} reflects the carboxylation rate allowed by the main biochemical limitation, combining equations (1 and 2) as

$$A_{net} = min\{W_c W_j W_p\}\left(1 - \frac{T^*}{C}\right) - R_d \quad (3)$$

W_c depends on kinetic properties of Rubisco and CO_2 and O_2 concentration at carboxylation site. W_j depends on the quantum light absorption and intrinsic properties of photosynthetic apparatus involved in electron transport chain and W_p depends on the rate of triose phosphate utilization renewing inorganic phosphate availability for ATP synthesis (Diaz-Espejo et al., 2012; Foyer and Spencer, 1986; Rebeille et al., 1983).

1.1. Limitation of carboxylation rate related to soil water availability and atmospheric evaporative demand

CO_2 and H_2O exchanges between plant and atmosphere are strictly correlated. CO_2 at carboxylation site, in the presence of carboxylation activity, goes towards depletion and it is replenished by atmospheric CO_2. Atmosphere, at the same time, causes strong evaporative demand that plants have to cope to maintain cellular turgor and allow cellular distension during growth. Plants H_2O and CO_2 combined relation with atmosphere not allows a hermetic isolation strategy, but it imposes a 2-directional *continuum*. Due to the different concentration scale of CO_2 and H_2O in atmosphere, for each molecule of CO_2 that diffuse into the leaf hundreds molecule of H_2O are lost by the plant and they need to be replenished by soil water withdrawal (Keller, 2020). Plants adopt complex mechanisms of regulation to make up for this extremely unbalance exchange maintaining an optimum between i) benefits due to elevated CO_2 availability for photosynthesis ii) availability of soil water in relation to the rate of water loss for evapotranspiration iii) metabolic costs of building and maintaining a conductive system that allows the replenishment of water loss (Deans et al., 2020).
The site of gas exchange between plant and atmosphere, in higher plants, is the stoma. Stomatal aperture is coordinated in response to a multitude of *stimuli* including light, CO_2 concentration in sub-stomatal chamber (C_i), temperature, vapor pressure deficit, hormonal and metabolic signals. Under water stress condition stomatal aperture limits H_2O diffusion to the atmosphere, as a consequence stomatal CO_2 conductance (g_{sc}) decreases and CO_2 becomes limiting for photosynthesis.
Photosynthesis limitation in response to water stress is one of the most studied phenomena of plant ecophysiology. In the last years, it has been placed particular attention whether the plant stomatal and photosynthetic responses to water stress are triggered and calibrated to substantial water limitations on evapotranspiration rate or are the result of complex signals that arise from utilization disequilibrium of photosynthetic products (Hagedorn et al., 2016).

1.2. Electron transport rate limitation related to intensity and quality of light

The driving force of photosynthesis is the light. The amount of energy carried by the light and the efficiency which plant absorbs and converts it in biochemical energy depends on both quantity and quality. Photon is the “vehicle” of light energy transport, its energy packet is inversely proportional to photon wavelength following the relation:

$$E_{phot} = \frac{hc}{\lambda} \quad (4)$$

Where E_{phot} is the photon energy, h is the Plank's constant, c is the light velocity and λ the wavelengths of the photon. Not all the light that impacts on plant photosynthetic organs is absorbed or used in photosynthetic processes; short and energetic wavelengths as the UV rays are stress factor that plants have to cope with auxiliary photoprotective pigments. The wavelength interval between 400 and 700 nm, but also up to 750 nm as recently claimed (Zhen and Bugbee, 2020), is called photosynthetic active radiation (PAR). Most of the PAR is absorbed by photosynthetic pigments, chlorophylls and carotenoids, and is directed to the photosynthetic process. Leaf PAR absorption is not homogenous, red and blue components are highly absorbed while green component is the least absorbed. Consequently, the quality of light exposition for plant under natural environment strongly depends on surrounding vegetation cover. Plants under direct solar light have access to the full energy of PAR spectrum and just a lower amount, characterized by elevated green/blue and far red/red energy ratio, is transmitted to the lower vegetation layers. The photosynthetic apparatus adaptation is oriented to provide sufficient (or less limiting) reduction power for plant requests during the whole light period. Under natural environment, plant light availability fluctuates and is common that light absorption exceeds the maximum energy supported by electron transport chain or the reduction power produced by the electron transport exceed CBC requests (Farquhar et al., 1980; Vialet-Chabrand et al., 2017). In these conditions energy imbalance is potentially dangerous bringing to photoinhibition. Plants, to prevent photoinhibition, have evolved a photosynthetic mechanism called non-photochemical quenching (NPQ) that dissipate excess light into heat.
Due to metabolic cost (as for the water transport), plants do not maximize their capacity of reduction power production from the incident light. The acclimation occurs as the result of a balance between the cost of increasing photosynthetic capacity, which can be underutilized (Oguchi et al., 2008; Terashima et al., 2006) and the risk of photooxidative damage if the mechanisms to dissipate excess energy received by the plant are not sufficient (Li et al., 2009). In this perspective, the light absorption properties of the photosynthetic apparatus tend to be optimized for intermediate light levels and not to the minimum or maximum levels of the light regime (Chabot et al., 1979; Watling et al., 1997).

1.3. Limitation concerning plant triose phosphate utilization capacity

The third form of biochemical limitation of photosynthesis depends to the limitation of triose phosphate utilization. The final products of CBC are all phosphorylated, that is why CBC uses ATP. ATP synthesis requires

inorganic phosphate but chloroplast phosphate concentration is almost stable in all environmental conditions including phosphate nutritional stress (Diaz- Espejo et al., 2012; Foyer and Spencer, 1986; Rebeille et al., 1983). The utilization of final product of CBC, followed by inorganic phosphate release, prevent chloroplast inorganic phosphate depletion and ATP synthesis inhibition. Starch synthesis uses 30-60 % of CBC products, 25-50 % are used in the sucrose synthesis, 7-12.5 % in the synthesis of amino acids, in particular glycine and serine (synthetized from photorespiration products and not from photosynthesis) and the remained part, at really low percentage, are linked to other form of metabolism (McClain and Sharkey, 2019).
The photochemical efficiency and the CBC enzymes are strongly regulated by inorganic phosphate availability, in case of limited condition the electron transport rate and Rubisco activity are immediately down regulated to prevent energetic imbalance and photoinhibition. Risk of limitation of triose phosphate utilization is predominant under high light and high CO_2 concentration, low temperature (caused by high sensitivity to temperature of enzyme involved in photosynthetic product utilization) or to a dramatic reduction of sink activity of photosynthetic products (Yang et al., 2016). Different experiments can be explained by sink activity limitation, for example defruited plants shown a significant down regulation of photosynthesis (King et al., 1967), artificial increase of sugar concentration into the leaf reduces sucrose synthesis, limits the triose phosphate utilization capacity and inhibits photosynthesis (Paul and Foyer, 2001). Starch builds up under artificial highly favorable photosynthetic condition causes a decline in photosynthetic rate (Ramonell et al., 2001). It must be said that plants show a high capacity to adapt triose phosphate utilization to the photosynthetic rate that they assume to experience. This acclimation capacity is so pronounced that recently is questioned the existence of triose phosphate limitation in natural ecosystems (Rogers et al., 2021).
Water stress is a cause of metabolic disequilibrium in photosynthesis products utilization that could bring a inhibitory signal on photosynthetic rate. This signal should not be the direct imbalance between production and utilization of triose phosphate in the chloroplast, but hormonal signals coming from sink organs (Lovisolo et al., 2010) and primary metabolism that target mesophyll and stomatal cells (Gago et al., 2016) reducing electron transport rate (Kiirats et al., 2009; Sharkey, 1988), the activation state of Rubisco and consequently carboxylation (Cen and Sage, 2005; Sharkey et al., 1986; Socias et al., 1993; Viil et al., 2004) allowing stomatal closure.

1.4. The gas exchange analysis

Heteroatomic molecules of gas as CO_2 and H_2O have a specific spectrum of absorption in the infrared; this peculiarity is not present in diatomic

molecule as N_2 and O_2. This behavior has meant that the easiest way to measure CO_2 concentration in air is through analysis of the CO_2 infrared specific component extinction in an optical pathway through air. The instrument that made this kind of analysis is the infrared gas analyzer (IRGA), an instrument that is composed of 4 main elements: a broad band infrared source, a gas cell, an optical filter and a detector. The infrared light beam emitted by the infrared source crosses the gas cell that shows a precise optical pathway; the optical filter pass only the CO_2 absorbed infrared component and the detector detects the residual infrared light intensity. Fixing the optical path length, CO_2 concentration is inversely proportional to the infrared intensity hitting the detector. The H_2O absorption spectrum partially overlaps the CO_2 one and atmospheric H_2O concentration is far above the atmospheric CO_2. For these reasons, measurement of CO_2 is coupled with water vapor concentration measurement that allows calculating an adjustment factor. Water vapor concentration measurement can be conducted with a specific IRGA or other instrumental methodology.

IRGAs are widely used in plant physiology and represent the easiest to use and the most diffuse system for photosynthesis measurements. Photosynthesis measurements should be made with close, semi-close or open systems. No net air-flow is present in the first two; air after IRGA measurement is recycled in the hermetic cuvette containing the leaf or the target plant organ and, in case of positive A_{net}, CO_2 concentration inevitably decreases until CO_2 compensation point, unless reintegration through CO_2 source (as the semi-clos system). The open system provides a net air-flow; new air is continuously introduced into the chamber while that contaminated by plant exchanges is expelled. Commercial solutions for leaf gas exchange analysis adopt open systems and always consist of at least 4 elements: a flow generator, a flow meter, a transparent chamber and an IRGA. These instruments blow a known volume of air inside the cuvette and perform twice CO_2 and H_2O measurements; the first time on the air entering the chamber, the second time on the air outing the chamber (depending on the instrument specifics these measurements could be conducted simultaneously, if there are 2 measurement cells for CO_2 and 2 measurement cells for H_2O, or consequentially). These collected data are sufficient to calculate through von Caemmerer and Farquhar' equation (1981) A_{net} and water loss through transpiration (E).

$$E = \frac{u_e(w_o - w_e)}{(1 - w_o)} \quad (5)$$

$$A_{net} = u_e(c_o - c_e) - E\, c_o \quad (6)$$

Where u_e, w_e and c_e are respectively molar air flow, water vapor concentration and CO_2 entering the chamber and w_o and c_o respectively the water vapor concentration and CO_2 outing the chamber. $E \cdot c_o$ is an adjustment factor considered for c_o dilution with water vapor released by E.
From E measurement it is possible to derive other important parameter as stomatal conductance (g_s), that define the facilities which H_2O penetrate out to the leaf surface through stoma and diffuse to the atmosphere. g_s is proportional to g_{sc} following the relation

$$g_{sc} = \frac{g_s}{1.56} \quad (7)$$

Being the stoma a resistance to CO_2 diffusion inside the leaf, C_i is different by CO_2 concentration (C_a) and could be calculate according to Fick's law:

$$C_i = C_a - \frac{A_{net}}{g_{sc}} \quad (8)$$

As gas exchange measurements can be made on photosynthetic organs, the same measurements can be made on not-photosynthetic organs or under environmental condition (e.g. in the dark or under stress condition) where carboxylation is not predominant in the net exchange of CO_2 between plant and atmosphere and CO_2 release through R_d (in not photosynthetic organs) and R_d and V_o (in photosynthetic organs) overcome V_c resulting in negative values of A_{net} calculated from the gas exchange analysis data (equation 1, 6).
As just mentioned, A_{net} changes in space and time, in commercial gas exchange systems, which mostly compartmentalize small portions of leaf and soil. During the years, custom-made gas exchange systems have been developed. These systems are orientated to measure a balance of net CO_2 flow on whole plant scale coupled to automatic and continuous monitoring. The obtained information is essential to deepen the complex responses and timing of acclimation of plants to the environmental stresses and to couple photosynthetic with respiratory metabolisms (Drake et al., 2019; Hagedorn et al., 2016).

1.5. References

Busch, F.A., 2018. Photosynthetic Gas Exchange in Land Plants at the Leaf Level. *Photosynthesis: Methods and Protocols* (ed. Covshoff, S.) 25–44.

Cen, Y.-P., Sage, R.F., 2005. The Regulation of Rubisco Activity in Response to Variation in Temperature and Atmospheric CO2 Partial Pressure in Sweet Potato. Plant Physiology 139, 979–990.

Chabot, B.F., Jurik, T.W., Chabot, J.F., 1979. Influence of Instantaneous and Integrated Light-Flux Density on Leaf Anatomy and Photosynthesis. American Journal of Botany 66, 940–945.

Deans, R.M., Brodribb, T.J., Busch, F.A., Farquhar, G.D., 2020. Optimization can provide the fundamental link between leaf photosynthesis, gas exchange and water relations. Nat. Plants 6, 1116–1125.

Diaz-Espejo, A., Bernacchi, C.J., Collatz, G.J., Sharkey, T.D., 2012. Models of photosynthesis, in: Loreto, F., Medrano, H., Flexas, J. (Eds.), Terrestrial Photosynthesis in a Changing Environment: A Molecular, Physiological, and Ecological Approach. Cambridge University Press, Cambridge, pp. 98–112.

Drake, J.E., Furze, M.E., Tjoelker, M.G., Carrillo, Y., Barton, C.V.M., Pendall, E., 2019. Climate warming and tree carbon use efficiency in a whole-tree 13CO2 tracer study. New Phytologist 222, 1313–1324.

Farquhar, G.D., von Caemmerer, S., Berry, J.A., 1980. A biochemical model of photosynthetic CO2 assimilation in leaves of C3 species. Planta 149, 78–90.

Foyer, C., Spencer, C., 1986. The relationship between phosphate status and photosynthesis in leaves : Effects on intracellular orthophosphate distribution, photosynthesis and assimilate partitioning. Planta 167, 369–375.

Gago, J., Daloso, D. de M., Figueroa, C.M., Flexas, J., Fernie, A.R., Nikoloski, Z., 2016. Relationships of Leaf Net Photosynthesis, Stomatal Conductance, and Mesophyll Conductance to Primary Metabolism: A Multispecies Meta-Analysis Approach. Plant Physiology 171, 265–279.

Hagedorn, F., Joseph, J., Peter, M., Luster, J., Pritsch, K., Nickel, U., Kerner, R., Molinier, V., Egli, S., Schaub, M., Liu, J., Li, M., Sever, K., Weiler, M., Siegwolf, R., Gessler, A., Arend, M., 2016. Recovery of trees from drought depends on belowground sink control. Nature Plants 2, 16111.

Keller, M. (Ed.), 2020. Preface to the third edition, in: The Science of Grapevines (Third Edition). Academic Press, pp. xi–xii.

Kiirats, O., Cruz, J.A., Edwards, G.E., Kramer, D.M., Kiirats, O., Cruz, J.A., Edwards, G.E., Kramer, D.M., 2009. Feedback limitation of

photosynthesis at high CO2 acts by modulating the activity of the chloroplast ATP synthase. Functional Plant Biol. 36, 893–901.
King, R.W., Wardlaw, I.F., Evans, L.T., 1967. Effect of assimilate utilization on photosynthetic rate in wheat. Planta 77, 261–276.
Li, Z., Wakao, S., Fischer, B.B., Niyogi, K.K., 2009. Sensing and responding to excess light. Annu Rev Plant Biol 60, 239–260.
Lovisolo, C., Perrone, I., Carra, A., Ferrandino, A., Flexas, J., Medrano, H., Schubert, A., 2010. Drought-induced changes in development and function of grapevine (Vitis spp.) organs and in their hydraulic and non-hydraulic interactions at the whole-plant level: a physiological and molecular update. Functional Plant Biol. 37, 98–116.
McClain, A.M., Sharkey, T.D., 2019. Triose phosphate utilization and beyond: from photosynthesis to end product synthesis. Journal of Experimental Botany 70, 1755–1766.
Oguchi, R., Hikosaka, K., Hiura, T., Hirose, T., 2008. Costs and benefits of photosynthetic light acclimation by tree seedlings in response to gap formation. Oecologia 155, 665–675.
Paul, M.J., Foyer, C.H., 2001. Sink regulation of photosynthesis. Journal of Experimental Botany 52, 1383–1400.
Ramonell, K.M., Kuang, A., Porterfield, D.M., Crispi, M.L., Xiao, Y., McClure, G., Musgrave, M.E., 2001. Influence of atmospheric oxygen on leaf structure and starch deposition in Arabidopsis thaliana. Plant Cell Environ 24, 419–428.
Rebeille, F., Bligny, R., Martin, J.-B., Douce, R., 1983. Relationship between the cytoplasm and the vacuole phosphate pool in Acer pseudoplatanus cells. Archives of Biochemistry and Biophysics 225, 143–148.
Rogers, A., Kumarathunge, D.P., Lombardozzi, D.L., Medlyn, B.E., Serbin, S.P., Walker, A.P., 2021. Triose phosphate utilization limitation: an unnecessary complexity in terrestrial biosphere model representation of photosynthesis. New Phytologist 230, 17–22.
Sharkey, T.D., 1988. Estimating the rate of photorespiration in leaves. Physiologia Plantarum 73, 147–152.
Sharkey, T.D., Seemann, J.R., Berry, J.A., 1986. Regulation of Ribulose-1,5-Bisphosphate Carboxylase Activity in Response to Changing Partial Pressure of 02 and Light in Phaseolus vulgaris' 4.
Socias, F.X., Medrano, H., Sharkey, T.D., 1993. Feedback limitation of photosynthesis of Phaseolus vulgaris L grown in elevated CO2. Plant, Cell & Environment 16, 81–86.
Terashima, I., Hanba, Y.T., Tazoe, Y., Vyas, P., Yano, S., 2006. Irradiance and phenotype: comparative eco-development of sun and shade leaves in relation to photosynthetic CO2 diffusion. Journal of Experimental Botany 57, 343–354.

Vialet-Chabrand, S., Matthews, J.S.A., Simkin, A.J., Raines, C.A., Lawson, T., 2017. Importance of Fluctuations in Light on Plant Photosynthetic Acclimation. Plant Physiology 173, 2163–2179.

Viil, J., Ivanova, H., Pärnik, T., Pärsim, E., 2004. Regulation of Ribulose-1,5-bisphosphate Carboxylase/Oxygenase in vivo: Control by High CO2 Concentration. Photosynthetica 42, 283–290.

von Caemmerer, S., Farquhar, G.D., 1981. Some relationships between the biochemistry of photosynthesis and the gas exchange of leaves. Planta 153, 376–387.

Watling, J.R., Ball, M.C., Woodrow, I.E., 1997. The utilization of lightflecks for growth in four Australian rain-forest species. Functional Ecology 11, 231–239.

Yang, J.T., Preiser, A.L., Li, Z., Weise, S.E., Sharkey, T.D., 2016. Triose phosphate use limitation of photosynthesis: short-term and long-term effects. Planta 243, 687–698.

Zhen, S., Bugbee, B., 2020. Substituting Far-Red for Traditionally Defined Photosynthetic Photons Results in Equal Canopy Quantum Yield for CO2 Fixation and Increased Photon Capture During Long-Term Studies: Implications for Re-Defining PAR. Frontiers in Plant Science 11.

2. Objectives

I focused my PhD thesis on the aspects limiting plant carbonic assimilation, above detailed, adopting different experimental setups and investigating different ecophysiological aspects. In all experiments, I set up gas exchange systems for whole plant and/or organ (shoot, root) measurements, with the goal to perform a C balance integrating CO_2 fluxes entering and exiting the targets (organs or whole-plants).

One of the objectives of my doctoral work was to identify solutions to the engineering difficulties encountered in the construction of gas exchange chambers on a whole plant. To do this, we have designed and built two prototypes of different sizes with the aim of highlighting the different instrumental solutions necessary to monitor the gas exchange of small plants grown in a controlled environment and large plants grown in an environment mimicking the natural one. One of the salient features of the work was to separate the shoot and root compartments to perform simultaneous measurements of canopy photosynthesis and root respiration. Particular attention was paid to implementing the ease of use of the equipment, making assembly faster and speeding up data acquisition.
This work led to the drafting of a methodological article reported here below (3.1) and accepted by Plant Science (Elsevier), https://doi.org/10.1016/j.plantsci.2022.111505, titled: '**Technical advances for measurement of gas exchange at the whole plant level: design solutions and prototype tests to carry out shoot and rootzone analyses in plants of different sizes'**. Some engineering challenges that I solved are the result of the collaboration with Prof. Davide Ricauda's group, a mechatronics expert of DISAFA.

In a second paper here reported, titled '**Effects of light quality on photosynthesis and growth of *Lactuca sativa* L.**' (3.2), submitted to Plant Growth Rgulation (Springer), limitations to the quality of light in lettuce (1.2) have been addressed.
The goal of the work was to understand whether the spectrum of LED light to which lettuce plants are subjected can have an effect on growth, acclimation of the photosynthetic apparatus and respiration. To do this, we exposed lettuce plants to 3 different light spectrum regimes (Red-Blue light, Red-Green-Blue light and Full Spectrum light) and conducted gas exchange analyzes on shoot and root to run a carbon balance. In parallel, we conducted fluorescence and molecular analyzes to identify differences in the composition of the photosystems.
Part of this work was conducted at the University of Verona, by working in the group of Prof. Matteo Ballottari, a group that I already frequented during a *post-laurea* period before to take the PhD course. I also

collaborated with the company of Turin Prisma s.r.l. at the realization of LED lamps with specific spectra, essential for the research goals on light limitation of assimilation.

In the third paper, '**Photosynthetic recovery in drought-rehydrated grapevines is associated with high demand from the sinks, maximizing the fruit-oriented performance**' (3.3), accepted for publication by The Plant Journal (Wiley), https://doi.org/10.1111/tpj.16000, I reported the results of my research focused to stomatal (1.1) and metabolic (1.3) limitations introduced by the analysis of the model of Farqhuar et al. 1980 under water stress and water stress release.
The goal of this work was to understand how carbon limitation induced by water stress can trigger a competition of the products of photosynthesis between fruit and root, and how this resolves following the rehydration of plants. The strategy we used was to continuously carry out a balance of C between photosynthesis and respiration of the plant during the period of stress and recovery from stress and to quantify the allocation of C to the different sinks through a pulse labeling experiment with marked C.
In this work, which benefited a funding from the CRT bank foundation (Carbostress project), I designed and realized a chamber for CO_2 labelling experiments in collaboration with the company of Turin Intek s.r.l. In this chamber, thank to the collaboration with prof. Daniel Said Pullicino (a soil chemist of DISAFA), I set up a system for CO_2 feeding and labeling for a pulse-chase experiment on grapevine. The functional question was the plant response at rehydration after a period of water stress. We pointed to understand the fruit sink importance of crop plants compared to the root sink activity role.
The bio-molecular aspects have been conducted in collaboration with Dr. Giorgio Gambino and Irene Perrone and their collaborators of IPSP, CNR, Torino and CREA, Conegliano.
In this experiment helped me several thesis students belonging to bachelor and master courses given by Prof. Claudio Lovisolo, that I coordinated in the acquisition of the research outputs.

In the second year of experiments (season 2020) the opportunity to frequent the laboratories of DISAFA at Grugliasco campus was interrupted by COVID-19 restriction. During this season I set up my systems for gas exchange measurement at whole plant scale on tobacco plants (results not presented in this PhD thesis; Figure 1) and I conducted preliminary experiments on lettuce to optimize the selection of spectra to test for lettuce growth and photosynthetic responses (Figure 2).

Figure 1. Gas exchange measurements of tobacco plant during COVID-19 lockdown (Aprli 2020).

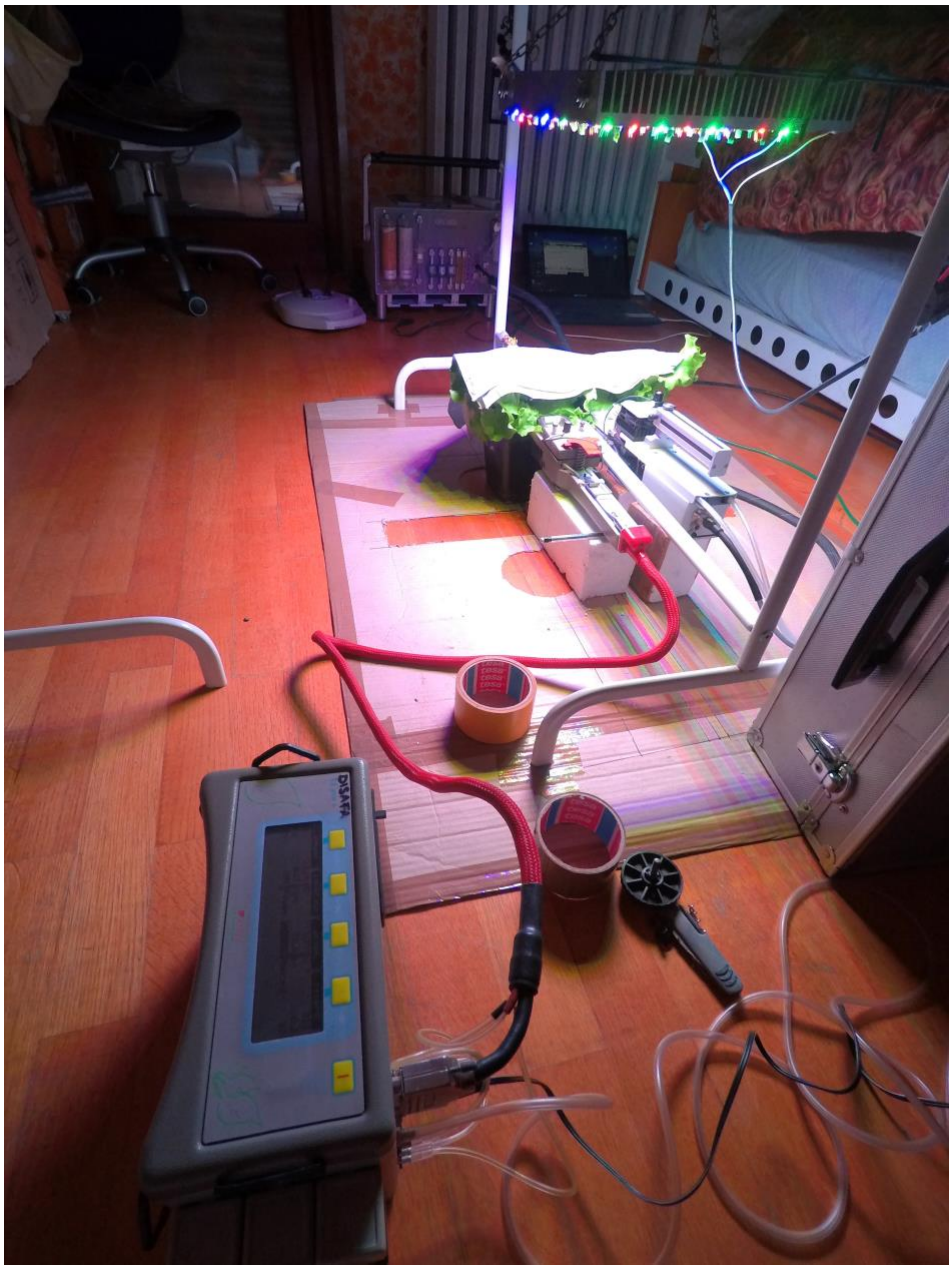

Figure 2. Preliminary experiment on lettuce plants for spectrum selection.

3. Results

3.1. accepted by Plant Science (Elsevier) following request of revisions
https://doi.org/10.1016/j.plantsci.2022.111505

Technical advances for measurement of gas exchange at the whole plant level: design solutions and prototype tests to carry out shoot and rootzone analyses in plants of different sizes.

Davide L. Patono[1], Leandro Eloi Alcatrão[1], Emilio Dicembrini, Giorgio Ivaldi[1], Davide Ricauda Aimonino[1], Claudio Lovisolo[1,2,*]

[1]Dept. Agricultural, Forest and Food Sciences, University of Turin, Grugliasco, Italy
[2]Institute for Sustainable Plant Protection, National Research Council, Turin, Italy
[*]Corresponding author

Abstract

To measure gas exchange at the whole plant (WP) level, design solutions were provided and prototypes of gas-exchange systems (GESs) were tested to carry out root and shoot analyses in plants of different sizes. A WP-GES for small herbaceous plants was tested on the ability to maximize the net assimilation rate of CO_2 in lettuce plants grown either under blue-red light or upon full spectrum artificial light. A WP-GES for large woody plants was tested during an experiment describing the drought stress inhibition of grapevine transpiration and photosynthesis. Technical advances pointed to optimize: i) the choice of cuvette material and its technical configuration to allow hermetic isolation of the interface shoot-root, to avoid contamination between the two compartments, and to allow climate control of both shoot and root cuvettes, ii) accurate measurements of the mass air-flow entering both cuvettes, and iii) an adequate homogenization of the cuvette air volume for stable and accurate detection of CO_2 and H_2O concentration in cuvettes before and after CO_2 and H_2O contamination of the air volumes exerted by plant organs.

Keywords

Gas exchange; transpiration; photosynthesis, respiration.

Introduction

Gas exchange measurement is a powerful tool in plant biology with a wide range of applications. One of the strengths of this methodology is the versatility of operating on different scales, from the small portion of plants (e.g. leaf, petiole, stem, root portion) to the ecosystem scale (Cernusak, 2020). Although some of the pioneering studies aimed at realizing a gas exchange system (GES) for whole plant (WP) measurements (Heinicke and Childers, 1937), the development of compact and easy-to-use commercial solutions on single leaf or portions of soil have made the latter predominant approach.

The prediction of plant dry matter production and yield requires a carbon (C) balance of the WP (integral for a chosen period of net shoot photosynthesis – root and soil respiration) (Matthews al., 2017), and the up-scaling of organ information to the WP is hampered by inhomogeneous distribution of gas exchange rates between the various organs (van Iersel and Bugbee, 2000; Leonardos and Grodzinski, 2011; Ryan and Asao, 2019). Rootzone respiration in soil, for example, responds to a temperature and humidity gradient in the soil, to the structure of the soil, to the presence of nutrients and organic matter, or to the greater or lesser diffusion of roots in the soil (Stoyan et al., 2000; Epron et al., 2004). As below - the above ground measurements are also influenced by the surrounding environment: the microclimate present around the leaves due to the structure of the canopy and the age of the leaves are just some important examples of the complexity of the factors that shape the photosynthetic performance of leaves and consequently the photosynthesis of the canopy. Furthermore, the respiratory contribution of organs such as the trunk or fruit is often not considered (Roux et al., 2001).

Modeling the C balance in WP starting from measurements on organ portions has some important disadvantages, including the need for multiple measurements to obtain representative values of spatial differences and greater mathematical complexity to cope with a large number of control hypotheses. The models are often incomplete with a high level of uncertainty and a direct measurement of the WP gas exchange is required for their validation (Tarara et al., 2011).

The ever-present scientific need to collect precise information on a plant scale has led over the years to the realization of numerous WP-GESs (e.g. Kölling et al., 2015 for herbaceous species; Poni et al., 2014 for perennial plants), each with customized solutions based on experimental needs. However, only a few WP-GESs had the goal of simultaneous measurement of shoot-atmosphere and soil-atmosphere exchanges (Walsh and Layzell, 1986; Harris and Paul, 1991; Cen et al., 2001; Kläring et al., 2014; Drake et al., 2019; Birami et al., 2020; Kläring and Körner, 2020; Osuebi-Iyke et al., 2022).

The main challenges to address for designing a WP-GES with separate compartments between shoot and the total soil volume hosting the rootzone could be summarized in: i) choice of cuvette material and its technical configuration to allow hermetic isolation of the interface shoot-rootzone, to avoid CO_2 and H_2O contamination between the two compartments, and to allow climate control of both shoot and rootzone cuvettes, ii) make accurate measurements of the mass air-flow entering both cuvettes, iii) allow for an adequate homogenization of the cuvette air volume for stable and accurate detection of CO_2 and H_2O concentration in cuvettes before and after contamination of the air volumes exerted by plant organs.

The aim of this technical article was to show how to solve the aforementioned challenges for using WP-GESs on different sized plants. We designed two different prototypes of WP-GES with separate compartments for shoot and rootzone for the measurement of either small herbaceous plants under in-lab actively controlled climatic conditions or woody plants growing in climatic conditions resuming environmental ones. We built and tested the two prototypes by addressing two biological phenomena. A WP-GES for small herbaceous plants (s-GES) was tested on the ability to maximize the net assimilation rate of CO_2 under blue-red light (Li et al., 2020) compared to a control full spectrum light in lettuce; preliminary measurements here described as tests pointed to understand if there is an adaptation of the photosynthetic apparatus to the spectrum of light, and especially to green an far-red light components, whose consequences have an impact on stomatal function and plant biomass accumulation (Kim et al., 2004; Son & Oh, 2015; Pennisi et al., 2019; Yan et al., 2019; Pennisi et al., 2020; Legendre & van Iersel, 2021). A WP-GES for large woody plants (b-GES) was tested during an experiment describing the water stress inhibition of grapevine photosynthesis, to compare our prototype with others described WP-GESs (Miller et al., 1996; Long et al., 1996; Poni et al., 1997; Moutinho-Pereira et al., 2010; Tarara et al., 2011).

Materials and methods

s-GES cuvette materials and design

The s-GES shoot cuvette was made in polycarbonate, adopting a cubic shape 90x90x90 mm. The shoot cuvette was connected to the rootzone cuvette by an aluminum junction ring. The rootzone cuvette consisted of a polycarbonate cylinder (80 mm diameter x 130 mm height) glued to the junction ring and an expanded polyvinyl chloride (PVC) basement. Shoot-root interface consisted in a polycarbonate disk with a central hole for plant shoot growth. A 12DC brushless fan was installed in both cuvettes to homogenize the air. Air-flow was supplied by a brushless diaphragm pump equipped with an analogue (0-5 V) speed control system (3KD Series-BLDC Motor, Boxer GmpH, Germany). The air-flow was monitored with two hot wire mass air-flow meters with air-flow range 0-10 l min^{-1} (Top-Trak 822, Sierra Instruments, USA). Flow was partially diverted in a silica gel column for dehumidification and to a 200 W Peltier cell for temperature control. An InfraRed Gas Analyzer - IRGA (Li-850 with internal air sample pump, Licor, USA) - was connected through a 4-way valve to root and shoot outlet and air reference, the air pathway sampled was manually selected. A t-type thermocouple was installed inside the cuvette for temperature measurement. A 120 Watt white LED or red-blue LED light lamp (Prisma, Italy) was positioned over the s-GES.
In details, the s-GES cuvette consisted of four elements: 1) polycarbonate shoot cuvette (Figure 1A), 2) polycarbonate rootzone cuvette (Figure 1B), 3) aluminum junction ring (Figure 1C) and 4) disk interface (Figure 1D). The polycarbonate shoot cuvette was made with a cubic shape made of 6 rigid panels 90x90x3 mm glued with neutral transparent silicone. On the lower face of the cube, a hole D85 mm was drilled and a 30 mm high slice polycarbonate pipe OD90x2 mm was glued to the hole perimeter. Two holes for installation of 2 bulkhead pneumatic push-in fittings were made on 2 specular side faces (Figure 1E). A 40x40x10 mm 12V DC brushless fan (Figure 1F) was glued on an internal side face for cuvette air homogenization a thermocouple was clamped in front of the fan, electrical wires pass the face in a through hole that was subsequently sealed with neutral silicone. The connection between shoot and rootzone cuvettes was assembled by the use of a custom aluminum junction ring made with CNC. This aluminum ring has two O-ring seats, one to hermetic adhesion with shoot compartment polycarbonate cylinder slice (nitrile rubber O-ring ID79x3.5 mm; Figure 1G), one for the hermetic adhesion to the root-shoot interface (nitrile rubber O-ring ID75x2.5 mm; Figure 1H). Aluminum junction ring has two radial through holes, one for electrical wires passage and the other for pneumatic push-in fitting assembling (rootzone cuvette air outlet).
The s-GES rootzone cuvette consisted of a slice of polycarbonate pipe D80X2mm 130 mm high glued with polyurethane sealant to the aluminum

junction ring at the top and an expanded PVC basement at the bottom. A U shape hole in the PVC basement (Figure 1J) created the inlet air path and a 12V DC fan (Figure 1K) was glued in its proximity inside the rootzone cuvette. Plants needed to be grown in cylindrical plastic pots (Figure 1L) of maximum OD50 mm and 100 mm high; plastic pots that we used were pipe slices closed at the bottom with 0.5 mm mesh plastic net. Shoot-root interface consisted of a D85x3 mm light gray polycarbonate disk with a central hole D3 mm (Figure 1D). The polycarbonate disk was fit to the plant after emergence of cotyledons. During growth, the stem autonomously plugged the central disk hole. At time of measurements plastic pots were inserted inside the rootzone cuvette and interface disk was screwed to the top surface of the aluminum junction ring.

b-GES cuvette materials and design

The b-GES shoot cuvette consisted in an inflated polyethylene balloon, while the rootzone cuvette was a custom '18-gallon' metal drum whose cover was used as a shoot-root interface. The air flow was supplied by a custom made 350W three-phase centrifugal fan dimensioned to allow at 50 Hz an air flow of 360 m^3 h^{-1} with pressure drop of 270 Pa (PBN, Italy); the fan speed was regulated by an inverter (VFD007EL23A, Delta, Taiwan). The flow was measured with a hot wire anemometer (AVUL-3DA1, Dwyer, USA) installed in the PVC pipeline. A T-type thermocouple was installed at the outlet of the balloon. A PAR sensor (SQ-515-SS, Apogee Instrument, USA) was installed outside the balloon under the same balloon polyethylene cover. A 220V AC brushless diaphragm pump (D7 series, Charles Austin, UK) with maximum air-flow 26 l min^{-1} was connected to the rootzone cuvette. The b-GES balloon was installed in a multi-chamber module that controls a series of 4 balloons; tests here conducted and the technical solution reported were focused on the one-balloon outputs and not on the automation of the multi-chamber system.
In details, the b-GES shoot compartment was designed as a balloon cuvette sustained directly by the air-flow through without a frame. We used a transparent polyethylene (PE) film (Long Life, Eiffel, Italy) that is developed for table grape growth. PE transparency was tested by comparing irradiance measurements performed with a spectroradiometer (MS-720, EKO instruments, Netherlands) inside the balloon with measurements carried out outside (Figure 2A). The relative transmittance (ratio between the two measurements) is close to the unity for wavelengths greater than 450 nm; below (in the blue and in the UV region) the transparency gradually decays up to a 15% relative transmittance at 350 nm (Figure 2B). It is a low thermality material stabilized for sulfur treatments with a lifespan of 2-3 years under full sunlight. Balloon film was thermo-sealed with a clamp heat sealer (Superpoly 630 SP, Ferplast, Italy). The geometry of the balloon was a prism with hexagonal base (maximum width 1.5 m, 1.2 m high) that is close above and below with

hexagonal pyramid prism (0.4 m high) per a total volume about 2.1 m^3 (Figure 3A). Along the entire balloon length a pressure polyethylene zip (Minisac S.n.c; Italy; Figure 3B) was thermo-sealed to allow fast opening and closing for sampling or plant substitution. When the balloon was well inflated the shape was pretty close to a sphere (Figure 3C). The efflux from the balloon was a PVC pipe curve OD63 mm (Figure 3D) cover with a closed cell foam adhesive tape at one extremity. An aperture at the top of the cuvette pyramid was sealed around the foam with a metal clamp. The PVC curve was also the seat of a thermocouple and a polytetrafluoroethylene (PTFE) probe (Figure 3E) connected to the IRGA for outlet air analysis. The inlet of the balloon was a PVC T OD100 mm (Figure 3F) clamped in the same way at the lower pyramid base.
The b-GES rootzone cuvette was realized starting from a metal drum ID450 mm and 450 mm high (about 70 l capacity) with 3 ¾" holes with screw cap closure (Figure 3G) at the bottom to allow water drainage, if needed. The interface between shoot and rootzone cuvette was the original cap of the tank with for 2" holes with screw cap closure (Figure 3H) to allow plant watering and soil sampling. A D100 mm hole was applied to the middle of the tank to allow the insertion of one PVC T junction that was sealed with polyurethane sealant. Before bud break PVC T was inserted inside the plant trunk and the space between trunk and PVC was foam filled (Figure 3F) to allow hermetic separation between shoot-rootzone compartments. Plants could be grown directly inside the rootzone cuvette or in a smaller pot and inserted in the tank at time of measurements. Theoretically the same b-GES could measure more plants during the season with the limitation that each plant should be inserted in a PVC T inside the tank cap at the beginning of the vegetative season. Shoot and rootzone air homogenization was obtained installing two 12V DC brushless fans 120x120x20 mm (Figure 3I).

Mass flow control and measurements - s-GES

Driving force of the air-flow in the s-GES was guaranteed by a 24V DC brushless diaphragm pump (Figure 4A) with 0-5 V signal for speed control (3KD Series-BLDC Motor, Boxer GmpH, Germany) regulated by a potentiometer (Figure 4B). The pneumatic pathway started with a 1000 l tank (Figure 4C) connected to the suction side of the pump to reduce fluctuation in atmosphere H_2O and CO_2 concentration. The tank was internally ventilated with a 120X120X40 mm 12V DC fan to prevent air pockets; to permit air renewal, a 4-meter high probe allowing air intake was connected to the cap of the tank (Figure 4D). The first element installed downstream the pump was a needle valve partially closed (Figure 4E) that dampened air pulsation due to pump operation. A Y fitting diverted part of the flow to a silica gel column (Figure 4F); air partition directed to the silica gel was regulated by a manual flow regulator (Figure 4G). After air dehumidification a cooling module was introduced. The

cooling module consists of a 200W Peltier cell glued from one side to a ventilated heatsink and to the other to an aluminum plate coil for heat exchange with air (Figure 4H). The Peltier operating power has been controlled manually with power supply current input. Another Y fitting split flow in two lines for rootzone and shoot cuvette and one flow regulator installed to the rootzone line control flow partitioning (Figure 4I). Prior to getting into the cuvettes air-flow was measured by two hot wire mass air-flow meters with free flow range 0-10 l min^{-1} (Top-Trak 822, Sierra Instruments, USA; Figure 4J). At pump full speed total flow (sum of the flow directed to the two cuvettes) was about 10 l min^{-1}. A T junction was installed immediately after the temperature module (Figure 4K) and one air probe connected to the IRGA allowed air sampling for reference gas analysis. The cuvette outlet consisted of push-in T-fittings (Figure 4L), one side of the T was connected to the air probe for sample gas analysis and other allowed air efflux. A 4-way manual valve selected the probe for the IRGA (Figure 4M).

Mass flow control and measurements - b-GES

In the b-GES the air-flow through the balloon was generated by a custom three-phase 350W centrifugal blower (PBN, Italy; Figure 5A) controlled with an inverter (Figure 5B) to regulate the frequency of the electrical engine and consequently the air-flow. The blower was dimensioned to the balloon multi-chamber module that presents a pipeline pressure drop of 270 Pa at a maximum flow of 360 m^3 h^{-1} (90 m^3 h^{-1} to each balloon; calculated according to pressure loss tables). Pipeline consisted of a 4 meter vertical pipe OD125 mm (Figure 5C) connected from one side to the suction port of the blower and to the other side to a 180° PVC curve to prevent water suction during rainfall. The blower air delivery port was connected to a branched pipeline with three T-pieces (Figure 5D) that allowed splitting the main flow in 4 lines. Each line, prior to the junction of the balloon PVC T surrounding the trunk, presented a diameter reduction from OD125 mm to OD63 mm (Figure 5E) where a hot wire anemometer was installed (Figure 5F) in a linear section of one meter. The reduction in the pipeline section was intended to increase air velocity (at same air-flow) to decrease anemometer error. The connection between pipeline and balloon was realized with 1 meter long PVC-copper flexible suction hose for air (Figure 5G). Pressure drop due to PVC curve restriction at balloon outlet (Figure 5H) was sufficient to maintain the balloon fully inflated in the range 20-90 m^3 h^{-1} of air.
Rootzone cuvette air-flow was generated by a diaphragm pump (Figure 5I) that pushes air into the cuvette through a PTFE pipeline ID4 mm- OD6 mm (inlet flow). On the PTFE pipeline, prior to being connected to the tank cap, a hot-wire flow meter was installed (Figure 5J). All the connections with the PTFE pipeline were realized with pneumatic push in fittings (Figure 3J). Considering pipeline pressure drop, the rootzone cuvette flow

was 16.0 □ 0.1 l min^{-1}. Cuvette efflux consisted of one 2" holes on the tank cap that was left open (Figure 3H). An air probe was connected to another push in fitting threaded to the tank cap allowing air sampling for IRGA analysis of the cuvette outlet. A manual 4-way valve (Figure 5K) opened the probe path selected for the IRGA (Figure 5L).

Tests of gas exchange measurements - Plant processing before, during, and after measurements in the s-GES

For the s-GES test, seeds of *Lactuca sativa* cv. Rebelina (Gautier, Eyragues, France) were sown in seedling trays filled with peat and left for 2 weeks to germinate in a plant incubator (temperature 23°C, RH 60%, white LED light of 215 µmol m^2 s^{-1}, and photoperiod of 16:8 h of day : night) (Figure 6A). With the aid of a spectroradiometer (MS-720, EKO instruments, Netherlands), light intensity was maintained at 215 µmol m^2 s^{-1} PPFD over the plant canopy throughout the experiment, following set up of Pennisi et al. (2019, 2020).
Seedlings were transplanted inside 0.4 l OD50 mm plastic pots filled with sand and transferred in groups of 10 potted plants on two different shelves in a growth chamber (Figure 6B).
Plants were irrigated twice a week with full strength Hoagland solution during three weeks of growth to study putative adaptations of lettuce photosynthetic apparatus to the spectrum of light and their consequences on indoor plant biomass accumulation (Figure 6C). We exposed plants to two different LED lighting conditions: a LED array showing narrow bands in RB and RGB regions was compared with a full spectrum (FS) LED that has a continuous emission in all the PAR regions, as it is in the sunlight. Both white and red-blue lights were set in order to have the same total PAR intensity of 215 µmol m^{-2} s^{-1}.
Gas exchange in shoot and rootzone was measured under 215 µmol m^2 s^{-1} of red-blue or white light. Steady state measurements of whole canopy assimilation (A), transpiration (E) and rootzone respiration (R) were performed in the s-GES, and the same measurement was conducted with a portable IRGA (GFS-3000, Walz, Germany) on single leaves (SL). No WALZ light source was used. SL measurements were performed under LED illumination used for lighting the s-GES. SL and WP net CO_2 assimilation (A), transpiration (E), and rootzone respiration (R) were calculated following von Caemmerer and Farquhar's equations (von Caemmerer & Farquhar, 1981) (Figure 6D).
As soon as the measurement was completed, the rosette was removed and the leaf area (LA) was quantified by scanning the leaves. The root was separated from the soil with a sieve and rinsed with water to remove the sand that remained stuck, after which it was dried and weighed. The rootzone respiration was scaled to the dry weight of the root (Figure 6E).

Tests of gas exchange measurements - Plant processing before, during, and after measurements in the b-GES

For the b-GES test, plants of *Vitis vinifera* cv Barbera grafted onto *Vitis riparia* × *Vitis berlandieri* 420A rootstocks were grown for 3 years in 70 L pot. In February, vines were winter-pruned and taken out from their growing pots, soil was removed and 12 plants with similar root volume were selected (Figure 7A).
Selected grapevines were transplanted in February in custom metal drums with 60 l of 3:2 v/v sand-peat mixture and 9 g of grapevine granular fertilizer (12+12+17+2 MgO + 20 SO_3) (Figure 7B) growing till July upon full irrigation. At the beginning of July, plant canopies were green-pruned to a similar leaf area (LA) (≈ 0,5 m^2) (Figure 7C).
On a sunny day of July, their canopies have been closed in balloons and two irrigation treatments were compared in order to have control plants (permanently well irrigated, WW) and water stress plant (WS). Measurements were performed after reaching stable H_2O and CO_2 values at the outlet of both balloon and rootzone cuvettes. Canopy A, E and rootzone R were measured on all 12 plants and, at the end of the measurement, single leaf measurements with portable IRGA have been assessed on 3 full expanded leaves per each plant randomly chosen on the canopy. Whole-canopy A, E and rootzone R were calculated following von Caemmerer and Farquhar's equations (von Caemmerer & Farquhar, 1981). Plant gas exchange measurements were performed in a period of high pressure and consequent highly-evapotranspirative atmosphere (Figure 7D).
During the experiment the relative soil humidity (RSH) in WS pots ranged between 30 and 40% and the pre-dawn leaf water potential (Ψ_{PD}) was checked (Rodriguez-Dominguez et al., 2022) every two days to maintain the designed stress level by replenishing water losses accordingly. In WS plants Ψ_{PD} was held around -0.18 ± 0.04 MPa, while the well-watered (WW) condition corresponded to RSH>80% and Ψ_{PD} of -0.05 ± 0.01 MPa.
Grapevine leaf area (LA) has been calculated *in vivo* by linear relationship between leaf square maximum width (diameter) and single-leaf area (Vitali et al., 2013).

Results

Preliminary test of devices

First of all, two tests of the hermetic seal were carried out on the s-GES. The first consisted to close inlet and outlet of s-GES cuvettes with a pneumatic plug and to submerge the system in a water tank 1 meter depth (negative pressure of 100 mbar): no water infiltration has been observed. In the second test, the s-GES was connected to the diaphragm pump and a leak detector spray was used to check any leaks, to increase cuvettes positive pressure during test at the outlet of the cuvettes a needle valve partially close was inserted. No leak has been observed.
The greenhouse effect of the shoot cuvette was tested inside the lettuce growth chamber at 23°C under LED light illumination intensity of 215 PPFD. The air supplied to the cuvette was directly taken from the chamber and shoot air-flow was set to 1.5 l min^{-1} (minimal shoot operational flow). Cuvette temperature after stabilization was +6°C.
Peltier cell worked efficiently at low delta temperature, the s-GES during gas exchange measurement needed continuous ambient air renewal. If the ambient air temperature was similar to the set cuvette temperature (for example during our spring tests) the Peltier cell properly controlled the cuvette temperature but, as the case of summer tests, the difference in temperature was too high and Peltier cell did not compensate sufficiently. We needed to introduce another aluminum plate coil (Figure 4O) that was positioned against the inox wall of the growth chamber (Figure 4P) to reduce temperature difference between external air and cuvette temperature prior to Peltier cell temperature control. This precaution allowed temperature control in the range of 23 □ 1.5°C, being the external temperature about 35°C.
To precisely measure gas exchange a fine measurement of air molar flow, CO_2 and H_2O concentration is essential. We tested the following sources of error: i) oscillation in the molar flow measurements due to diaphragm pump pulsation; ii) oscillation in reference air and sample air H_2O and CO_2 concentration due to atmospheric air CO_2 and H_2O fluctuations and presence of air pockets in the shoot and rootzone cuvettes; iii) CO_2 and H_2O contamination between shoot cand rootzone cuvettes. We used one lettuce plant growth under full spectrum white light to define the shoot and rootzone cuvette air-flow to impose during lettuce measurements. Considering that IRGA has <1 ppm of measurement noise, we chose to impose a flow rate that defines a delta CO_2 between reference and sample in the range of 10-30 ppm for shoot and >5 ppm for root. The first test suggested an air-flow in the shoot cuvette of 5.0 l min^{-1} and the minimal air-flow of 1.5 l min^{-1} in the rootzone cuvette, it was not possible to further reduce the flow in rootzone cuvette because IRGA pump was set to 0.75 l min^{-1} and we were willing to exclude external air contamination at the site of the air probe sampling.

Reducing pump speed to target air-flow increased flow oscillation > 0.3 l min^{-1}, doubling the accuracy of the flow meter (1.5% full scale corresponding to 0.15 l min^{-1}). In addition, we introduced a needle valve just downstream of the pump to dampen air oscillation due to pump membrane vibration, as suggested by Long and Hallgren (1985).
Interface leakages have been checked monitoring sample CO_2 of one cuvette and breathing to the inlet pipe of the other cuvette, no evidence of interface air contamination have been observed in both cuvettes.
Once the centrifugal blower had been turned on, we checked at which blower regime the balloon was completely swollen, this regime was from 20 Hz to 50 Hz. For air-flow measurement we installed the anemometer following device suggestion, it was positioned 10 duct diameters downstream any disturbances and 5 duct diameters upstream of any disturbances. Anemometer depth was defined by calibration with a mass flow meter at variable area (VFC-133-EC, Dwyer, USA) temporally installed downstream of the anemometer. Depth was offset 5 mm from the duct middle. We checked for shoot-root interface leakage submerging with water the T PVC that contained the trunk and we used leak detector spray to check leakage between the sealing between PVC T and tank cap. We imposed a blower frequency of 35 Hz corresponding to an air-flow volume about 39 m^3 h^{-1}. This blower velocity allowed the better compromise between balloon internal temperature and delta CO_2 and H_2O between reference and sample. The grapevine measurements were done in August, with this air-flow we observed a maximum greenhouse effect of +4°C.

Experimental tests - Outputs of measurement routines in the s-GES

To test the the s-GES we performed gas exchange measurements on lettuce in controlled climatic conditions; the predetermined temperature and relative humidity were respectively 23 °C and 60% with a consequent absolute concentration of H_2O in air of 17000 ppm. During the measurements, the external temperature varied from 25 °C at 09.00 a.m. to a peak of 32.5 °C at 04.00 p.m. with a variation in atmospheric humidity respectively from 65% to 41% and with variations in absolute air humidity in the span of the day from 18890 to 21780 ppm. The Peltier air conditioning system operated at maximum current intensity during the hottest hours and at 80% during the first hours of measurement. During the measurements it was necessary to use the dehumidifier with small adjustments throughout the day addressing the flow toward the silica gel cylinder. The temperature during the course of the measurements was maintained at the established temperature with a maximum deviation of 1.5 °C; as regards absolute air humidity, the deviation was a maximum of 700 ppm. 5.0 l min-1 of air were directed to the shoot cuvette and 1.5 l to the rootzone cuvette, no flow adjustment was set among one measurement and the following ones to maintain the same turbulence

conditions inside the cuvette. The steady state condition was reached about 45 minutes after the start of the measurement routine; deltas of CO_2 concentration between reference air and sample air recorded were between 11 and 24 ppm, while air H_2O deltas were between 2000 and 5000 ppm. The absolute CO_2 and H_2O values sequently measured for the reference and the sample (shoot and rootzone) were the average (AV) of 60 s of measurement (Figure 8).
In this period of time, fluctuations in CO_2 and H_2O were observed respectively in the order of ±0.6 ppm and ±40 ppm, falling within the background noise of the instrument. This result highlights how the ventilated 1000 l tank and the probe placed at a height of 4 meters sufficiently dampened the fluctuations in the concentration of CO_2 and H_2O of the atmospheric air and how this homogenization of the air was maintained throughout the air pathway, including the cuvette. As regards the gas exchange of the root, the CO_2 delta observed between the reference and the sample air was in the range of 3.8-8.8 ppm, while the H_2O concentration of the sample was considered to be saturated vapor (Figure 8).
Gas exchange data showed how the difference in A between Red-Blue light and Full Spectrum light observable on single leaf (SL) measurements was also observable on whole plant (WP) measurements, where plants under Red-Blue light showed a significantly higher A. Significant differences in E were not detectable in either SL or WP. As for the coefficients of variation (= standard deviation / average * 100), no consistent differences were observed between the two measurement systems (Table 1).

Experimental tests - Outputs of measurement routines in the b-GES

To test the b-GES, grapevines grown in pots under control irrigation (WW) and water stress (WS) conditions were measured. The test pointed to an instantaneous measure of both photosynthesis rate of the shoot and respiration of the rootzone representative of the environmental growing conditions. The closure of the balloons through the compression zip and the waiting time for the balloon to be perfectly inflated was 3, 4 minutes, while the plateau of both CO_2 and H_2O deltas between reference and sample was reached in about 2 minutes. The frequency of the centrifugal blower was set at 35 Hz which, depending on the plant measured, resulted in a flow in the range of 34.7-39.3 $m^3\ h^{-1}$ with a noise during the measurement in the order of 0.8 $m^3\ h^{-1}$. The small differences in the flow between one tested plant and another were mainly due to the bulk and shape of the trunk inside the T-piece, thus revealing an obstacle to the flow of air that is not entirely negligible.
Measurements followed a repeated 90 s run including a period of air purging (about 30 s) and 60 s thereafter to determine the mean steady state value, for averaging the measurement output (M or REF). The

measurements were conducted following the sequence: 1 reference (REF), 6 replicate samples (M), 1 REF, 6 Ms, 1 REF. Each routine consisted of 1 + 6 + 1 + 6 + 1 = 15 measurements. H_2O and CO_2 were measured simultaneously. As for reference CO_2 there was greater stability than for reference H_2O, but by averaging the 3 references, a stable value was obtained in both shoot (Figure 9A) and rootzone (Figure 9B).

Our flow intensity determined deltas of CO_2 and H_2O respectively in the range of 15-22 ppm and 4300-5400 ppm for WW plants, and 3-7 ppm and 1900-2800 ppm for plants under WS. Given measurement speed, the temperature rise recorded was a maximum of 2 °C. CO_2 and H_2O concentration noise was respectively about 1 ppm and 150 ppm, slightly higher than instrument noise. Differential CO_2 concentration in rootzone cuvette was pretty high, in the range of 30-70 for WS plants and in the range of 70-100 in the WW plants, the time needed to reach the CO_2 plateau at the outlet of rootzone cuvette was pretty long, around 20 min.

Both measurements carried out on a SL and those carried out on a WP showed a clear difference in A and E between WW plants and plants under WS. No significant differences were observed between the two measurement methods; however, in measurements of WW plants A tended to be higher on the WP than in SL. A high CV is also observed for WP measurements under WS conditions. From the data of R it was observed that the water availability of the soil has a strong impact on the gas exchange of the root, as expected (Table 1).

Discussion

Technical advances of s-GES and b-GES systems

The whole plant gas exchange measurement systems presented here have highlighted some technical advances.
Both systems have a semi-simultaneous measurement system of the rootzone in parallel with that of the canopy, from whose outputs it is possible to deduce belowground respiration data hardly present in literature. These data can be fundamental for identification or calibration of predictive models for the assimilation / consumption of carbon in both sources and sinks on either herbaceous or perennial plants.
Through the analysis of construction details and measurement performance, we were able to compare two systems very different from a design point of view, but which respond to the same need, on two different scales. There are points for and against both systems, here detailed and described, in response to the design traits.
Finally, it was possible to discuss the functionality of these systems in more controlled environmental conditions (s-GES), or as natural as possible (b-GES), highlighting the constructive critical points that are most affected by environmental settings.
Proposed technical advances responded to three major challenges arising in the design and setup of gas exchange systems (GESs) for whole plant (WP) measurements: i - cuvette technical configuration, ii - measurements of mass air-flowing, and iii - stable and accurate detection of air CO_2 and H_2Or concentrations. From the analysis of our prototype operational skills and from results of the experimental tests a series of problems and possible outcomes can be deduced.

Problems related to the choice of materials

In the choice of materials, various factors must be taken into account: mechanical properties of the materials, transparency of the shoot cuvette, thermal properties of the material and interaction-permeability of the material with CO_2 and H_2O. As explained above, the artificiality of the environment created in the s-GES system allowed the use of materials during the design that simplified the construction of the cuvette. In literature, plexiglass is the most widely used material for rigid plastic cuvettes (Garcia et al., 1990; Harris and Paul, 1991; Donahue et al., 1997; van Iersel and Bugbee, 2000; Cen et al., 2001, Medhurst et al., 2006; Langensiepen et al., 2012; Ferrari et al., 2016; Birami et al., 2020); this choice is most often due to the very high transparency of the material. However, for a laboratory system we preferred the use of transparent polycarbonate as it does not splinter during processing and is easily glued. On the other hand, modern LED technology allows the

achievement of high light intensities at low cost, and the search for transparency becomes negligible.
The aluminum junction ring, on the other hand, was made of metal and CNC to ensure precise sizing of the O-Ring seats for the hermetic seal of the cuvette. In addition, the entire pipeline system (with the exception of the 1000 l tank) was made of PTFE or aluminum, materials with very low gas permeability and low water absorption (Dixon and Grace, 1982), minimizing possible artifacts during measurements.
The b-GES, on the other hand, had to reproduce light conditions similar to environmental ones inside the balloon. The material used was developed for the cultivation of table grapes; its high transparency and low thermal properties made it the preferred material for our purpose. Furthermore, the material we have chosen can be applied for long periods to vine plants as it is nickel-based additive to give it resistance to plant protection chemicals and is also transparent and resistant to UV rays at the same time. This allows the environmental trigger that determines a response in the secondary metabolism of the plant, and at the same time a prolonged life of the film (2 years in full sun). The balloon system was chosen because it does not require a frame, is light and transportable and allows the creation of customized shapes. Our hexagonal base shape and the slight elasticity of the materials determined an almost spherical shape when the balloon was perfectly inflated; spherical shapes are preferable to edgy shapes to reduce the scattering effect which reduces the ratio between direct light and diffused light and, when the angle of incidence of sunlight is tangential to the surfaces of the balloon, leads to phenomena of total reflection (Corelli-Grappadelli and Magnanini, 1997). However, this problem was negligible for the s-GES since the light source was fixed and perpendicular to the cuvette making the cubic shape more practical.
The greenhouse effect has been minimized in the b-GES thanks to the white color of the PVC pipes and the low-thermal material of the balloon. For quick measurements, such as those carried out by us, the rise was less than 2 °C. If prolonged measurements were to be carried out, as demonstrated by the preliminary tests, on particularly hot and sunny days the rise of 3-4 °C could be decisive in the response of the plant controlling its rates of A, E and R. The flow we set determines a rechange of air inside the balloon every 6 minutes and, in the experiment with vine plants, provides about 10 l of air per m^2 of leaf. In the literature, an entire air exchange every 30 s has been suggested on grapevine plants to reduce the greenhouse effect to about 3 °C (Poni et al., 1999; Perez-Peña and Tarara, 2004) and 3 to 4 l of air per m^{-2} of leaf surface s^{-1} to maintain adequate detection of the differential of gas exchanges (Poni et al., 2014). There are number of studies that have built chambers for grapevines that ranged from field grown vines (Petrie et al., 2003; Perez-Peña and Tarara, 2004; Dragoni et al., 2006; Intrigliolo et al., 2009; Tarara et al., 2011; Prieto et al., 2020), field-like canopies on potted vines (Poni et al., 1997, 1999, 2014; Smith et al., 2019) and then young potted vines, as in our b-

GES. Grapevine A and E we measured in the b-GES are consistent with the literature where values have been reported on a leaf area basis. We recorded A of 13.4 µmol m^{-2} s^{-1} compared to peaks of ~ 8 to 12 µmol m^{-2} s^{-1} measured by Tarara et al. (2011), ~ 6 to 11 µmol m^{-2} s^{-1} measured by Petrie et al. (2003), and about 12 µmol m^{-2} s^{-1}, reported by Smith et al. (2019). In canopies of field grown vines there are often shaded leaves, and with some training systems, canopies can be very dense. We probably measured high rates of A and E due to the spherical shape slightly oversized of the shoot balloon-cuvette and good spatial arrangement of the canopy in the balloon, dealing our prototype with young potted vines.
Undoubtedly, in both our work and previous ones on vines, plastic ballons determined a greenhouse effect; a possible implementation of our b-GES could be the conditioning of the incoming air, already implemented in other WP-GES plants used on other plant species (Barton et al., 2010; Birami et al., 2020). In the s-GES, the air conditioning system presented by us is a valid solution for experiments where the internal temperature of the cuvette differs by a few degrees from the ambient temperature; greater freedom in regulating the internal temperature of the cuvette can be obtained with air conditioning systems consisting in a refrigeration unit and a heat exchanger with refrigerant fluid.

Problems concerning the measurement of the mass flow of air

The mass flow of incoming air is one of the traits that most affects the accuracy of the final measurement; for small systems with air volumes from a few hundred ml min^{-1} to a few tens of l min^{-1}, the use of mass flow meters is ideal. Hot wire technology is one of the cheapest and most widely used. However, attention must be paid to calibration; the type of gaseous mixture, the presence of humidity, temperature and pressure are parameters that can have a significant impact on the accuracy of the estimate. In our case, we asked for a calibration with dry air at 21 ° C at atmospheric pressure. In our range of use, humidity had an influence of up to 1.5% on the final estimate. Since the s-GES is a pneumatic system powered by a diaphragm pump, the pressure in the pipes could exceed several hundreds of millibars. To minimize errors in estimating the measurement, we placed all the elements that cause pressure drops, with the exception of the cuvettes, upstream of the flow detectors so that the pressure inside the detector was as close to the ambient pressure as possible. As for the b-GES, direct mass flow measurements can be very expensive. To overcome this problem, we opted for the use of a hot-wire anemometer which, however, required calibration.
Other types of flow measurements can be performed either with other types of anemometers, for example a plate anemometer (Burkart et al., 2007), or with differential pressure measurements with Pitot tubes (Alterio et al., 2006) or orifice plates (Corelli-Grappadelli and Magnanini, 1993;

Poni et al., 1999). However, calibration is always required, as it is an indirect flow measurement. In other works, calibration was performed by measuring the flow by diluting a known constant gas flow (Corelli-Grappadelli and Magnanini, 1993) or by considering the filling time of a known volume (Goulden and Field, 1994); in our case we decided to use a variable air-flow meter.

Problems arising to obtain stable and accurate detection of air CO_2 and H_2Or concentrations

As regards the measurement of H_2O and CO_2 concentration, the tests have shown that in the s-GES the 1000 l tank adequately ventilated and with the air renewal pipe placed at a height of 4 meters determines an exceptional dampening of the environmental fluctuations of CO_2 and H_2O. Furthermore, the stability of the air-flow due to the presence of restrictions during the path which dampen the flow oscillations due to the pump, the adequate ventilation of the cuvettes and stable environmental conditions (light and temperature) preserved the stability of the air CO_2 and H_2O contents also at the outlet. The large amount of air directed to the balloons in the b-GES system has made it impossible to create an adequately sized tank to dampen the environmental fluctuations of CO_2 and H_2O. This limitation is observed in the background noise observed in the measurement of the reference and sample CO_2 and H_2O; however, if the greenhouse effect is reduced, as in our case, the air-flow can be reduced by determining differential concentrations of CO_2 and H_2O that make this background noise negligible. For both the s-GES and the b-GES the separation system of shoot-root interface was found to be suitable. In the first case, our strategy follows what was done by Donahue et al. (1997), who demonstrated that plant growth can be exploited to hermetically seal a small hole in an insulating plastic film, adopting a rigid plastic material and thus opening the possibility of using materials with different properties. This strategy restricted the measurement time window to a couple of weeks. In our lettuce test, contamination between the two cuvettes was still noted during the first 3 weeks of plant growth in the cuvette. The measurement phase (Figure 6D) lasted about two weeks, following the aforementioned 3 weeks; meanwhile, single leaf measurements were also carried out and the transpiration and photosynthesis performances did not vary in this time window. The fixed size of the hole, however, remains a weak point of the system and one could think of a root shoot interface-hole in a more extensible material to be able to extend the measurements longer. In the b-GES, the use of the metal barrel closure makes assembly quick.
The achievement of a final steady state measurement in an open gas exchange system follows an exponential trend. 95% of the final value is reached after a time of 3τ, where τ is a constant that corresponds to the volume of the system / flow (Weiss et al., 2009). At the time of closure,

the balloon had a very high flow relative to volume and therefore the concentration of CO_2 exiting the balloon during the whole inflation was very similar to the stationary concentration of CO_2. As for the rootzone cuvette, the 3τ we estimated was about 13 min. Moreover, since the pot was not very ventilated until the pump was switched on, the initial CO_2 concentration inside the cuvette was also 10 times higher than the final concentration, for this reason a time of 3τ was not sufficient to give a sufficient accuracy of the measurement, having to go to a turnover of almost 5τ, corresponding to the achievement of 99% of the final value. Since the final CO_2 deltas are very high, a future solution could be to use a higher air delivery in order to reduce τ while remaining in an accurate CO_2 delta range considering the background noise and the accuracy of the IRGA.

Comparison between SL measures and WP measures

In lettuces mesaured in the s-GES, WP assimilation scaled per leaf square meter is about half of that measured in SL, both in conditions maximizing photosynthesis (RB light) and in control conditions (FS light). The whole plant measurements consider the integral of all the leaves of the rosette, both those well exposed to light, and those that remain embedded in lower layers obscured by those in full light. This situation therefore gives the idea that in a lettuce rosette the most internal leaves almost do not photosynthesize anymore and the more exposed ones have a photosynthesis that is equal to that measured in SLs, when the well extended leaf is measured in total incident light. The average of the s-GES therefore renders an estimation of the integral of this gradient (from a putative 0% to 100%), giving us an average value that is approximately half of the maximum (the one detected by the SL measurement).
In b-GES-growing grapevines, on the other hand, light is not a limiting factor. The plants are small in comparison to the volume of our balloon and all leaves receive sunlight, which is the same receiving single leaves with portable IRGAs. The advantage of having the direct integral of the whole plant value remains undoubted, without having to model taking into account canopy architecture and physiological, leaf aging-related, microclimatic and environmental factors, not negligible, on the contrary, to extend punctual SL measurements to models of the whole canopy (Cernusak, 2020).

Conclusions

In light of the measurements described and the results of both preliminary and experimental tests, our prototypes were found to be of useful application for gas exchange measurements with performances comparable to the SL systems available on the market, but with the

undoubted advantage of providing information on whole-canopy. In addition, the semi-simultaneous measurement system of the rootzone, in parallel with that of the canopy, allowed the measurement of belowground respiration data, hardly present in literature. These data can be fundamental for identification or calibration of predictive models for the assimilation / consumption of carbon in both sources and sinks on either herbaceous or perennial plants.

Acknowledgements

The authors thank Klaas De Backer, Samuele Bolassa, Corrado Domanda, Matteo Dellapiana, Mauro Caviglione, Marco D'Oria for technical help during experiments. Financial support: CARBOSTRESS project – CRT - Cassa Risparmio Torino Foundation.

Author Contributions

DLP and CL conceptualized and wrote the original draft. DLP, LEA, GI and ED carried out the experimental part under supervision from DRA. LEA, ED and DRA critically reviewed the draft. All authors read and approved the manuscript.

References

Alterio, G., Giorio, P., Sorrentino, G., 2006. Open-system chamber for measurements of gas exchanges at plant level. Environ. Sci. Technol. 40, 1950–1955.

Barton, C.V.M., Ellsworth, D.S., Medlyn, B.E., Duursma, R.A., Tissue, D.T., Adams, M.A., Eamus, D., Conroy, J.P., McMurtrie, R.E., Parsby, J., Linder, S., 2010. Whole-tree chambers for elevated atmospheric CO_2 experimentation and tree scale flux measurements in south-eastern Australia: the Hawkesbury Forest Experiment. Agric. For. Met. 150, 941–951.

Birami, B., Nägele, T., Gattmann, M., Preisler, Y., Gast, A., Arneth, A., Ruehr, N.K., 2020. Hot drought reduces the effects of elevated CO_2 on tree water-use efficiency and carbon metabolism. New Phytol. 226, 1607–1621.

Burkart, S., Manderscheid, R., Weigel, H.-J., 2007. Design and performance of a portable gas exchange chamber system for CO_2- and H_2O-flux measurements in crop canopies. Env. Exp. Bot. 61, 25–34.

Cen, Y.P., Turpin, D.H., Layzell, D.B., 2001. Whole-plant gas exchange and reductive biosynthesis in white lupin, Plant Physiol. 126, 1555–1565.

Cernusak, L. A., 2020. Gas exchange and water-use efficiency in plant canopies. Plant Biol (Stuttg). 22, 52–67.

Corelli-Grappadelli, L., Magnanini, E., 1993. A whole-tree system for gas-exchange studies. HortSci. 28, 41–45.

Corelli-Grappadelli, L., Magnanini, E., 1997. Whole-tree gas exchanges: can we do it cheaper? Acta Hort. 279–286.

Dixon, M., Grace, J., 1982. Water uptake by some chamber materials. Plant Cell Env. 5, 323–327.

Donahue, R.A., Poulson, M.E., Edwards, G.E., 1997. A method for measuring whole plant photosynthesis in Arabidopsis thaliana. Photos. Res. 52, 263–269.

Drake, J.E., Furze, M.E., Tjoelker, M.G., Carrillo, Y., Barton, C.V.M., Pendall, E. (2019) Climate warming and tree carbon use efficiency in a whole-tree $^{13}CO_2$ tracer study. New Phytol. 222, 1313–1324.

Epron, D., Nouvellon, Y., Roupsard, O., Mouvondy, W., Mabiala, A., Saint-André, L., Joffre, R., Jourdan, C., Bonnefond, J.-M., Berbigier, P., Hamel, O., 2004. Spatial and temporal variations of soil respiration in a Eucalyptus plantation in Congo. For. Ecol. Manag. 202, 149–160.

Ferrari, F.N., Parera, C.A., Passera, C.B., 2016. Whole plant open chamber to measure gas exchange on herbaceous plants. Chil. J. Agric. Res. 76, 93–99.

Garcia, R.L., Norman, J.M., McDermitt, D.K., 1990. Measurements of canopy gas exchange using an open chamber system. Rem. Sens. Reviews. 5, 141–162.

Goulden, M.L., Field, C.B., 1994. Three methods for monitoring the gas exchange of individual tree canopies: ventilated-chamber, sap-flow and Penman-Monteith measurements on evergreen oaks. Funct. Ecol. 8, 125.

Harris, D., Paul, E.A., 1991. Techniques for examining the carbon relationships of plant-microbial symbioses. Academic Press, Inc, United States.

Heinicke, A.J., Childers, N.F., 1937. The daily rate of photosynthesis during the growing season of 1935, of a young apple tree of bearing age. Cornell Univ.Agric. Exp. Sta. 201, 3–52.

Kläring, H.-P., Körner, O., 2020. Design of a Real-Time Gas-Exchange Measurement System for Crop Stands in Environmental Scenarios. Agronomy. 10, 737.

Langensiepen, M. Kupisch, M., van Wijk, M.T., Ewert, F., 2012. Analyzing transient closed chamber effects on canopy gas exchange for optimizing flux calculation timing. Agricultural and Forest Meteorology. 164 (2012) 61–70.

Leonardos, E.D., Grodzinski, B., 2011. 4.14 - Photosynthesis and Productivity of Vascular Plants in Controlled and Field Environments. In: Moo-Young, M. (Ed.), Comprehensive Biotechnology (Second Edition), Academic Press, Burlington, 177–189.

Li, Y., Xin, G., Liu, C., Shi, Q., Yang, F., Wei, M., 2020. Effects of red and blue light on leaf anatomy, CO_2 assimilation and the photosynthetic electron transport capacity of sweet pepper (*Capsicum annuum* L.) seedlings. BMC Plant Biol. 20, 318.

Long, S.P., Farage, P.K., Garcia, R.L., 1996. Measurement of leaf and canopy photosynthetic CO_2 exchange in the field. J. Exp. Bot. 47, 1629–1642.

Long, S.P., Hallgren, J.-E., 1985. Chapter 6 - Measurement of CO_2 assimilation by plants in the field and the laboratory. In: Coombs, J., Hall, D.O., Long, S.P., Scurlock, J.M.O. (Eds.), Techniques in Bioproductivity and Photosynthesis (Second Edition), Pergamon, 62–94.

Matthews, J.S.A., Vialet-Chabrand, S.R.M., Lawson, T., 2017. Diurnal Variation in Gas Exchange: The Balance between Carbon Fixation and Water Loss. Plant Physiol. 174, 614–623.

Medhurst, J. Parsby, J., Linder, S., Wallin, G., Ceschia, E., Slaney, M., 2006. A whole-tree chamber system for examining tree-level physiological responses of field-grown trees to environmental variation and climate change. Plant Cell Environ. 29, 1853–1869.

Miller, D., Howell, G., Flore, J., 1996. A Whole-plant, Open, Gas-exchange System for Measuring Net Photosynthesis of Potted Woody Plants. HortSci. 31, 944–946.
Moutinho-Pereira, J.M., Bacelar, E.A., Gonçalves, B., Ferreira, H.F., Coutinho, J.F., Correia, C.M., 2010. Effects of Open-Top Chambers on physiological and yield attributes of field grown grapevines. Acta Physiol. Plant. 32, 395–403.
Perez-Peña, J., Tarara, J., 2004. A portable whole canopy gas exchange system for several mature field-grown grapevines. Vitis 43, 7–14.
Poni, S., Intrieri, C., Magnanini, E., 1999. Set-up, calibration and testing of a custom-built system for measuring whole-canopy transpiration in grapevine. Acta Hort. 149–160.
Poni, S., Magnanini, E., Rebucci, B., 1997. An Automated Chamber System for Measurements of Whole-vine Gas Exchange. HortSci. 32, 64–67.
Poni, S., Merli, M.C., Magnanini, E., Galbignani, M., Bernizzoni, F., Vercesi, A., Gatti, M., 2014. An improved multichamber gas exchange system for determining whole-canopy water-use efficiency in grapevine. Amer. J. Enol. Vitic. 65, 268–276.
Roux, X.L., Lacointe, A., Escobar-Gutiérrez, A., Dizès, S.L., 2001. Carbon-based models of individual tree growth: A critical appraisal. Ann. For. Sci. 58, 469–506.
Ryan, M.G., Asao, S., 2019. Clues for our missing respiration model. New Phytol. 222 (2019) 1167–1170.
Stoyan, H., De-Polli, H., Böhm, S., Robertson, G.P., Paul, E.A., 2000. Spatial heterogeneity of soil respiration and related properties at the plant scale. Plant Soil. 222, 203–214.
Tarara, J.M., Peña, J.E.P., Keller, M., Schreiner, R.P., Smithyman, R.P., 2011. Net carbon exchange in grapevine canopies responds rapidly to timing and extent of regulated deficit irrigation. Funct. Plant Biol. 38, 386–400.
van Iersel, M.W., Bugbee, B., 2000. A Multiple Chamber, Semicontinuous, Crop Carbon Dioxide Exchange System: Design, Calibration, and Data Interpretation. Jashs. 125, 86–92.
Vitali, M., Tamagnone, M., Iacona, T.L., Lovisolo, C., 2013. Measurement of grapevine canopy leaf area by using an ultrasonic-based method. OENO One. 47, 183–189.
Walsh, K.B., Layzell, D.B., 1986. Carbon and Nitrogen Assimilation and Partitioning in Soybeans Exposed to Low Root Temperatures. Plant Physiol. 80, 249–255.
Weiss, I., Mizrahi, Y., Raveh, E., 2009. Chamber response time: a neglected issue in gas exchange measurements. Photosynt. 47, 121–124.

Table 1. Experimental tests of ecophysiological measurements in the different cuvettes. Assimilation (A), transpiration (E) and whole-root respiration (R) of lettuce plants grown under Full Spectrum (FS) and Red/Blue (RB) light at 23°C air temperature and 60% relative humidity measured either with a commercial IRGA equipped with a single-leaf (SL) cuvette or with our prototype of a whole-plant (WP) gas-exchange system s-GES; A, E and R of grapevine plants under water stress (WS) and well watered (WW) conditions measured either with a commercial IRGA equipped with a SL cuvette or with our WP b-GES. Statistical analysis of data was performed using the one-way analysis of variance (ANOVA) followed by a *post hoc* Tukey's test. Letters denote statistically significant variations ($p < 0.05$). Coefficients of variation (CV = standard deviation / average * 100) are reported for each trait.

	s-GES for lettuce plants					
	A µmol m^{-2} s^{-1}	E mmol m^{-2} s^{-1}	R µmol g^{-1} s^{-1}	CV_A %	CV_E %	CV_R %
SL FS	8,8 ± 0,6 b	1,4 ± 0,2 a	/	6	16	/
WP FS	3,5 ± 0,2 d	0,8 ± 0,2 b	0,07 ± 0,02 a	7	19	28
SL RB	9,9 ± 0,4 a	1,8 ± 0,2 a	/	4	8	/
WP RB	4,3 ± 0,4 c	0,9 ± 0,1 b	0,08 ± 0,02 a	9	14	24
	b-GES for grapevines					
	A µmol m^{-2} s^{-1}	E mmol m^{-2} s^{-1}	R µmol g^{-1} s^{-1}	CV_A %	CV_E %	CV_R %
SL WW	10,7 ± 2,1 a	3 ± 0,8 a	/	20	26	/
WP WW	13,4 ± 2,5 a	2,8 ± 0,8 a	0,81 ± 0,07 a	18	29	8
SL WS	4,4 ± 0,8 b	1,2 ± 0,4 b	/	19	34	/
WP WS	3,4 ± 2,2 b	1 ± 0,6 b	0,52 ± 0,09 b	63	62	17

Figure legend

Figure 1. Design of shoot and rootzone s-GES cuvettes. Key elements of the s-GES: A) polycarbonate shoot cuvette with cubic shape, B) polycarbonate rootzone cuvette enclosed between an aluminum junction ring and an expanded PVC basement, C) aluminum junction ring realize with CNC, D) polycarbonate disk interface with hole in the middle for plant growth, E) push-in fittings for shoot cuvette air inlet and outlet, F) 40x40x10 mm 12V DC fan for shoot cuvette air homogenization, G) nitrile rubber O-ring ID79x3.5 mm for hermetic isolation of shoot cuvette, H) nitrile rubber O-ring ID75x2.5 mm for hermetic isolation of disk interface, J) push-in fitting positioned over the U-shape hole for air inlet of the rootzone cuvette and K) 40x40x10 mm 12V DC fan for rootzone cuvette air homogenization.

Figure 2. Test of transparency of the baloon-polyethylene film (Long Life, Eiffel, Italy). Transparency was tested by comparing A) irradiance measurements performed with a spectroradiometer (MS-720, EKO instruments, Netherlands) inside the balloon with measurements carried out outside. B) The relative transmittance describes the ratio between the two measurements.

Figure 3. Design of shoot and rootzone b-GES cuvettes. Key elements of the b-GES: A) thermo-sealed polyethylene balloon of hexagonal base, B) pressure polyethylene zip, C) spherical-like shape when inflated, D) PVC OD63mm curve for efflux and seat of E) thermocouple and balloon air sample probe, F) PVC T for balloon air inlet connection sealed with foam for root-shoot interface isolation, G) metal drum as rootzone cuvette with 3-$^{3}/_{4}$'' holes with screw cap for water drainage, H) metal drum cap as shoot-root interface with 4-2" holes for air efflux, plant watering and soil sampling, I) 120x120x20 mm 12V DC fan for shoot and rootzone cuvette air homogenization, and J) push-in fittings for rootzone air inlet and rootzone air sampling connection.

Figure 4. s-GES air pathway and climate control. Scheme of the air pathway and the elements of climate control: A) Diaphragm pump, B) potentiometer for diaphragm pump speed control, C) 1000 l tank with D) 4-meter high probe to allow air intake and dampen atmospheric CO_2 and H_2O fluctuation during air renewal, E) needle valve partially close to dampen pump air pulsation, F) silica gel column, G) needle valve for air partitioning in silica gel column, H) Peltier cell with ventilated heatsink and aluminum plate coil; I) needle valve for air partitioning between shoot and rootzone cuvettes, J) hot wire air-flow meters, K) T push-in fitting for reference air sampling, L) T push-in fitting for air efflux and shoot and rootzone air sampling, M) 4-way valve for probe selection, N) IRGA and

O) additional aluminum plate coil for heat exchange between air and inox wall of P) lettuce growth chamber.

Figure 5. b-GES air pathway and climate control. Scheme of the air pathway and the elements of climate control: A) three-phase centrifugal blower, B) inverter for blower frequency control, C) 4-meter PVC pipe for atmosphere air renewal, D) PVC T junctions to split main flow in 4 different lines, E) PVC reduction OD125 mm to OD63 mm to increase air velocity, F) hot wire anemometer, G) PVC-copper flexible suction hose for flexible connection from pipeline to balloon air inlet, H) PVC OD63 mm for balloon efflux, I) diaphragm pump and J) hot wire mass flow meter for rootzone cuvette air-flow supply, K) 4-way valve for probe selection and L) IRGA .

Figure 6. Plant processing before, during, and after measurements in the s-GES. A) 2-week germination; B) transplant inside 0.4 l OD50 mm plastic pots filled with sand; C) 3-week growth under differential light spectrum; D) gas exchange measurement in shoot and rootzone, see Figure 8; E) assessment of leaf area (LA) and dry weight of the root (DW).

Figure 7. Plant processing before, during, and after measurements in the b-GES. A) winter-pruning and selection of plants with similar root volume; B) transplant in February in custom metal drums with 60 l of 3:2 v/v sand-peat mixture and 9 g of grapevine granular fertilizer (12+12+17+2 MgO + 20 SO_3); C) green-pruning in July to set a similar leaf area (LA) (≈ 0,5 m^2); D) plant gas exchange measurements in shoot and rootzone , see Figure 9.

Figure 8. Measurement routines in the s-GES. Absolute CO_2 and H_2O in-air concentrations consequently measured for the reference (REF) and the sample (M shoot and M rootzone) as the average (AV) of 60 s of measurement. H_2O and CO_2 were measured simultaneously.

Figure 9. Measurement routines in the b-GES. Absolute CO_2 and H_2O in-air concentrations recorded following a repeated 90 s run including a period of air purging (about 30 s) and 60 s thereafter to determine the mean steady state value, for averaging (AV) the measurement output (M or REF). The measurements were conducted following the sequence: 1 reference (REF), 6 replicate samples (M), 1 REF, 6 Ms, 1 REF. Each routine consisted of 1 + 6 + 1 + 6 + 1 = 15 measurements. H_2O and CO_2 were measured simultaneously either in the shoot (A) or in the rootzone (B).

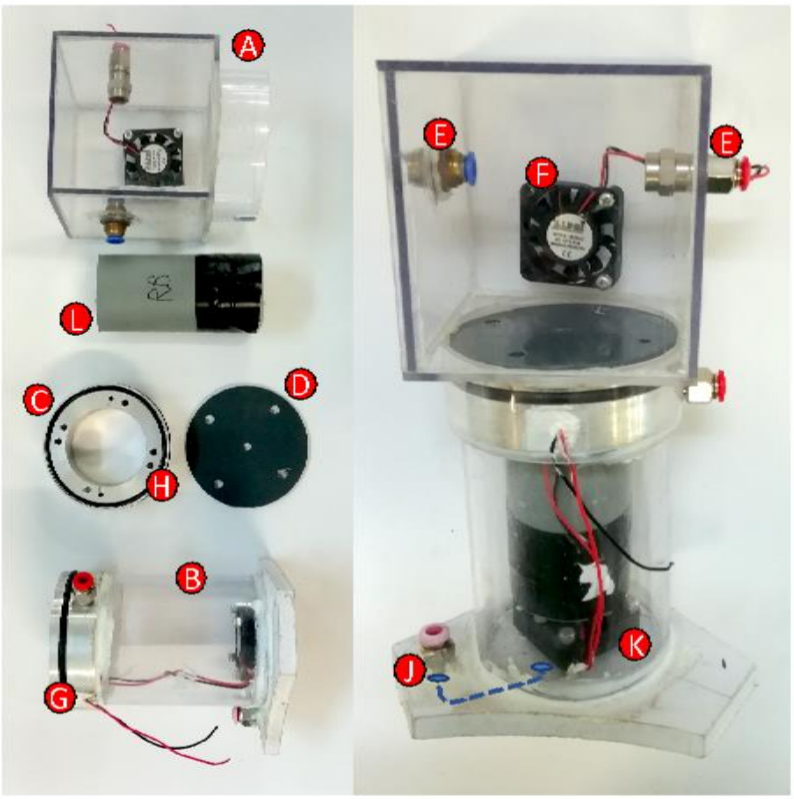

Figure 1. Design of root and shoot s-GES cuvettes.

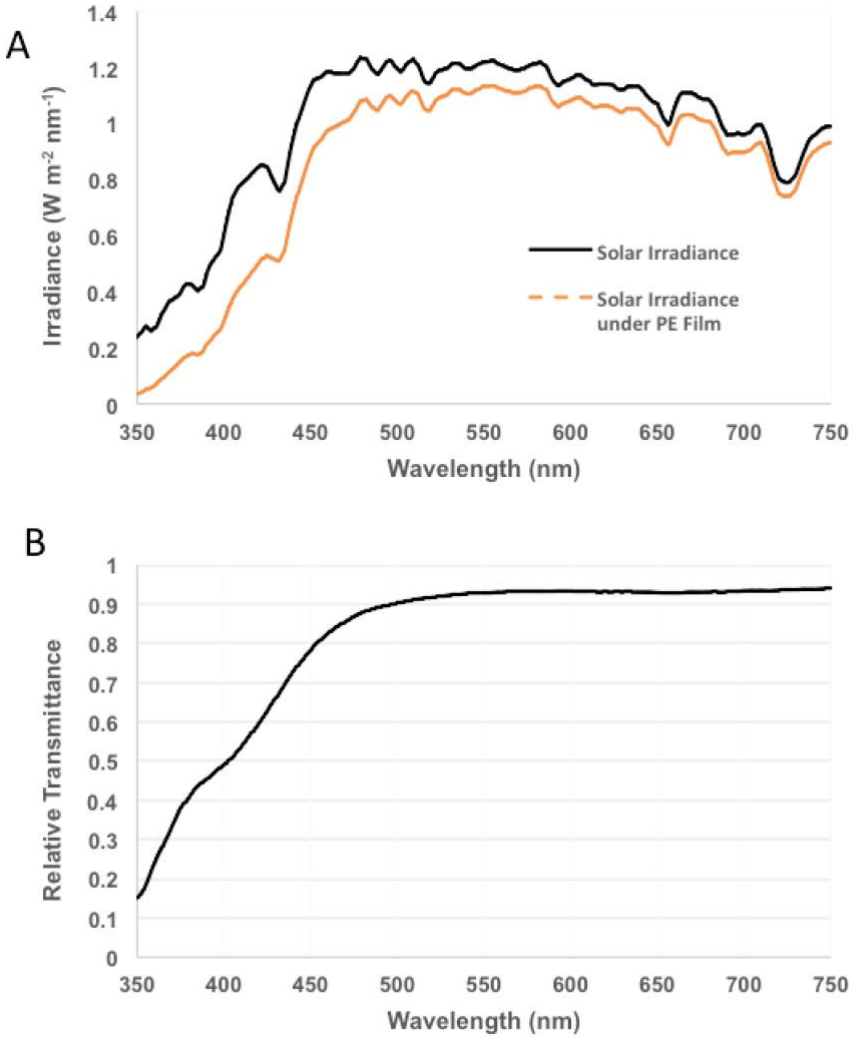

Figure 2. Test of transparency of the baloon-polyethylene film (Long Life, Eiffel, Italy).

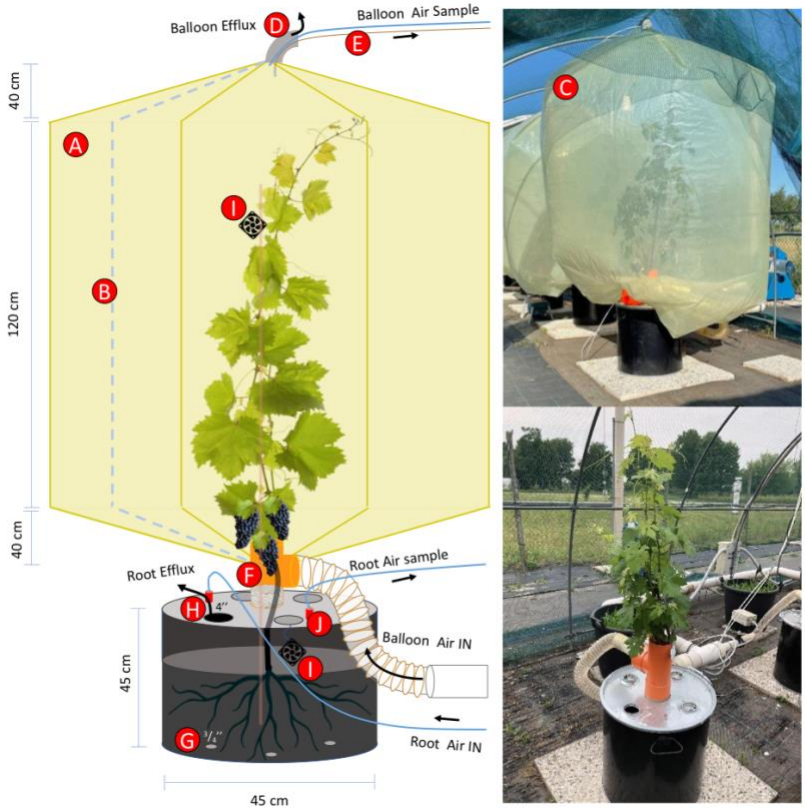

Figure 3. Design of root and shoot b-GES cuvettes.

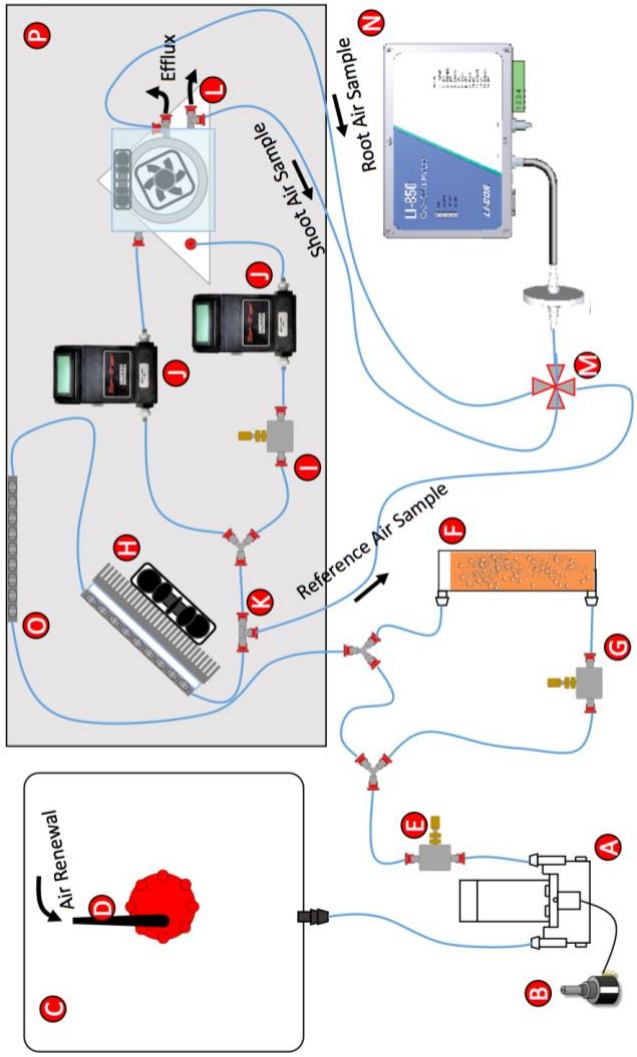

Figure 4. s-GES air pathway and climate control.

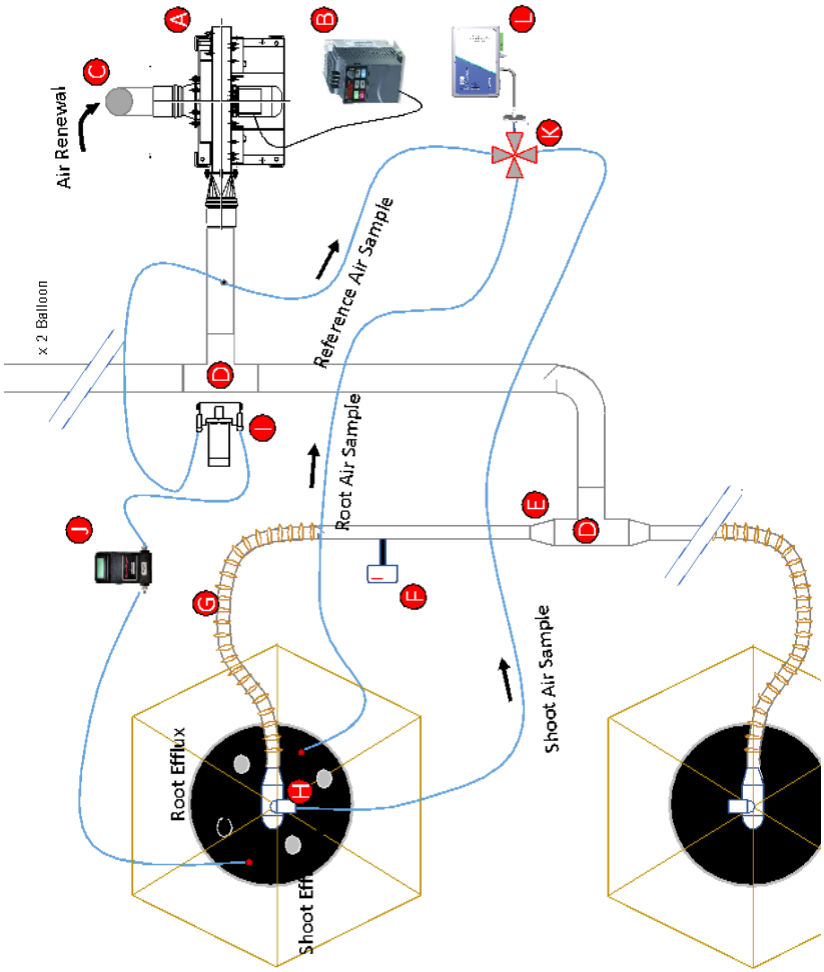

Figure 5. b-GES air pathway and climate control.

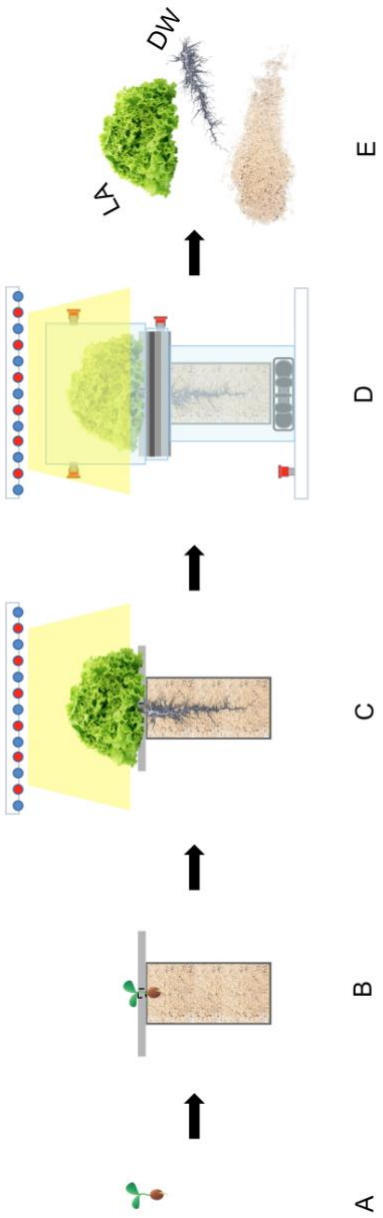

Figure 6. Plant processing before, during, and after measurements in the s-GES.

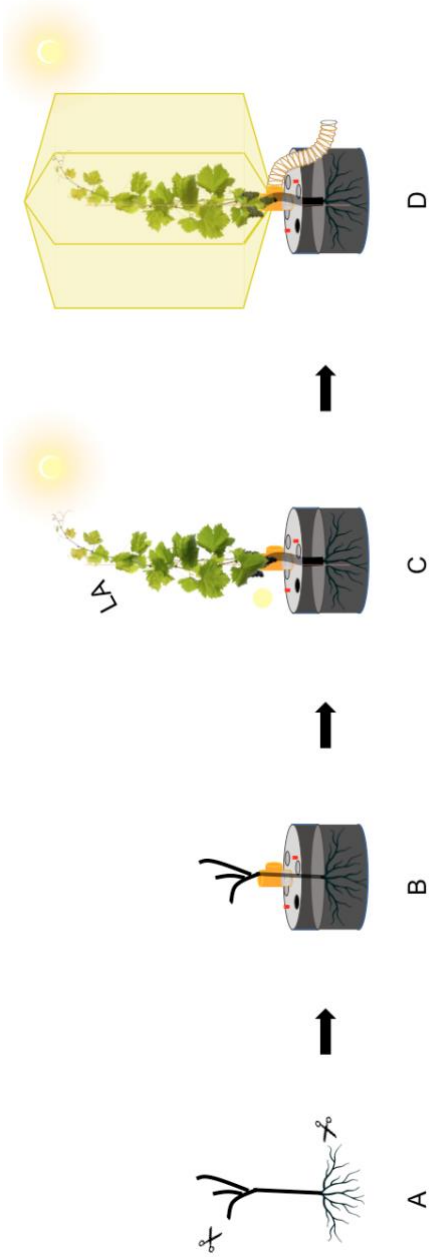

Figure 7. Plant processing before, during, and after measurements in the b-GES.

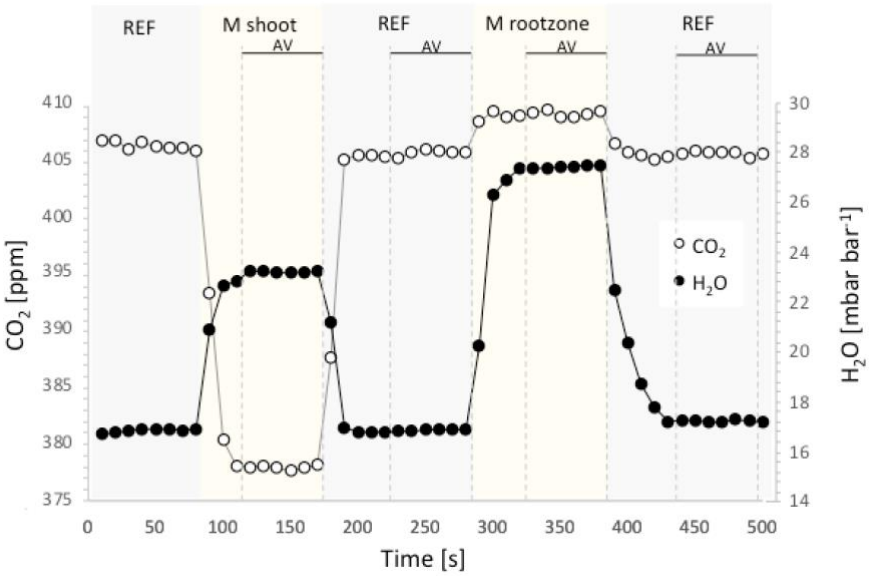

Figure 8. Measurement routines in the s-GES.

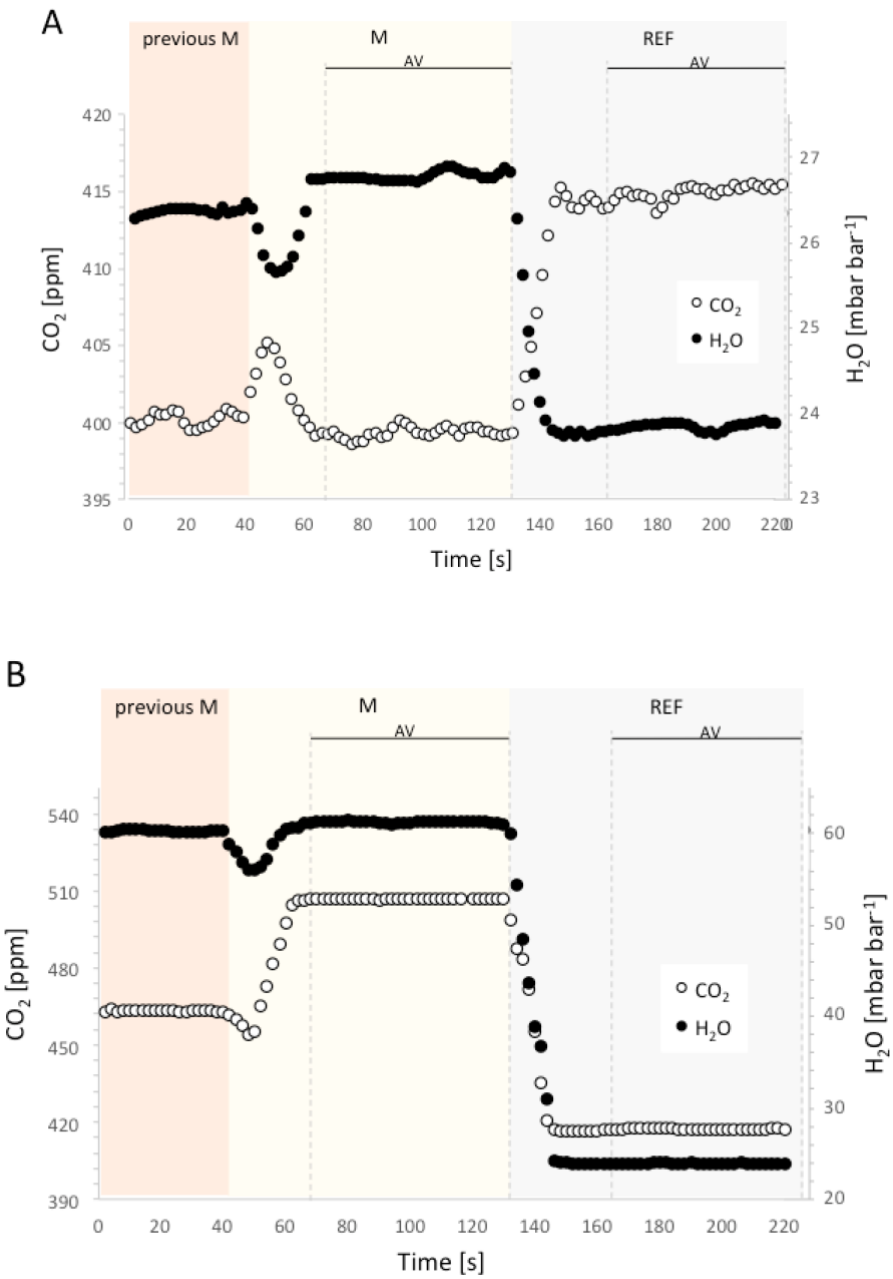

Figure 9. Measurement routines in the b-GES.

3.2. submitted to Plant Growth Regulation (Springer)

Effects of light quality on photosynthesis and growth of *Lactuca sativa* L.

Davide L. Patono[1], Flavio Martini[2], Stefano Cazzaniga[2], Matteo Ballottari[2], Claudio Lovisolo[1*]

[1]Department of Agriculture, Forest and Food Sciences, University of Torino, Largo Braccini 2, 10095 Grugliasco, Italy
[2]Department of Biotechnology, University of Verona, Strada Le Grazie 15, 37134 Verona, Italy
[*]Corresponding author.

Main Conclusion
Plants growing under light spectra optimized for photosynthesis invest less carbon in leaf blade extension and leaf growth than root, showing a reduced photosynthetic active surface, which incorporates less carbon than its photosynthetic potential.

Abstract
Understanding the responses of plants to light quality becomes increasingly important to optimize plant indoor cultivation with artificial light. In this comparative study of lettuce grown with different light spectra, photosynthesis, root and shoot respiration, and growth traits through chlorophyll fluorimetry essays, biochemical and molecular characterization of photosystems, and plant-to-atmosphere gas exchange assessment have been measured. Red and blue (RB) light maximized photosynthetic activity, but this advantage did not lead to greater biomass accumulation, which was greater in plants under red, green and blue (RGB) and further under full spectrum (FS) light. Plants subjected to the RB light regime invest less carbon in leaf blade extension and incorporate less carbon than what has been assimilated. RB leaves have a smaller PSII antenna size and the cyclic electron transport around PSI is higher, implying a lower NADPH / ATP ratio. Exposure to RB light affects plant overall metabolic biosynthetic pathways at the expense of growth, while RGB and especially FS light, by not triggering this acclimation, are more suited to constant low light indoor growing conditions.

Keywords
Chlorophyll fluorimetry; light spectrum; photosystems; photo-protection; carbon assimilation; root and shoot respiration.

Introduction

The limited scope for further expanding traditional farming and its heavy reliance on fertilizers and pesticides is driving advances in controlled farming techniques in greenhouses and indoor plant cultivation. One of the main parameters still to be optimized is the light source whose quality and intensity regulate the growth and development of plants (Yeh and Chung, 2009).

Photosynthetically active radiation (PAR) is the region between 400-700 nm of the solar spectrum whose energy is used by photosynthesis , but not all of this range is absorbed by photosystems with the same efficiency. The main light absorbing pigments are the chlorophylls (Chls) that consist in a porphyrin ring esterified with a long phytol chain; in vascular plants, only Chl a and Chl b are present (Smith and Benitez, 1955). The absorption spectra of the Chls present two main bands: the Qy transition and the Soret band. The Qy transition peaks around 670-680 nm and corresponds to the electron transition from S0 to S1 (first excited state). The Soret band corresponds to transitions to higher Sn state and its maximum is around 430-450 nm (Livingston, 1960). Besides chlorophylls, in plants, carotenoids are present absorbing in the blue-green region with pronounced absorption bands between 450-530 nm, enlarging the range of absorbed wavelengths. Thanks to these pigments, the photosynthetic apparatus mainly absorbs light in the red (630-710 nm) and blue (420-530 nm) regions, while only a small part of green (520-560 nm) and yellow (560-630 nm) light are used (Liu & van Iersel, 2021). The efficiency of light in triggering photosynthesis, measured as O_2 evolved and/or CO_2 fixed per mole of photons, is highest for red photons followed by blue and green photons (McCree, 1971). When light with wavelengths that are weakly absorbed by plants are provided, a potential energy loss can occur; in addition, not-used wavelengths show the additional problem of increasing the temperature of the indoor growing system that needs to be then cooled with additional energy cost. Another important factor is the intensity of the light provided that needs to be strictly controlled. If the light intensity is limiting, plants will not reach the optimal yield. If the light is too high, the flow of energy that reaches the reaction centers saturates the electronic transport capacity, causing an energy imbalance that triggers photoprotective mechanisms (Demmig-Adams & Adams, 1992). The most effective short-term photoprotection mechanisms is non-photochemical quenching (NPQ) which disperses light energy in the form of heat; this excess light, emitted as NPQ, is not used to increase biomass and it is a waste of energy that increase the cost of the process (Horton et al., 1996).

The advent of LED technology had allowed easy and efficient solutions for these aspects (Nakamura et al., 2000). LEDs are gradually gained popularity for use in controlled environment agriculture since (i) they produce little radiant heat which allows them to be placed closer to plants,

(ii) the intensity of light output can be strictly regulated and (iii) they have a long lifetime. The main advantage of the LED technology is that they emit in specific spectral regions and are available with peaks at many different wavelengths, providing higher flexibility than older artificial light technologies. This feature allows to select LEDs with specific spectral ranges that are absorbed by plants increasing the light conversion efficiency and minimizing energy waste that is one of the main bottlenecks of indoor growing systems. Understanding the effect of the different light range on plants would allow to select the wavelength that maximize plant yield and productivity (Chen and Blankenship, 2011; Leone et al., 2021).
The selection of the right wavelength is still matter of discussion. In initial studies, the different wavelengths were generally provided by monochromators or filters resulting in large peaks that comprehended many wavelengths and it was difficult to evaluate the effects of the single light components. The first generation of LED lamps for horticulture was red and blue (RB), since it was believed that the highest rate of net photosynthesis, at the same light intensity, could be obtained exclusively with red and blue light, while green light was considered inefficient and received less attention in photosynthetic research (McCee, 1971). On the contrary, modern LEDs provide narrow peaks that in less than 10 nm go below 10% of light absorbance. With these new technologies the specific effect of the different wavelengths could be studied avoiding superimposition between different wavelengths.
Studies showed the improvement of photosynthesis using green light (Kim et al., 2004; Terashima et al., 2009). The growth effect of green light was attributed to its ability to penetrate deeper into leaves and canopy. Red and blue photons are absorbed within a few layers from the leaf surface, while green ones can penetrate further and activate photosynthesis also on lower layers or leaves inside the canopy. The advantage is twofold: the deep layers of the leaf contribute to the total photosynthetic performance, while the surface layers of the leaf are subjected to an effective lower photon absorption, reducing the risk of energy saturation of photosynthetic apparatus and NPQ activation (Liu and van Iersel, 2021).
The aim of this work was to understand if there is an acclimation of the photosynthetic apparatus to the spectrum of light whose consequences have an impact on plant biomass accumulation. To this aim, we compared the biomass production of lettuce plants grown under RB LED light and red, green and blue (RGB) light with the one achievable under full spectrum (FS) LED light condition. An in-depth analysis of the acclimations of the photosynthetic apparatus to these three conditions was conducted, and thanks to a whole-organ (shoot and root) gas exchange analysis technique (Patono et al. 2022a, 2022b), we calculated a daily plant relative growth rate (RGR) for each light condition. In this way, it was possible to achieve an index of the carbon balance in the three different light conditions, suggesting differences in growth strategy and in plant acclimations to different light regimes.

Materials and Methods

Plant material and growth condition

Seeds of *Lactuca sativa cv*. Rebelina (Gautier, Eyragues, France) were sown in seedling trays filled with peat and left for 2 weeks to germinate in a plant incubator maintaining an air temperature of 23°C, a RH of 60%, and a photoperiod of 16:8 h of day : night. Plants were illuminated with white LED light of 215 μmol m^2 s^{-1} PPFD according to Pennisi et al. (2019). Seedlings were transplanted in sand inside 0.4 l plastic pots and transferred in groups of 10 potted plants on three light-shielded compartments in a growth chamber.

To study putative acclimations of lettuce photosynthetic apparatus to the spectrum of light and their consequences on indoor plant biomass accumulation we exposed plants to three different LED lighting conditions: two LED arrays showing narrow bands in RB and RGB regions and a FS LED array mimicking the sunlight. In the LED panel with only red and blue (RB) light, the ratio between R and B was of 3:1 according to previous works that established this as the ratio with the highest productivity in lettuce (Pennisi et al., 2019). To evaluate the role of green light we used another LED panel with the same ratio between red and blue lights, but with additional green LEDs (RGB). The intensity of the green light was set to give the same light intensity of the blue light, as it is meanly in solar light. These two setups were compared with a full spectrum (FS) LED that had a continuous emission in all the PAR regions (Figure 1).

In order to expose plants at the three different light spectra conditions, each compartment was illuminated by dimmable LED lamps (Prisma, Italy) with RB, RGB or FS LED arrays and fully shielded by the light present in the other compartments. With the aid of a spectroradiometer (MS-720, EKO instruments, Netherlands), light intensity was maintained at 215 μmol m^2 s^{-1} PPFD over the plant canopy throughout the experiment. Plants were treated for 14 days with RB, RBG and FS light, maintaining throughout the experiment the same temperature, humidity and photoperiod of the first two weeks of growth post-germination. Plants were irrigated daily with full strength Hoagland's solution. Biomass production quantification, physiological and biochemical analysis were performed after 14 days of differential light spectrum exposure.

The experiment was carried out 4 times to perform all the analyses considered and to confirm the repeatability of the data obtained: the first experiment was conducted to optimize the setup of environmental conditions and to have preliminary estimation of biomass accumulation and gas exchange, the second to harvest plants for biochemical and molecular characterizations (n = 10), the third for the quantification of biomass and for gas exchange measurements (n = 5) and for fluorimetric

measurements (n = 4), and the fourth to repeat the quantification of biomass and gas exchange measurements (n = 10).

Quantification of biomass and gas exchange measurements

Gas exchange analysis was performed on either whole-shoot or whole-root through a gas exchange system (GES) designed for organs of small herbaceous plants, allowing subsequent measurements of shoot and root gas exchange, described by Patono et al. (2022a).
The GES consisted of 2 cuvettes, one for the root and one for the leaf canopy (shoot), which could be assembled around the plants that had grown in the 0.4 l plastic pots. The measurements were carried out with 3 GESs, one per growth-chamber compartment, subsequently moving the GES from one plant to another. The plant was positioned appropriately during the measurement, so that the upper part of the canopy received 215 µmol m^2 s^{-1} PPFD inside the GES shoot cuvette. The steady state condition for both shoot and root was reached about 45 min after the start of every measurement routine, on the 14^{th} day of differential light treatment on 10 total replicates per treatment.
Net CO_2 assimilation (*A*), shoot respiration (R_{shoot}) and root respiration (R_{root}) were calculated following von Caemmerer and Farquhar's equations (von Caemmerer & Farquhar, 1981), by using outputs of gas exchange measurements performed during the day to obtain *A* and during the night to obtain R_{shoot}. R_{root} was the weighted average of daily (16 hr) and nocturnal (8 hr) outputs recorded in the root cuvette.
At the end of day and night gas exchange measurement routines, for every replicate plant, leaf area of the whole shoot was measured by scanning all the leaves, root and shoot were harvested and dried at 60°C for 72 h, and dry weight was quantified.

Membrane and pigments isolation

Thylakoid membranes were isolated from a pool of 10 lettuce plants as previously described by Casazza et al. (2001). Pigments coming from ten 0.8 cm^2 leaf discs per treatment and the complexes isolated from the thylakoids were extracted with 80% acetone (v/v) and then quantified with Jasco V-550 ultraviolet-visible spectrophotometer fitting the spectra of the acetone extracts with the spectra of individual pigments, as described previously (Croce et al., 2000).

Photosynthetic complexes separation and immunoblotting

Purified thylakoids corresponding to 30 µg of Chls were solubilized with 0.6% and 1.2% dodecyl-α-D-maltoside (α-DM) and loaded in each lane of a non- denaturing Deriphat-PAGE as described by Peter et al. (1991). Sucrose fractionation was performed on membranes corresponding to

500 µg of chlorophyll (Chl) after being washed in 5 mM EDTA and solubilized with 0.6% α-DM by ultracentrifugation (19 h at 40000g, 4°C) in a 0.5 M sucrose gradient containing 0.03% α-DM, 10 mM HEPES, pH 7.8 and protease inhibitors. Immunoblot was performed on 0.37, 0.75, 1.5 and 3 µg corresponding Chls of thylakoids electroblotted on nitrocellulose membranes and detected with antibody conjugated to alkaline phosphatase. αPSAA (AS06 172), αCP47 (AS04 038) and αLHCII (AS01 003); all the antibodies were purchased by Agrisera (Sweden). The protein level was quantified by densitometric analysis.

Photosynthetic parameters

The photosystem II (PSII) activity was conducted on dark-acclimated plants with a Dual-PAM 100 fluorometer (Walz, Effeltrich, Germany) using a saturating light pulse of 5000 µmol photons m^2 s^{-1}, 0.6 s, and white actinic light ranging from 200 to 2400 µmol photons m^2 s^{-1}. The maximum PSII yield (F_v/F_m), the yield of the Photosystem II (Y(II)), the non-photochemical quenching (NPQ), the reduction fraction of plastoquinone pool (1-qL) and the relative electron transport rate (ETR) were calculated according to the equations of Van Kooten and Snel (1990). For each light intensity, independent measurements were carried out on four replicate plants acclimatized to the dark. Proton motive force upon exposure to different light intensities was measured by electrochromic shift (ECS) on leaves un-treated and vacuum infiltered with 50 µM dichlorophenyl dimethylurea (DCMU) (Malkin et al., 1981) with MultispeQ V2.0 (PhotosynQ) (Kuhlgert et al., 2016). PSI activity was measured with Dual-PAM 100 fluorometer with a dual wavelength (830/875 nm) unit.

Relative Growth Rate (RGR)

The relative growth rate (RGR) (Poorter, 2002) was calculated on lettuce plants at day 14 of the light treatments using outputs of gas exchange measurements (*A*, R_{shoot} and R_{root}) and biometric plant traits by following the equation proposed by Evans (1972) :

$RGR = SLA * LMF * \frac{PS_A * FCI}{[C]}$.

- SLA, is the Specific Leaf Area (m^2 leaf area * g^{-1} leaf dry weight);
- LMF (Leaf Mass Fraction), is the ratio between biomass of the shoot and the total plant biomass (g shoot dry weight * g^{-1} total dry weight);
- PS_A is the plant Photosynthesis per unit leaf Area (*A*) integrated over the day (mol C fixed * m^{-2} * day^{-1});
- FCI, is the Fraction of daily C which is not respired but Incorporated for growth, i.e. the day integral of (A-R_{shoot}-R_{root}) * A^{-1} (mol C incorporated * mol^{-1} C fixed);

- [C], is the carbon concentration of the plant per biomass unit (mol C * g^{-1} dry weight); in our work was considered 0.032 according to values found in literature (Kawasaki et al., 2015).

Results

We exposed two weeks old lettuce seedlings, which were previously germinated and grown under FS light, for 14 days under the three light treatments in growth chambers under climate-controlled conditions. All the three light treatments were set in order to have the same PPFD of 215 µmol m^{-2} s^{-1}. FS plants accumulated the greatest amount of root and leaf biomass and had the highest leaf area. The plants accumulating the least biomass and showing the lowest leaf area (LA) were those grown under RB light. Plants treated with RGB spectrum were intermediate (Figure 2A).

Contrary to what might be expected from biomass production data, measurements of steady-state gas exchange parameters, showed that plants exposed to FS and RGB light had assimilation (*A*) lower than plants exposed to RB light. Shoot respiration (R_{shoot}) measured during the night was lower in FS-trated plants than in plants growing under RB spectrum. Plants RGB-treated were intermediate. Root respiration (R_{root}) measured during 24 hr did not show significant differences among light treatments (Figure 2B).

The impact of the different light regimes on photosystems organization and photosynthetic parameters was then evaluated. Lettuce plants grown under different light spectra showed an altered Chl pigment distribution. RB and RGB showed a higher Chl a/b ratio compared to FS. The total Chl content was similar in all the samples even if RB and RGB showed a higher, but not significant, value (Table 1).

In order to identify possible effects of the different light spectra on photosynthesis, photosynthetic parameters on mature leaves were analyzed, focusing on Y(II), NPQ, ETR and 1-qL. F_v/F_m was identical among treatments (Table 1). Under low actinic light (200 µE µmol m^{-2} s^{-1}) all the plants grown at different light conditions showed no variations of the major photosynthetic parameters ranging from the efficiency of PSII to the fraction of closed PSII centers. When the PPFD was raised over 400 µmol m^2 s^{-1}, FS plants showed high levels of NPQ and closed PSII centers due to higher oxidation of plastoquinone pool (1-qL), leading to a lower yield of photosystem II and ETR compared to the other treatments. No significative difference was observed in these parameters between RB and RGB plants at all the light intensities tested (Figure 3A-D).

The activity of Photosystem I (PSI) was then analyzed by transient absorption following light dependent absorption changes at 830 nm, reflecting oxidation of P700, the reaction center of PSI. The maximum oxidation of P700 was analyzed in the presence of DCMU and dibromothymoquinone (DBMIB) (Trebst, 2007) to block both the electron flow-from PSII and the cyclic electron transport (CEF), adding an electron donor (ascorbate) and acceptor (methyl viologen) of electrons. No differences were observed on the maximum PSI activity on Chl basis for

any light treatment. To evaluate if the different light treatments induced a variation in the generation of the protonic gradient upon illumination, the total ECS was measured at different light intensities. The values of ECS measured were similar in RGB and FS treated leaves but reduced in RB samples. The same measurements were performed in presence of DCMU, an inhibitor of PSII and consequently of linear electron flow: in presence of DCMU the ECS values represent the cyclic component of the electron flow (CEF) (Trebst, 2007). The ratio between the ECS in the presence of DCMU on the total ECS of RB and RGB plants was higher than FS at low actinic lights suggesting that in FS plants the linear transport of electrons was promoted, at the expense of cyclic electron flow (Figure 4).

Finally, thylakoid membranes were isolated from lettuce plants grown for three weeks under FS, RB and RGB light spectra to analyze major variations on the organization of pigment-binding complexes. Thylakoid membrane composition was then analyzed by native Deriphat-PAGE electrophoresis (Dreyfuss and Thornber, 1994) upon solubilization with 0.6 or 1.2% α-DM). As reported in Figure S1, a similar pigment binding complexes separation was obtained either upon solubilization with 0.6% or 1.2% α-DM: no major differences could be observed for the different Chl-pigment proteins for FS, RB or RGB samples. Thylakoid membrane composition was then investigated by membrane solubilization with 0.6% α-DM and fractionation in sucrose gradient by ultracentrifugation to separate the major Chl-binding proteins (Figure 5A). The distribution of complexes in sucrose gradient was similar for all the samples analyzed, consistently with the results obtained by native Deriphat-PAGE electrophoresis. The First three major G bands in the upper part of the gradients correspond to the PSII-LHCII components being monomeric LHCB, the trimeric LHCII and the PSII core complex referred as B2, B3 and B4, respectively (Dall'Osto et al., 2014). The PSI-LHCI complex (B5) was detected in the lower part of the gradient, whereas no traces of PSII super-complexes were observed (Figure 5A). All the bands were confirmed analyzing the absorption spectra in the visible spectra (Figure S2).

In order to investigate deeper into details the relative distribution of the major components of the photosynthetic apparatus, an immunoblot analysis on thylakoid proteins was carried out. The amount of the main outer antenna of PSII (LHCII) and the PsaA subunit of the PSI core complex were correlated to the amount of CP47, i.e. the inner antenna of PSII in order to estimate respectively the relative LHCII/PSII and PSI/PSII ratio. Plants grown under FS light showed a higher LHCII/PSII ratio compared to both RB and RGB treatments, in line with a lower Chl a/b in FS (being Chl b only bound by antenna complexes), although this difference was significant only with the RGB light spectrum. In general, no differences were observed at the level of PsaA/CP47 (PSII/PSI) ratio (Figure 5B).

The RGR, an index defining how much plant biomass is accumulated daily starting from the already existing biomass, gives the description of growth velocity under the imposed growing conditions. The RGR factorization adopted by Poorter (2002) is detailed enough to offer some indications on the development strategy of the plant, integrating biometric data (SLA and LMF) and canopy carbon assimilation and respiration of both shoot and root (PS_A e FCI).

SLA was lower in RB-treated than in both FS- and RGB-treated shoots. The PS_A detected had mirror values to the SLA. FCI was greater in plants acclimated to FS than in those that grew 14 days under RB and RGB spectra. From the combination of these 4 factors in the growth index equation, the RGR was higher in FS-treated plants than in RB-treated plants. In the RGB-treated plants it was intermediate, and not significantly different from both.

The PS_A and FCI factors must represent the daily integral of the measured phenomenons. Through gas exchange measurements in the GESs repeated under constant conditions during day and night, we were able to have a good estimate of the integral by extending every measured steady state value over the day (*A*), over the night (R_{shoot}), and daily (R_{root}) hours (Table 2).

Discussion

Possible roles that peculiar light components play for different light spectra

In this work, we used a FS LED with a spectrum similar to sunlight, and we evaluated the role of green light using a blue/green ratio similar to one present in the sunlight spectrum. Depending on the light spectrum, the optimal light intensity varies considerably to maximize the light use efficiency for indoor plant growth. On lettuce plants under narrow-band RB light or fluorescent white light conditions, the maximum biomass production is achieved at an intensity between 200 and 300 PPFD, generally considered a low light intensity condition (Kang et al., 2013; Yan et al., 2019; Pennisi et al., 2019, 2020).
Beside red, blue and green, the FS LED used as control presents also a far-red (FR) component that could theoretically affect the plant growth. FR radiation (700-800 nm) is poorly absorbed by leaves and can penetrate in the inner layer of the canopy where the R/FR ratio decreases. This decrease is sensed by phytochromes that can activate shade-avoidance and shade-tolerance responses leading leaves to grow thinner, larger and with higher chlorophyll content and stems to elongate, trying to capture more light (Smith and Whitelam, 1997). In addition, FR can also regulate photosynthesis. The reaction center chlorophylls in PSII and PSI absorb around 680 and 700 nm, respectively. FR light is preferentially absorbed by PSI, while shorter wavelengths by PSII. The two photosystems operate in series to drive electrons from H_2O to NADP+ and the PSII/PSI excitation should be approximately equal to achieve the highest efficiency. The FR light could provide more photons for the PSI and maintain that balance. Thus, the difference between RB and FS LED could be due to a possible effect of FR on leaves development and light phase of photosynthesis (Zhen et al., 2022). This does not seem the case for the light setup used in this work. Plants were all germinated below the same white light with the same FR light to stimulate photo-morphogenesis. During the experiments under differential light spectra, the FR component in the FS used was limited to the 7% of the total light with an intensity of around 13 µmol m^{-2} s^{-1}. Such a small amount of FR has already been demonstrated not to have significant effect on lettuce leaf width and length and on biomass accumulation (Legendre & van Iersel, 2021). Therefore, the presence of a small FR fraction in the FS light could not be considered the main reason for the difference between treatments.
Green light has a photomorphogenic effect that is not yet well understood, also linked to plant responses to shading (Zhang et al., 2011). Green light is less absorbed by the external layers of the upper leaves and can reach the inner layer while the red and blue light in the RB treatment is promptly captured by external layer and the excess of light absorbed is dissipated

and not transferred to the inner part. This effect increases in conditions where the light intensity is high, determining an improvement in photosynthesis, but it is possibly not an important factor for the 215 µmol m^{-2} s^{-1} PPFD used in this work (Terashima et al., 2009; Liu & van Iersel, 2021).

Effects of growing light regimes on biomass accumulation

Comparing the biomass production of lettuce plants grown indoors at 215 µmol m^2 s^{-1} with RB and RGB LED light with that obtainable with FS LED light (condition with a spectrum similar to the sunlight) we show that plants accumulate more biomass in FS conditions than in RB conditions, while plants growing with RGB light are in an intermediate position.
In our experiments, we note that the high growth performance (biomass accumulation in shoot and root) under FS and RGB light is not due to a higher assimilation of carbon on the basis of the leaf surface unit than that found in plants subjected to the RB light regime. Thanks to the measurements on the whole plant, we can be sure that this effect was not due to photosynthetic deficiencies occurring in the event of a putative greater leaf crowding and / or mutual shading interference among the leaves in plants under FS light, as could be argued if we were based only on single leaf measurements, putatively masking this effect. An effect of light competition among leaves in the WP-measurement condition, compared with the optimal measurement in SL, occurred certainly in all treatments, as reflected by the absolute values of A_{WP} measured and scaled per leaf area unit, which were about double those of A_{SL}. However, the reciprocal relationships between different spectral treatments were the same in both assimilation measurements on SL and WP.
Also for the root, measurement artifacts caused by impediments to growth exerted by the pot cannot be imputed, as biomass accumulation and gas exchange measurements were made after two weeks of differential light treatment following two weeks post-germination, an insufficient time to cause impediments to root growth exerted by the pot. According to Poorter et al. (2012), an interference of the pot on root development would already occur when the ratio between total plant biomass and the volume of rooting space (BVR) was higher than 2 g of dry weight l^{-1} pot volume; in our plants, the maximum BVR was 1.95, reached in plants subjected to FS light.

Effects of growing light regimes on photosynthetic activity

To resolve our biomass-accumulation/carbon-assimilation paradox, an in-depth investigation was carried out on photosynthetic traits, focusing both on energy traits measured by Chl fluorimetry and on the molecular characterization of leaf photosystems. From a theoretical point of view, with low and sub-saturating light intensity, the main limiting factor for

carbon fixation should be the light energy to synthetize ATP and NADPH (Matuszyńska et al., 2019).
Leaves respond in different ways to illumination with the same light intensity of full spectrum radiation or of specific wavelength selected for the highest photosynthetic yield. The leaves under FS seemed more capable of directing excitation energy towards photosynthetic electron transport chain. This is related to the relative higher Chl b and increased LHCII/PSII content found in this condition with respect to RB and RGB. The antenna size of the PSII can change depending on the light condition; it is increased under low or limiting light condition in order to capture all the available light and it is decreased when the light intensity increase in order to avoid excessive light energy absorption and saturation of the electron transport chain (Ballottari et al., 2007). The NPQ of FS plants is activated at lower light intensities compared with leaves under RB or RGB. Both higher antenna size and lower threshold of NPQ activation indicate that FS light, with a photon distribution also in the low-absorbance regions of the PAR, activate in the leaves a response more similar to the low light condition than RB and RGB lights. Thus, FS-treated plants were possibly better able to capture light energy and use it in the electron transport chain toward NADPH production. Furthermore, FS leaves showed a higher level of oxidized PSII (1-qL) and a reduced CEF compared to the other two light treatments, implying an increased NADPH / ATP photosynthetic production ratio compared to RB and RGB light conditions.
Here we report that RB and RGB plants have a higher Y(II) and do not activate NPQ except at very high light intensities (2400 μmol m^2 s^{-1} PPFD), managing to keep the ETR higher since they have lower 1-qL (a proxy measurement of the presence of closed photosystems) and therefore more oxidized PSII capable of supporting a greater flow of electrons. The molecular analysis showed in parallel how this was due to an effect of the spectrum on the light harvesting apparatus. Plants exposed to RB light, as well as RGB, had a higher Chl a / b ratio. Taken together with the immunoblot data, the Chl a/b results suggest that there is an acclimation aimed at decreasing the relative abundance of antenna proteins compared to the reaction center complexes. This acclimation in RB and RGB plants is therefore functional and permits a higher energy flow through the photochemical pathway (Ballottari et al., 2007).
As noted previously, FS plants have an acclimation that points in the opposite direction, that is to implement the antenna proteins and consequently the ability to intercept photons while reducing the maximum operational capacity of the photochemical pathway.
Plants under RB light certainly have an assimilative advantage over plants under FS light, linked to the performance of the light phase of photosynthesis. In RB plants growing in indoor conditions of low light intensity this advantage did not lead to a greater accumulation of biomass, while the reduction of the NADPH / ATP ratio could have affected overall

metabolic biosynthetic pathways for plant acclimtion to the light regime at the expense of growth.

Effects of growing light regimes on carbon balance in whole plants

Since the energetic and molecular results related to the light phase of photosynthesis did not fully explain our dilemma, we shifted the focus to the carbon economy of the WP.
Via gas exchange analysis of the WP through customized growth/measurement chambers, we calculated the RGR of the plant for each light condition. It was possible to obtain an explanatory index of the carbon balance allocation factors between root and shoot in the 3 different light conditions to define growth strategy and probable photo-morphogenic acclimations.
The RGR calculation algorithm couples the output of WP gas exchange measurements with plant growth traits. Daily RGR was significantly higher in plants grown under FS LED lamps than in those grown under RGB light, which was in turn higher than RGR for the RB treatment. Based on the measurements and calculations of the RGR, we showed that the plants subjected to the RB light regime (i) invest less carbon in the distension of the leaf blade, i.e. the leaf thickens instead of spreading out, as evidenced by looking at the SLA values; (ii) have the highest daily integral of photosynthesis per leaf area unit (PS_A), but, as the specific leaf area is low (iii) incorporate little carbon in relation to what has been assimilated.
In conclusion, the fact that SLA is lower in plants subjected to RB illumination, indicates how the RB spectrum at low light intensity determines a growth acclimation, which is normally induced upon acclimation to high light conditions (Poorter, 2002). An imbalance of energy metabolism in favor of respiration is well evidenced by the FCI index, which is lower in RB plants. The greater energy demand in the leaf of RB plants is also highlighted by a greater recruitment of cyclic photosynthesis as evidenced by the ECS analyzes. This greater energy requirement of the leaf as photosynthesis increases has been studied for long time (Ludwig et al., 1975) and is linked to all the energy needs that occur due to a high rate of photosynthesis, increasing in turn plant respiration requirement (Thornley, 2011). FS (and RGB) plants, on the other hand, do not trigger this photoprotective acclimation and their growth advantage lies in adopting a growth strategy that conforms to growing indoor light conditions (Robson et al., 2022).

References

van Amerongen H, Croce R (2013) Light harvesting in photosystem II. *Photosynth. Res*. 116, 251–263. https://doi.org/10.1007/s11120-013-9824-3

Ballottari M, Dall'Osto L, Morosinotto T, Bassi R (2007) Contrasting behavior of higher plant photosystem I and II antenna systems during acclimation. *J. Biol. Chem.* 282, 8947–8958. https://doi.org/10.1074/jbc.M606417200

von Caemmerer S, Farquhar GD (1981) Some relationships between the biochemistry of photosynthesis and the gas exchange of leaves. *Planta* 153, 376–387. https://doi.org/10.1007/BF00384257

Casazza AP, Tarantino D, Soave C (2001) Preparation and functional characterization of thylakoids from Arabidopsis thaliana. *Photosynth. Res.* 68, 175–180. https://doi.org/10.1023/A:1011818021875

Chen M, Blankenship RE (2011) Expanding the solar spectrum used by photosynthesis. *Trends Plant Sci*. 16, 427-431. https://doi.org/10.1016/j.tplants.2011.03.011

Croce R, Cinque G, Holzwarth AR, Bassi R (2000) The Soret absorption properties of carotenoids and chlorophylls in antenna complexes of higher plants. *Photosynth. Res.* 64, 221–231. https://doi.org/10.1023/A:1006455230379

Dall'Osto L, Cazzaniga, S, Wada M, Bassi R (2014) On the origin of a slowly reversible fluorescence decay component in the Arabidopsis npq4 mutant. *Philos. Trans. R. Soc. B Biol. Sci.* 369, 20130221. https://doi.org/10.1098/rstb.2013.0221

Demmig-Adams B, Adams WW (1992) Photoprotection and other responses of plants to high light stress. *Ann. Rev. Plant Physiol. Plant Mol. Biol.* 43, 599-626. https://doi.org/10.1146/annurev.pp.43.060192.003123

Dreyfuss BW, Thornber JP (1994) Organization of the Light-Harvesting Complex of Photosystem I and Its Assembly during Plastid Development. *Plant Physiol.* 106, 841–848. https://doi.org/10.1104/pp.106.3.841

Evans GC (1972) The Quantitative Analysis of Plant Growth. University of California Press, Berkeley.

Horton P, Ruban AV, Walters RG (1996) Regulation of light harvesting in green plants. *Annu. Rev. Plant Physiol. Plant Mol. Biol.* 47, 655–684. https://doi.org/10.1146/annurev.arplant.47.1.655

Kang JH, KrishnaKumar S, Atulba SLS, Jeong BR, Hwang SJ (2013) Light intensity and photoperiod influence the growth and development of hydroponically grown leaf lettuce in a closed-type plant factory system. *Hortic. Environ. Biotechnol*. 54, 501–509. https://doi.org/10.1007/s13580-013-0109-8

Kawasaki S-I, Tominaga, J, Uehara N, Ueno M, Kawamitsu Y (2015) Effects of long-term exposure to different O_2 concentrations on growth and phytochemical content in red leaf lettuce. *Env. Control Biol*. 53, 7. https://doi.org/10.2525/ecb.53.117

Kim H-H, Goins G, Wheeler R, Sager, J (2004) Stomatal conductance of lettuce grown under or exposed to different light qualities. *Ann. Bot.* 94, 691–697. https://doi.org/10.1093/aob/mch192

van Kooten O, Snel JFH (1990) The use of chlorophyll fluorescence nomenclature in plant stress physiology. *Photosynth. Res*. 25, 147–150. https://doi.org/10.1007/BF00033156

Kuhlgert S, Austic G, Zegarac R, Osei-Bonsu I, Hoh D, Chilvers MI, Roth MG, Bi K, TerAvest D, Weebadde P, Kramer DM (2016) MultispeQ Beta: a tool for large-scale plant phenotyping connected to the open PhotosynQ network. *R. Soc. Open Sci.* 3, 160592. https://doi.org/10.1098/rsos.160592

Legendre R, van Iersel MW (2021) Supplemental far-red light stimulates lettuce growth: disentangling morphological and physiological effects. *Plants* 10, 166. https://doi.org/10.3390/plants10010166

Leone G, De la Cruz Valbuena G, Cicco SR, Vona D, Altamura E, Ragni R, Molotokaite E, Cecchin M, Cazzaniga S, Ballottari M, D'Andrea C, Lanzani G, Farinola GM (2021) Incorporating a molecular antenna in diatom microalgae cells enhances photosynthesis. *Sci. Rep*.11, 5209. https://doi.org/10.1038/s41598-021-84690-z

Liu J, van Iersel MW (2021) Photosynthetic physiology of blue, green, and red light: light intensity effects and underlying mechanisms. *Front. Plant Sci.* 12, 619987. https://doi.org/10.3389/fpls.2021.619987

Livingston R (1960) The photochemistry of chlorophyll. Encyclopedia of Plant Physiology. 5 Part 1. Eds., Ruhland. W., Berlin, Springer, 830-883. https://doi.org/10.1007/978-3-642-94798-8_29

Ludwig LJ, Charles-Edwards DA, Withers, AC (1975) Tomato leaf photosynthesis and respiration in various light and carbon dioxide environments. In: Marcelle, R., eds Environmental and Biological Control of Photosynthesis. 29–36. Springer Netherlands. https://doi.org/10.1007/978-94-010-1957-6_3

Malkin S, Armond PA, Mooney HA, Fork DC (1981) Photosystem II Photosynthetic Unit Sizes from Fluorescence Induction in Leaves: CORRELATION TO PHOTOSYNTHETIC CAPACITY. *Plant Physiol.* 67, 570–579. https://doi.org/10.1104/pp.67.3.570

Matuszyńska A, Saadat NP, Ebenhöh O (2019) Balancing energy supply during photosynthesis – a theoretical perspective. *Physiol. Plant*. 166, 392–402. https://doi.org/10.1111/ppl.12962

Nakamura S, Senoh M, Nagahama, S-I, Iwasa N, Matsushita T, Mukai T (2000) Blue InGaN-based laser diodes with an emission wavelength of 450 nm. *Appl. Phys. Lett.* 76, 22- https://doi.org/10.1063/1.125643

McCree KJ (1971) The action spectrum, absorptance and quantum yield of photosynthesis in crop plants. *Agric. Meteorol.* 9, 191–216. https://doi.org/10.1016/0002-1571(71)90022-7

Patono DL, Eloi Alcatrão L, Dicembrini E, Ivaldi G, Ricauda Aimonino D, Lovisolo C (2022a) Technical advances for measurement of gas exchange at the whole plant level: design solutions and prototype tests to carry out shoot and rootzone analyses in plants of different sizes. *Plant Sci.* 2022, 111505, ISSN 0168-9452. https://doi.org/10.1016/j.plantsci.2022.111505

Patono DL, Said-Pullicino D, Eloi Alcatrão L, Firbus A, Ivaldi G, Chitarra W, Ferrandino A, Ricauda Aimonino D, Celi L, Gambino G, Perrone I, Lovisolo C (2022b) Photosynthetic recovery in drought-rehydrated grapevines is associated with high demand from the sinks, maximizing the fruit-oriented performance. *Plant J.* First published: 09 October 2022. https://doi.org/10.1111/tpj.16000

Pennisi G, Orsini F, Blasioli S, Cellini A, Crepaldi A, Braschi I, Spinelli F, Nicola S, Fernandez JA, Stanghellini C, Gianquinto G, Marcelis LFM (2019) Resource use efficiency of indoor lettuce (*Lactuca sativa* L.) cultivation as affected by red:blue ratio provided by LED lighting. *Sci. Rep*. 9, 1–11. https://doi.org/10.1038/s41598-019-50783-z

Pennisi G, Pistillo A, Orsini F, Cellini A, Spinelli F, Nicola S, Fernandez JA, Crepaldi A, Gianquinto G, Marcelis LFM (2020) Optimal light intensity for sustainable water and energy use in indoor cultivation of lettuce and basil under red and blue LEDs. *Sci. Hortic.* 272, 109508. https://doi.org/10.1016/j.scienta.2020.109508

Peter GF, Takeuchi T, Philip Thornber J (1991) Solubilization and two-dimensional electrophoretic procedures for studying the organization and composition of photosynthetic membrane polypeptides. *Methods* 3, 115–124. https://doi.org/10.1016/S1046-2023(05)80203-8

Poorter H (2002) Plant Growth and Carbon Economy. John Wiley & Sons, Ltd, ed. eLS. Wiley. https://doi.org/10.1038/npg.els.0003200

Poorter H, Niklas KJ, Reich PB, Oleksyn J, Poot P, Mommer L (2012) Biomass allocation to leaves, stems and roots: meta-analyses of interspecific variation and environmental control. *New Phytologist* 193, 30–50. https://doi.org/10.1111/j.1469-8137.2011.03952.x

Robson TM, Pieristè M, Durand M, Kotilainen TK, Aphalo PJ (2022) The benefits of informed management of sunlight in production greenhouses and polytunnels. *Plants, People, Planet*. https://doi.org/10.1002/ppp3.10258

Smith H, Whitelam GV (1997) The shade avoidance syndrome: multiple responses mediated by multiple phytochromes. *Plant Cell Env.* 20, 840-844. https://doi.org/10.1046/j.1365-3040.1997.d01-104.x

Smith JHC, Benitez A (1955) Chlorophylls: Analysis in Plant Materials. In: Paech, K., Tracey, M.V. (eds) Modern Methods of Plant Analysis /

Moderne Methoden der Pflanzenanalyse, vol 4. Springer, Berlin, Heidelberg. https://doi.org/10.1007/978-3-642-64961-5_6

Terashima I, Fujita T, Inoue T, Chow WS, Oguchi R (2009) Green light drives leaf photosynthesis more efficiently than red light in strong white light: revisiting the enigmatic question of why leaves are green. *Plant Cell Physiol*. 50, 684–697. https://doi.org/10.1093/pcp/pcp034

Thornley JHM (2011) Plant growth and respiration re-visited: maintenance respiration defined – it is an emergent property of, not a separate process within, the system – and why the respiration : photosynthesis ratio is conservative. *Ann. Bot.* 108, 1365–1380. https://doi.org/10.1093/aob/mcr238

Trebst A (2007) Inhibitors in the functional dissection of the photosynthetic electron transport system. *Photosynth. Res*. 92, 217–224. https://doi.org/10.1007/s11120-007-9213-x

Yan Z, He D, Niu G, Zhai H (2019) Evaluation of growth and quality of hydroponic lettuce at harvest as affected by the light intensity, photoperiod and light quality at seedling stage. *Sci. Hortic*. 248, 138–144. https://doi.org/10.1016/j.scienta.2019.01.002

Yeh N, Chung, J-P (2009) High-brightness LEDs—Energy efficient lighting sources and their potential in indoor plant cultivation, *Renewable and Sustainable Energy Reviews*. https://doi.org/10.1016/j.rser.2009.01.027

Zhang T, Maruhnich SA, Folta KM (2011) Green light induces shade avoidance symptoms. *Plant Physiol.* 157, 1528–1536. https://doi.org/10.1104/pp.111.180661

Zhen S, van Iersel MW, Bugbee, B (2022) Photosynthesis in sun and shade: the surprising importance of far-red photons. *New Phytologist*, accepted article. . https://doi.org/10.1111/nph.18375

	Chl a μg cm^{-2}	Chl b μg cm^{-2}	Chl tot μg cm^{-2}	Chl a/b	F_v/F_m
FS	3.63 ± 0.66 a	0.85 ± 0.16 a	4.48 ± 0.82 a	4.30 ± 0.19 b	0.847 ± 0.004 a
RB	4.07 ± 1.16 a	0.90 ± 0.27 a	4.97 ± 1.43 a	4.55 ± 0.16 a	0.846 ± 0.005 a
RGB	3.89 ± 1.21 a	0.86 ± 0.27 a	4.74 ± 1.47 a	4.55 ± 0.13 a	0.844 ± 0.006 a

Table 1. Measurement of Chl content and F_v/F_m during fluorimetry assessment. Chl quantification of leaf discs from lettuce plants grown for two weeks at FS, RB and RGB light treatments. F_v/F_m on dark adapted leaves. Values are means ± SD (n = 10 for chlorophyll quantification; n = 4 for F_v/F_m). Statistical analysis of data was performed using the one-way analysis of variance (ANOVA) followed by a *post hoc* Tukey's test. Letters denote statistically significant variations ($p < 0.05$).

	SLA $m^2 \cdot g^{-1}$	LMF $g \cdot g^{-1}$	PS_A mol C fixed m^{-2} day^{-1}	FCI μmol C·μmol C^{-1}	RGR $mg \cdot g^{-1} \cdot day^{-1}$
FS	0.048 ± 0.002 a	0.72 ± 0.01 a	0.20 ± 0.01 b	0.70 ± 0.01 a	154 ± 5 a
RB	0.038 ± 0.003 b	0.74 ± 0.03 a	0.25 ± 0.02 a	0.61 ± 0.03 b	129 ± 8 b
RGB	0.045 ± 0.001 a	0.73 ± 0.02 a	0.21 ± 0.01 b	0.61 ± 0.02 b	136 ± 10 ab

Table 2. Factors measured on root and shoot of lettuce plants grown for 2 weeks at FS, RB and RGB light treatment to assess their Relative Growth Rate: $RGR = SLA * LMF * \frac{PS_A * FCI}{[C]}$**.** Specific Leaf Area (SLA), Leaf Mass Fraction (LMF), plant Photosynthesis per unit leaf Area (*A*) integrated over the day (PS_A) and Fraction of daily C which is not respired but Incorporated for growth (FCI) measured at the end of the gas exchange analysis. Relative Growth Rate (RGR) calculated at day 14. Values are means ± SE (n = 10 plants). Statistical analysis of data was performed using the one-way analysis of variance (ANOVA) followed by a *post hoc* Tukey's test. Letters denote statistically significant variations ($p < 0.05$).

Figure legend

Figure 1. Spectra of the three experimental LED panels. The ratio between R and B was of 3:1 according to previous works that established this as the ratio with the highest productivity in lettuce. Spectra are normalized to the same area of light emission. To evaluate the role of green light we used another LED panel with the same ratio between red and blue lights, but with additional green LEDs (RGB). The intensity of the green light was set to give the same light intensity of the blue light, similar to what measured in the sunlight spectrum. These two setups were compared with a full spectrum (FS) LED that has a continuous emission in all the PAR regions.

Figure 2. Biomass accumulation and ecophysiological traits. (A) shoot and root dry weight (DW) and leaf area (LA); (B) outputs of gas exchange measurements: assimilation (*A*), shoot respiration (R_{shoot}) and root respiration (R_{root}) of lettuce plants grown for 2 weeks at RB, RGB and FS light regimes. Mean values ± SE (n = 10). Statistical analysis of data was performed using the one-way analysis of variance (ANOVA) followed by a *post hoc* Tukey's test. Letters denote statistically significant variations ($p < 0.05$).

Figure 3. Photosynthetic parameters of mature lettuce plants after 2 weeks of FS, RB and RGB light treatment. (A) quantum yield of PSII (Y(II)), (B) non-photochemical quenching (NPQ), (C) relative electron transport rate (ETR) and (D) reduction state of plastoquinone pool (1-qL) of lettuce shoots were measured by pulse-amplitude modulation (PAM) fluorimeter. Values are means ± SE (n = 4). Statistical analysis of data was performed using the one-way analysis of variance (ANOVA) followed by a *post hoc* Tukey's test. Letters denote statistically significant variations ($p < 0.05$).

Figure 4. Biochemical characterization. Activity of Photosystem I (PSI) and Electrochromic shift (ECS) of mature lettuce plants after 2 weeks of FS, RB and RGB light treatment. (A) Maximal P700 oxidation on a Chl basis, ECS measured on Chl bases without (B) or with (C) DCMU. Values are means ± SE (n = 10). Statistical analysis of data was performed using the one-way analysis of variance (ANOVA) followed by a *post hoc* Tukey's test. Letters denote statistically significant variations ($p < 0.05$).

Figure 5. Molecular characterization. Structural analysis of thylakoid membranes of lettuce plants grown for 2 weeks at FS, RB and RGB light treatment: (A) Sucrose gradient fractionation of solubilized thylakoids with 0.6% α-DM and (B) immunoblot of thylakoids proteins. Data of LHCII and PsaA proteins were normalized to CP47 and normalized to the FS treatment.

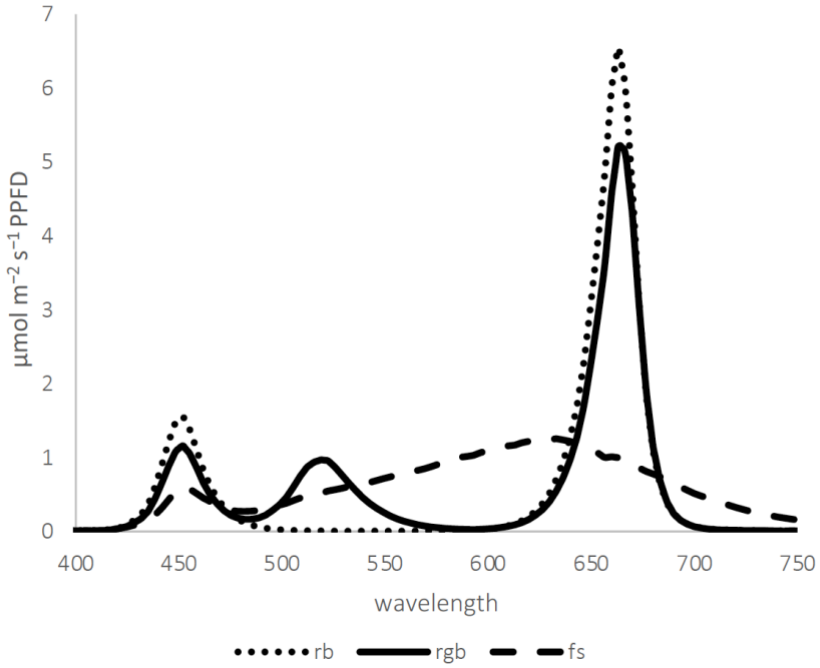

Figure 1. Spectra of the three experimental LED panels.

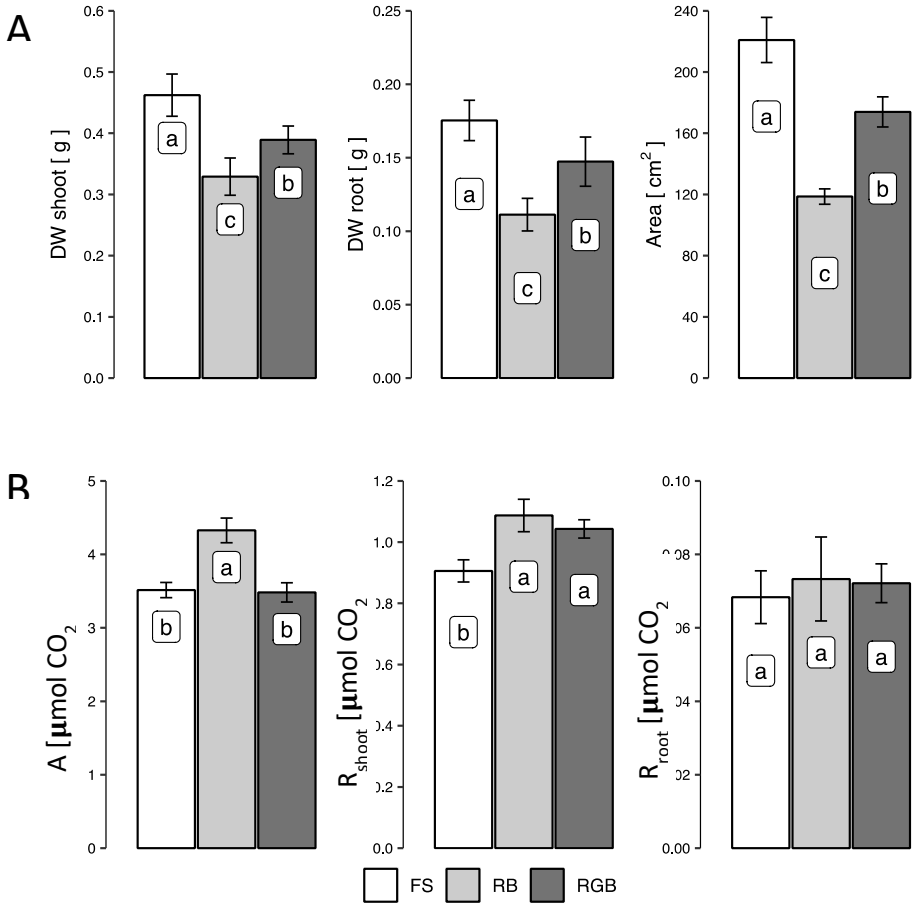

Figure 2. Biomass accumulation and ecophysiological traits.

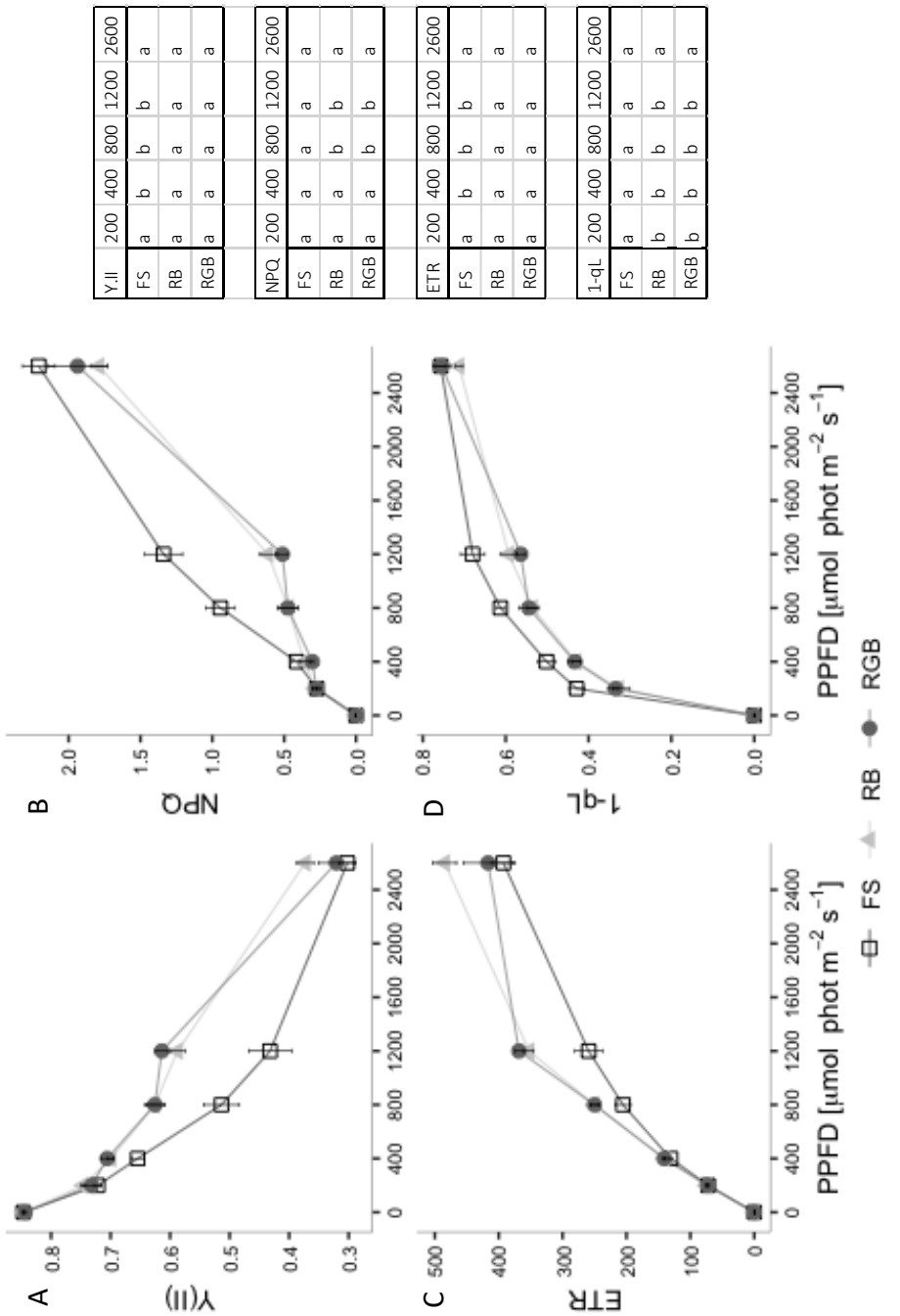

Figure 3. Photosynthetic parameters of mature lettuce plants after 2 weeks of FS, RB and RGB light treatment.

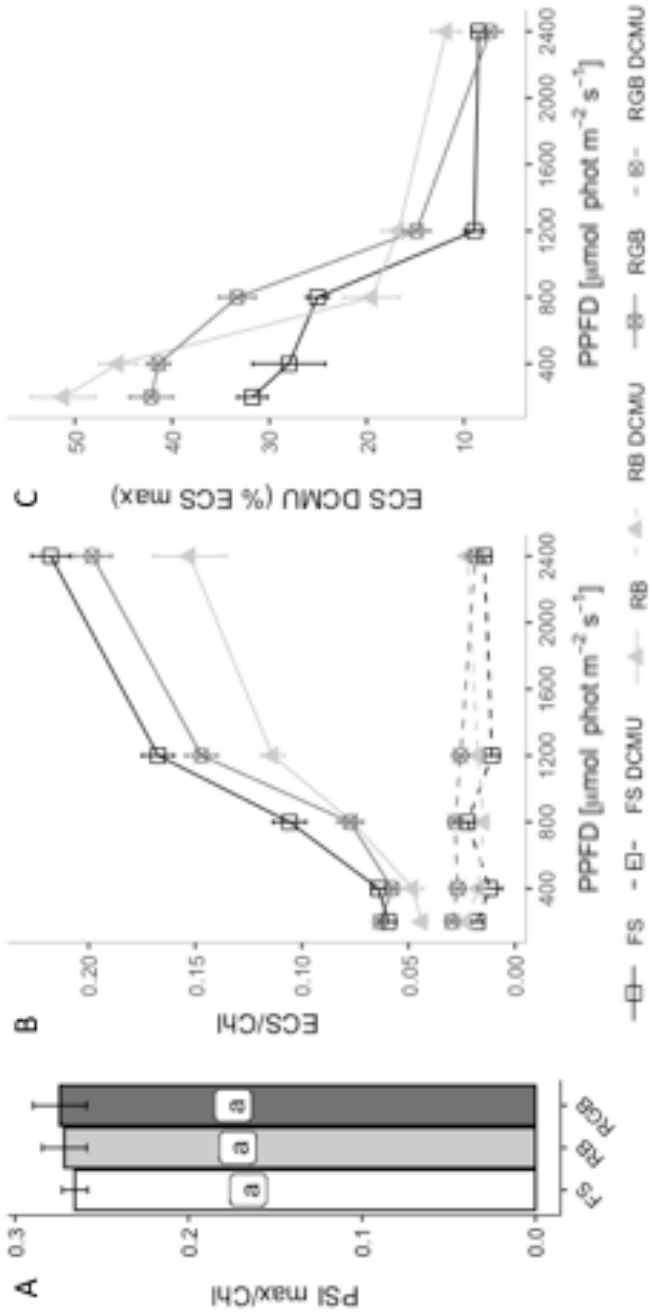

ECS/Chl	200	400	800	1200	2400
FS	a	a	a	a	a
RB	b	b	b	b	b
RGB	a	a	b	a	a
FS DCMU	b	b	a	b	b
RB DCMU	b	b	b	b	a
RGB DCMU	a	a	a	a	a

% ECS max	200	400	800	1200	2400
FS	b	b	b	b	ab
RB	a	a	b	a	a
RGB	a	a	a	ab	b

Figure 4. Biochemical characterization.

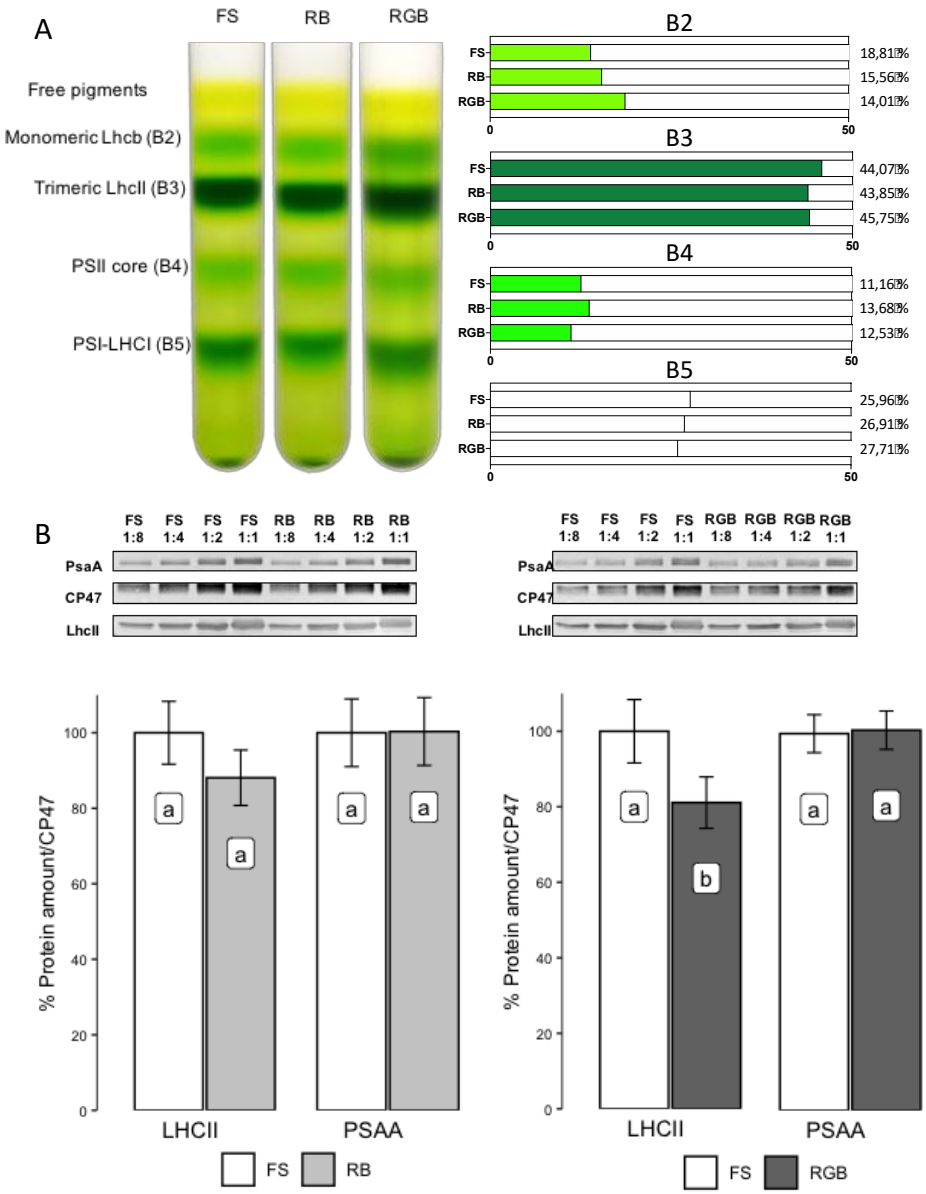

Figure 5. Molecular characterization.

Supplementary materials

Figure S1. Native Deriphat-PAGE of solubilized thylakoid membranes. Native Deriphat-PAGE of solubilized thylakoid membranes of lettuce plants grown for 2 weeks at FS, RB and RGB light treatment.

Figure S2. Absorption spectra of thylakoids bands isolated. Absorption spectra of thylakoids bands isolated from the sucrose gradient solubilized with 0.6% α-DM of lettuce plants grown under FS, RB and RGB spectrum of light.

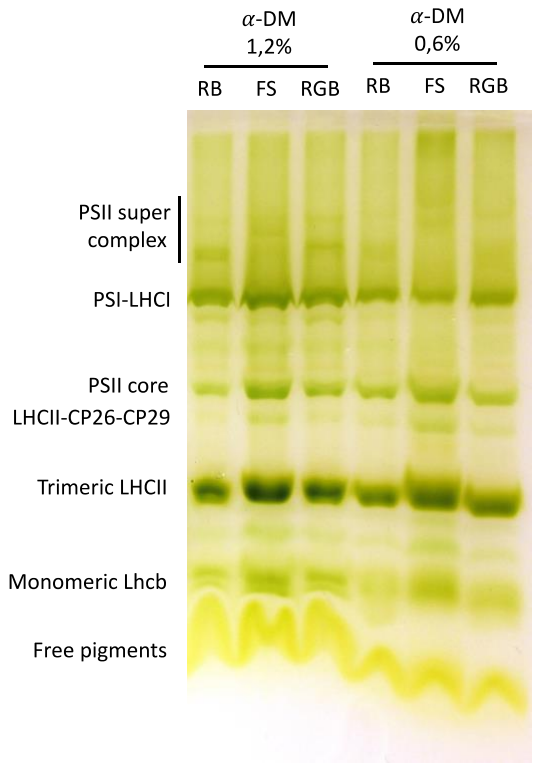

Figure S1. Native Deriphat-PAGE of solubilized thylakoid membranes.

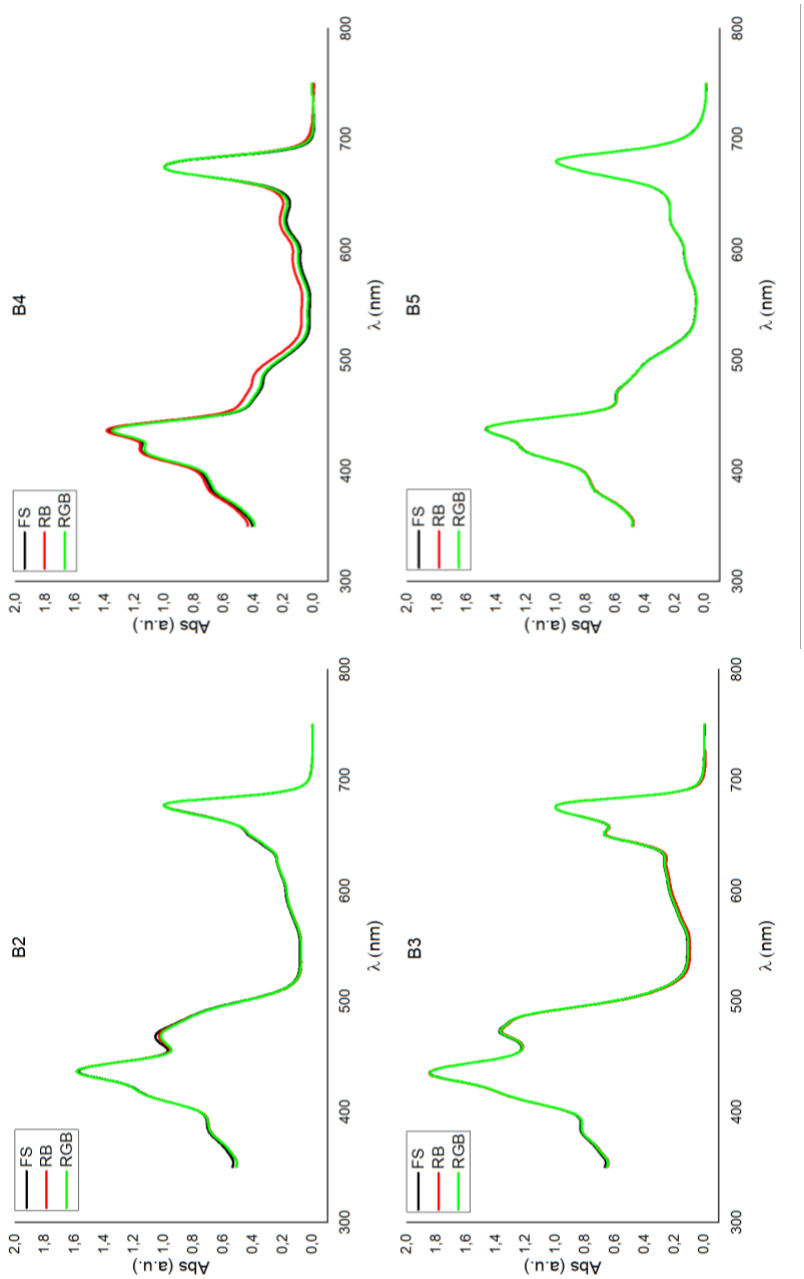

Figure S2. Absorption spectra of thylakoids bands isolated.

3.3. accepted for publication by The Plant Journal (Wiley)
https://doi.org/10.1111/tpj.16000

Photosynthetic recovery in drought-rehydrated grapevines is associated with high demand from the sinks, maximizing the fruit-oriented performance.

Davide L. Patono[1], Daniel Said-Pullicino[1], Leandro Eloi Alcatrão[1], Andrea Firbus[1], Giorgio Ivaldi[1], Walter Chitarra[2,3], Alessandra Ferrandino[1], Davide Ricauda Aimonino[1], Luisella Celi[1], Giorgio Gambino[2], Irene Perrone[2], Claudio Lovisolo[1,2,*]

[1]Dept. Agricultural, Forest and Food Sciences, University of Turin, Grugliasco, Italy
[2]Institute for Sustainable Plant Protection, National Research Council, Turin, Italy
[3]Council for Agricultural Research and Economics-Research Centre for Viticulture and Enology (CREA-VE), Conegliano (TV), Italy
[*]Corresponding Author

Keywords

Water stress; drought; rehydration; ^{13}C pulse-chase technique; photosynthesis, respiration; sugar metabolism; sucrose synthase (*VvSusy*); cell wall invertase (*VvcwINV*); *Vitis vinifera* L.

Abstract

To understand how grapevine sinks compete with each other during the phases of carbon (C) starvation due to water stress and subsequent rehydration, C allocation patterns in drought-rehydrated vines (REC) at the beginning of fruit ripening were compared with control vines maintained under drought (WS) or fully irrigated (WW). In the 30 days following rehydration, the quantity and distribution of newly fixed C between leaves, roots and fruits was evaluated through $^{13}CO_2$ pulse-labelling and stable isotope ratio mass spectrometry.
REC plants diverted the same percentage of fixed C towards the berries as the WS plants, though higher than that of WW plants. Net photosynthesis (measured simultaneously with root respiration in a multi-chamber system for analysis of gas exchange above- and below-ground) was about twice in REC compared to WS treatment, and comparable or even higher than in WW plants. Maximizing C assimilation and delivery in REC plants led to a significantly higher amount of newly fixed C than in both control treatments, already two days after rehydration in root, and

two days later in the berries, in line with the expression of genes responsible for sugar metabolism. In REC plants, the increase in C assimilation was able to support the requests of the sinks during fruit ripening, without affecting the reserves, as was the case in WS.
These mechanisms clarify what is experienced in fruit crops, when occasional rain or irrigation events are more effective in determining sugar delivery toward fruits, rather than constant and satisfactory water availabilities.

Introduction

In temperate climate regions, rainfall is less evenly distributed during the growing season and the occurrence of prolonged periods of drought alternating with periods of abundant rainfall are increasing (Vilonen *et al*., 2022). In fleshy fruit crops, where the productivity and quality of fruits strictly depend on water availability, it is strategic to understand in more detail the dynamics of plant response to alternations between low and high water availability (Ripoll et al., 2014).
The adaptation of grapevines to water deficit and recovery is a complex biological process (Herrera et al., 2022), where the most explored response mechanisms are linked to the hydraulic adaptation of the vine (Perrone et al., 2012), to stomatal regulation (Lavoie-Lamoureux et al., 2017), and to their impact on photosynthesis (Galmés et al., 2007) and water use efficiency (Faralli et al., 2022). Decades of research have focused on water transport in the event of drought stress (Lovisolo et al., 2010; Kuromori et al., 2022), while the transport of carbon (C) in the plant and the related metabolic activities of roots and shoots are less studied (Douthe et al., 2018; Gambetta et al., 2020).
Within plants, C source-sink relationships regulate photosynthate transport from sources towards other organs (sinks such as root tips, fruit and seeds) for further metabolism or storage. Currently there is a change in the paradigm from a source-limited model to a sink-limited model, source activity (photosynthesis) depending on sink activity (tissue growth) (Fatichi et al., 2014; Körner et al., 2015). In the last years, it has been demonstrated that photosynthetic activity in plants experiencing water stress is not only regulated by water transport, but is also controlled by the root C metabolism (Hasibeder et al., 2015). The first response of plants to the onset of water stress is the down-regulation of root respiration that leads to a lower unloading rate of sucrose from the phloem in root. This decrease in the flow rate results in an accumulation of sucrose in the leaf leading to a feedback inhibition of photosynthesis. Similarly, the recovery of root metabolic activity with rehydration is immediate, thus resolving the imbalance between production and use (Hagedorn et al., 2016; Rodrigues et al., 2019).
Plants have different sinks competing with each other for photo-assimilates, organized in a complex network (Knoblauch et al., 2016) that is based on a priority system, according to sink strengths (Ho, 2003), sink phenological phases, and environmental *stimuli* (Wardlaw, 1990). Photosynthetic performance and relative availability of C fluctuate throughout the day, as do phloem loading and source-sink regulation; although it is not yet clear how phloem cells perceive sugar concentration and modulate signalling and expression of transporters (e.g. Sugar Will Eventually be Exported Transporters – SWEET - genes) (Chen et al., 2012; Keller et al., 2021). In conditions of prolonged stress, such as drought, plants activate different adaptation responses that strongly

influence the mobilization and transport of C and, in turn, the source-sink performance (Lemoine et al., 2013).
In contrast to tree species, fruit crops such as grapevines introduce more complexity in the C sink relations: the root sink activity intersects berry growth and ripening that attracts large amounts of C during the growing season, in particular during fruit ripening (in grapevine, after *veraison*), competing strongly with the roots (Pastenes et al., 2014). This derives from an ancestral need to convey nutrients to the seed with a parallel need to make the fruits palatable to the herbivore for seed dissemination that ensures the continuity of the progeny. Furthermore, the selection of the most productive phenotypes has made the fruit sink quantitatively competitive against the root sink (Ryan et al., 2018) to a greater extent than what is observed in forest plants, where roots completely orchestrate the response to stress (Hagedorn et al., 2016).
In this study, we aimed to explore whether the rehydration process could act as regulator of crop performance in an environment with low water availability and a highly-evapotranspirative atmosphere. It could be hypothesized that in crop fruit plants, which show an increasing fruit sink strength from flowering to harvest, the root carries out its sink activity secondary to the fruit. The object of our research is to understand when, how much and how the root and fruit compete with each other, and if during water stress and/or during the subsequent rehydration, the competition can be accentuated. To this end, we have conducted analyses through i) the assessment of C allocation kinetics in the different plant sinks (root-shoot-fruit) competing in drought and post-drought rehydrated vines, ii) the measurement of the ecophysiological performances in root and shoot, and iii) the analysis of transcripts of key genes involved in controlling source-sink interrelationships. Carbon allocation patterns between different sinks can be adequately studied by means of ^{13}C pulse-labelling approaches in which temporal changes in the ^{13}C isotope content of different plant parts after labelling with ^{13}C enriched CO_2 ($^{13}CO_2$) can be used to trace the distribution of neo-photosynthates and follow C partitioning between sinks (Epron et al., 2012).

Materials and methods

Plant material, growth condition and water stress treatment

Plants of *Vitis vinifera cv* Barbera grafted onto *Vitis riparia* × *Vitis berlandieri* 420A rootstocks were grown for 3 years in 70 L pot. In February 2019, vines were taken out from their growing pots, soil was removed and 24 plants with similar root volume were selected. Twelve selected vines were placed in 450 mm internal diameter and 450 mm deep custom metal pots with an air tight lid (for simultaneous measurement of R_{bg} and whole plant gas exchange, Figure S3), while another 12 were transferred to 70 L plastic pots filled with 60 L of a 3:2 v/v sand-peat mixture and 9 g of grapevine granular fertilizer (12+12+17+2 MgO + 20 SO_3). Once the vines started to break dormancy, 4 shoots bearing a cluster were selected in each plant and, at the beginning of July, plant canopies were green-pruned to a similar leaf area (LA) ($\approx$ 0,5 m^2).
During the growth season, 3 irrigation treatments were compared in order to have: 8 control plants (permanently well irrigated, WW), 8 water stress plant (exposed to water stress from the end of July to the end of the experiment, WS) and 8 rehydrated plants (exposed to water stress from the end of July 2019 to the 20th of August 2019 and after well irrigated till to the end of the experiment, REC). For each treatment we randomly selected 4 plants in plastic pots and 4 plants in metal pots. A moderate water deficit level (Lovisolo et al., 2010; Lavoie-Lamoureux et al., 2017; Rienth and Scholasch, 2019) was achieved in about one week at the beginning of August and maintained until rehydration in REC plants and up to DAR 30 in WS plants. Water stress was achieved and maintained by progressively acting on soil moisture levels, checked gravimetrically approximately every two days. The design based on maintaining midday leaf water potential (Ψ_{MD}) levels, measured on detached leaves in the plants growing in metal pots by pressure chamber technique, weekly at the beginning of the imposition of water stress and more frequently as *veraison* approached. On REC plants, Ψ_{MD} restored in one day after re-hydration, as expected (Lovisolo et al., 2008a) (Figure 7).
During the experiment after re-hydration the relative soil humidity (RSH) in WS pots ranged between 30 and 40% and also the pre-dawn leaf water potential (Ψ_{PD}) was checked (Rodriguez-Dominguez *et al*., 2022), and single leaf gas exchange at 10.00 am (Lovisolo *et al*., 2010) was assessed every two days to maintain the designed stress level by replenishing water losses accordingly. In WS plants Ψ_{PD} was held around -0.18 $\pm$ 0.04 MPa, single leaf net CO_2 assimilation (A_{leaf}) around 4.7 $\pm$ 2.2 μmol of CO_2 m^{-2} s^{-1} and single leaf transpiration (E_{leaf}) around 1.2 $\pm$ 0.6 mmol of H_2O m^{-2} s^{-1}, while the well-watered (WW) condition corresponded to RSH>80%, Ψ_{PD} of -0.05 $\pm$ 0.01 MPa, A_{leaf} 10.3 $\pm$ 2.2 μmol of CO_2 m^{-2} s^{-1} and E_{leaf} 3.0 $\pm$ 0.9 mmol of H_2O m^{-2} s^{-1}.

The rehydration was carried out on 20th August at 8.00 am restoring the pot RSH to 80%, similar to that constantly maintained in the control WW plants. In all measurements we performed, 20th August was considered the day after rehydration (DAR) zero (0) and has been designed in order to coincide with 100% berry *veraison*.
As a linear correlation was observed between the square leaf maximum width (diameter) and leaf area (LA) of Barbera grapevine (Figure S4), LA of each plant was estimated *in vivo* by measuring maximum diameter of all leaves according to Vitali *et al*. (2013). LA of plants for gas exchange analysis were calculated before and after the measurement campaign (at DAR -7 and at DAR 8) and LA of plants for carbon labelling were measured at DAR -1, 15 and 30.
At DAR 30, plants in plastic pots were entirely sampled, and leaf, berry and root fresh and dry biomass quantified. Weight of the berry, production of grapes per plant, number of berries per plant, degree Brix (°Brix) of the berries, and their total acidity as tartaric acid were assessed.

Whole plant gas exchange measurements

All the plants in the metal pots were installed in a multi-chamber system for continuous gas exchange analysis between whole-canopy, soil and atmosphere (Figure S3). Aboveground measurement consisted of 3 custom centrifuge fans (PBN, Italy) blowing atmospheric air into 12 polyethylene (Long Life, Eiffel, Italy) balloons through PVC pipelines. Centrifuge fan velocity was controlled with 3 inverters (VFD007EL23A, Delta, Taiwan) and air flow incoming into balloons was continuously monitored with hot-wire anemometers. Temperature inside the balloon was monitored with 12 thermocouples. For soil gas exchange measurements, air flow was supported by 3 diaphragm pumps (D7 series, Charles Austin, UK) pushing air into metal pots through pneumatic pipelines connected to the pot with pneumatic fittings. Air flow was continuously monitored with mass flow sensors (Top Trak 822, Sierra, USA). Air-volume homogenization was guaranteed by 12V fans in both balloons and metal pots. Pneumatic probes were positioned to balloons and metal pots outlets and to centrifuge fans inlet and connect to a CO_2 and H_2O gas analyser (LI-850, LI-COR,USA). A manifold with 25 connections with a system of solenoid valves (320 series, Matrix, Italia) made possible to select the air sampling path.
In detail, there were 12 balloons divided into 3 modules; into each module from one to 2 plants per treatment were randomized. Measurements followed a repeated 120 s routine including 60 s of air purging and 60 s thereafter to determine the mean steady state value. The measurements were conducted following the sequence: 1 reference, 6 samples, 1 reference, 6 samples, 1 reference. Each routine consisted of 1 + 6 + 1 + 6 + 1 = 15 measurements * 120 s = 30 min. H_2O and CO_2 were measured simultaneously. As for reference CO_2 (ranging between 405 and 425 ppm)

there was greater stability than for reference H_2O (ranging between 13 and 19 mbar), but by averaging the 3 references, a stable value was obtained. No gradient was observed when measuring the reference in the 3 modules.
Differential CO_2 concentration, differential H_2O concentration and air flow were measured every 6 hours in the soil compartment.
All the electronic instrumentation was connected to a control system (Field Point, National Instruments, USA) and data collection was monitored with an external PC.
The single leaf respiration was measured in the night on replicate leaves with a portable infrared gas analyzer (GFS-3000, Walz, Germany) to estimate respiration of the whole-canopy during dark hours (R_{cd}). Whole-canopy A, E and R_{cd}, and belowground respiration (R_{bg}) were calculated following von Caemmerer and Farquhar's equations (von Caemmerer & Farquhar, 1981). Plant gas exchange measurements were performed in a period of high pressure and consequent highly-evapotranspirative atmosphere. Air temperature (T), photosynthetic photon flux density (PPFD) and air relative humidity (RH) were monitored and reported in Figure S5a, b, c.

$^{13}CO_2$ pulse-labelling

Three plants for each treatment were labelled with $^{13}CO_2$ at DAR 1 within an air-tight, transparent labelling chamber having an internal volume of 8.4 m^3. Before labelling the soil was sealed to minimize diffusion of the labelled CO_2 into the soil. During labelling the chamber temperature and relative humidity were set to 28°C and 60%, respectively, while natural light was integrated by artificial LED light. CO_2 concentration inside the chamber was monitored constantly with a portable IRGA that showed sensitivity to $^{13}CO_2$ that was previously determined to correspond to 11% of natural abundance CO_2. Labelling started at 8.00 am by repeatedly replacing CO_2 depleted by plant assimilation with 30 at% $^{13}CO_2$ generated through the reaction between 0.6 M $NaH^{13}CO_3$ (30 at%) and 4 M sulfuric acid to maintain the CO_2 concentrations in the chamber between 370-420 ppm throughout the labelling period (Figure S1). Plant labelling ended after 4 h after which tissue samples (leaves, berries and primary and secondary roots separated from a soil core) were immediately collected on all 9 labelled plants. In addition, three additional pots that remained unlabelled were sampled to provide the natural $\delta^{13}C$ background of plant compartments. All plant biomass samples were dried at 70°C, weighed, milled prior to $\delta^{13}C$ analysis. The same sampling procedure was performed at DAR 2, 3, 6, 15 and 30. After the pulse all 9+3 plants were enclosed in air ventilated balloon to reproduce the same condition of plant used for whole plant gas exchange analysis.

Isotope ratio mass spectrometry (IRMS) measurements

The $\delta^{13}C$ values and C contents of plant biomass samples were measured by high-temperature combustion in an elemental analyser (Vario Isotope Select, Elementar Analysensysteme GmbH, Hanau, Germany) coupled to an isotope ratio mass spectrometer (Isoprime 100, Elementar). The $\delta^{13}C$-values (‰) were calibrated relative to the international standard Vienna Pee Dee Belemnite (VPDB) by means of a three-point calibration using standard reference materials IAEA-600, IAEA-603 and IAEA-CH3. Measurement uncertainty was monitored by repeated measurements of internal laboratory standards and standard reference materials. Precision was determined to be ±0.1‰ based on repeated measurements of calibration standards and internal laboratory standards. Accuracy was determined to be ±0.1‰ on the basis of the difference between the observed and known δ values of check standards and their standard deviations. The total analytical uncertainty for $\delta^{13}C$ values was estimated to be ±0.2‰. To estimate $^{13}CO_2$ uptake by leaves and translocation to other organs, δ notations were first expressed in atom%, and subsequently the C content of an organ fraction was multiplied by with the ^{13}C excess (atom%) of this fraction (with respect to the ^{13}C of the unlabelled control), as follows:

$$^{13}C \text{ fixed (mg plant}^{-1}) = \frac{(at\%^{13}C_{labelled} - at\%^{13}C_{unlabelled})}{100} \cdot B \cdot \frac{C\%}{100}$$

Where B is the dry weight (DW) of plant biomass compartments (leaf, root or berry) and C% is the percentage of C in the sample. Changes in the total amounts of ^{13}C assimilated or delivered in the different plant organs with time were expressed as a percentage of the amount of ^{13}C fixed by the leaves at DAR 1 (the labelled ^{13}C), assumed to represent the total ^{13}C assimilated by the plant during labelling.
To model the total amount of C assimilated at DAR 1 that was directed to the different C pools and that persisted during the experimental period, we multiplied the integral amount of C assimilated at DAR 1 to the percentage of C partitioning determined from the $^{13}CO_2$ pulse labelling.

$$C \text{ allocation}_{pool,\,t} \text{ [mmol C]} = \text{Daily } A_{DAR\,1} \text{ [mmol]} * {}^{13}C_{pool,\,t} \text{ [\%]}$$

Where $C \text{ allocation}_{pool,\,t}$ is the total C assimilated at DAR 1 that is allocated and persisted at time t in the considered pool. Daily $A_{DAR\,1}$ is the integral of daily C assimilated at DAR 1. $^{13}C_{pool,\,t}$ is the percentage of the amount of ^{13}C fixed by the leaves at DAR 1, that is present in the C pool at time t. Leaf biomass was calculated using the linear correlation that exist between leaf diameter^2 and leaf DW (Figure S4), plant leaf diameters were measured at DAR 0, 6, 15 and 30. Root biomass was dried and weighted at DAR 30, no evidence of root growth were observed for WS

plants, but only for WW and REC plants (root lighter in colour with white root tips). In any case, the volume of new roots on the total root volume was negligible. For each plant a representative portion of the total root system was exanimated, primary and secondary roots were manually separated and weighted and the relative weight was normalized to the total weight of the root system. Total fruit dry mass was quantified at DAR 30. Average DW of berries sampled at DAR 1, 2 and 3 for each plant were compared to average DW of berries sampled at DAR 30. An 18 % increase of berry DW was observed and it was linearly distributed along the 30 days monitored. No difference in berry DW were observed between treatments.

Molecular analysis

At 4 hours (DAR 0), at 28 hours (DAR 1), and at 4 days from rewatering (DAR 4), at 12.00 am, leaf, berry and root samples collected from WW, WS and REC plants (3 biological replicates for each treatment) were sampled in liquid nitrogen. Plant materials were ground in liquid nitrogen; 40 mg of leaf and 200 mg of root and berry were used for total RNA extraction with Spectrum Plant Total RNA kit (Sigma Aldrich, USA). cDNA was synthesized from 1 μg of the total RNA with High Capacity cDNA Reverse Transcription Kit (Life Technologies, USA). RT-qPCR analyses were performed as described before (Chitarra et al., 2017), using the oligonucleotide sets listed in Table S1. Three technical replicates were run for each biological replicate, and the expression of transcripts was quantified after normalization to two housekeeping genes: ubiquitin (VvUBI) and actin (VvACT). One-way analyses of variance (ANOVA) with treatment as the main factor were performed with the SPSS 23.0 statistical software package (SPSS Inc., Cary, NC, USA). Tukey's HSD-test was applied when ANOVA showed significant differences ($P < 0.05$). The standard error of all means was calculated.

Results

Water treatments and gas exchange analysis

Since the beginning of March, three-year-old plants of grapevine *cv* Barbera with similar root volume were grown in pots and fully-irrigated (WW) to prevent water stress. At the end of July, 2/3 of the plants were exposed to water stress (WS) by drastically reducing the irrigation regime. On August 20th (day after re-hydration zero - DAR 0), one half of these plants were rehydrated (REC) to pre-stress conditions while the other half were maintained under water stress. A whole plant gas exchange analysis in a custom-built multi-chamber system was started one week before re-hydration. WW plants maintained a higher transpiration of the whole canopy (E, Figure 1a), net CO_2 assimilation of the whole canopy (A, Figure 1b), and belowground respiration (R_{bg}, Figure 2) than WS plants. While R_{bg} of REC plants was rapidly restored to the level of WW plants within the first 2 h after rehydration, the levels of E and A of REC plants reached those of WW plants after 8 h. During the subsequent days, R_{bg} and E of REC plants were comparable to those of WW plants. A of REC plants was similar to that of WW plants during DAR 1 and 2 with a trend of up-regulation in the central hours of the day that became statistically significant at DAR 3 and 4. From DAR 5 onwards, no differences in A between REC and WW plants were appreciable.

Carbon allocation patterns to the different sinks following rehydration

From 08.00 am to 12.00 am of DAR 1, nine plants (three for each treatment) were $^{13}CO_2$ pulse-labelled under climate-controlled conditions (Figure S1). Total $^{13}CO_2$ fixed by each plant immediately after labelling (DAR 1) corresponded to 9.2 $\pm$ 3.4 mmol ^{13}C plant^{-1} that was found exclusively in the leaves, without significant differences among treatments. Up to 90% of this pool of newly assimilated C was rapidly lost from the leaves by respiration and reallocation to other plant parts within 2 d from labelling (DAR 3), irrespective of the irrigation regime. WW and WS leaves showed a slight further reduction of the residual ^{13}C at DAR 6 but no further significant loss of C was observable at DAR 15 and DAR 30. REC plants did not lose ^{13}C from leaves between DAR 3 and 6 but showed a decrease thereafter. By DAR 30 all plants showed the same residual amount of ^{13}C in the leaves that amounted to about 5-8% of assimilated C (Figure 3a).
Allocation of ^{13}C to the berries increased with time over the first days after labelling and subsequently reached a stable amount by DAR 6 to 15 (between 16 and 30% of fixed ^{13}C) with no significant subsequent loss of ^{13}C. However, whereas the maximum proportion of ^{13}C was reached within DAR 6 in WW and WS plants, ^{13}C allocation to the berries of REC plants continued to increase until DAR 15. The final proportion of ^{13}C

allocated to the berries was higher in WS and REC plants with respect to WW ones (Figure 3b).
In contrast, ^{13}C allocation to the roots increased to a maximum by DAR 3 in WW, while in WS and REC root C allocation continued to increase slightly between DAR 3 and DAR 6. Subsequently, WW plants quickly lost ^{13}C between DAR 3 and 15 and all the ^{13}C remaining at DAR 15 persisted also at DAR 30. On the other hand, WS and REC plants showed a slower loss of ^{13}C that persisted also between DAR 15 and 30. By the end of the experiment, the residual proportion of fixed ^{13}C in the roots of WW, WS and REC plants (about 10 %) was not significantly different (Figure 3c).
Considering the total amount of fixed ^{13}C in the different pools, there was a strong decrease in fixed ^{13}C in the first 3 days that continued to decrease faster in WW plants with respect to WS and REC plants, resulting in a final proportion of fixed ^{13}C of about 40 % for WS and REC plants and 30 % for WW plants (Figure 3d).
Considering that the different irrigation treatments affected both net photosynthesis as well as the partitioning of newly assimilation C between the different sinks, we estimated the amount of C transferred to the sinks following re-hydration (DAR 0) by coupling daily integrals of A and total respiration ($R_{tot} = R_{bg} + R_{cd}$) at DAR 1 with the allocation of ^{13}C fixed at DAR 1 to the different sinks. In detail, plant gas exchange outputs at DAR 1 were integrated over 24 hours, and total daily A, R_{bg}, the respiration of the whole-canopy during dark hours (R_{cd}) and R_{tot} are reported in table 1, showing that the ratio between R_{tot} and A was significantly higher in WS plants than in WW and REC plants. We calculated the residual amount of C allocated to the different pools after sink respiration and/or re-mobilization by multiplying the proportion of residual ^{13}C in the different pools at DAR 1, 2, 3, 6, 15 and 30, with the integrated daily A of DAR 1 (the ^{13}C pulse day). Figure 4 reports this information and shows how total C allocated to berry and root was similar between WS and WW plants and higher in REC plants. Already from DAR 2 in root, and two days later in fruit, the amount of C in the REC treatment was significantly higher than in the control plants (both WW and WS). The WS plants allocated more C belowground than WW controls in the first 15 days, but then the consumption (respiration or translocation) brought the assimilated C to a level comparable to that of WW controls. Also in the REC roots, the maximum amount of C at DAR 6 tended to drop, indicating consumption and/or reallocation but the total amount of assimilated C that remained in the root at DAR 30 was significantly higher than WW and WS plants. On the contrary, C accumulation in the berries of REC plants remained stable and constant in time (Figure 4).
The amount of assimilated C that remained in the leaf at DAR 30 was much lower compared to the other two C pools, though nonetheless slightly higher in REC plants compared to WS and WW plants. Adding the total amounts of newly fixed C remaining in the roots, berries and leaves at DAR 30 to the daily R_{tot} we observed that the amount of daily C

assimilated was sufficient to support C accumulation and root and shoot respiration in WW and REC plants, but on the contrary, not sufficient in WS plants (Figure 5).
The accumulation levels of fresh and dry matter, measured at DAR 30 in berries, reflected the carbon fluxes described so far and the levels of water potential measured. The REC grapes generally showed higher levels than the WW ones, in turn higher than the WS ones (table 2).

Transcript expression analyses of key genes involved in source-sink interrelationships

The expression of different carbohydrate metabolism-related genes was analysed in source and sink tissues of WW, WS and REC plants over a time course characterizing the early phases after rewatering (DAR 0, DAR 1 and DAR4), in order to add information at the molecular level about carbon allocation dynamics (see Figures S2 a and b for DAR 0 and DAR 1 and Figure 6 for DAR 4. In general, the gene expression trends were similar during the early phases considered, thus we decided to describe more in detail the results occurring at DAR4 when ecophysiological measurements confirmed a fully recovery of REC plants (Figure 6). The sucrose synthase gene *VvSuSy* was expressed mainly in root and characterized by a lower expression level in WS treatment. An alternative route for sucrose breakdown in WS root was offered by the increased expression of the cell wall invertase (*VvcwINV*) gene, whose expression trend was in general complementary to that of *VvSuSy* in WW, WS and REC root samples. Interestingly, WS root showed an increased expression of threalose-6-phosphate phosphatase (*VvTPP*) gene, responsible for the synthesis of threalose from the precursor threalose-6-phosphate. The availability of new photosynthates after rehydration allowed the REC root to increase the starch synthesis (*VvSTA*, starch synthase) mirroring the WW root behaviour, whereas in WS root *VvSTA* did not increase the expression level. This result agrees with the high hexose mobilization confirmed by the increased expression level of the hexose transporter 3 (*VvHT3*) in WS root in respect to the same tissue of WW and REC plants. In berry, two transcripts among the genes analysed showed high expression, mainly in WW and REC plants: the Sugar Will Eventually be Exported Transporter 10 (*VvSWEET10*), responsible for phloem unloading in sink tissues, and the vacuolar hexose transporter 6 (*VvHT6*) driving the carbohydrates to storage in the vacuole. Similarly, the vacuolar invertase *VvGIN2* showed expression in the berry reinforcing the sucrose compartmentalization in the vacuole (Figure 6).

Discussion

Carbon balance in drought-rehydrated ripening grapevines

In this study, droughted vines rehydrated at *veraison* were pulse-labelled with $^{13}CO_2$ together with other vines maintained in water deficit or fully irrigated. The ^{13}C absorbed by the leaves with photosynthesis during labelling were subsequently used to trace the phloem flows of newly assimilated C towards the strongest sinks in the thirty days of the post-*veraison* phase, when the ripening processes of the grape occurred triggering C allocation towards the sinks. From the combined analysis of the ^{13}C allocation patterns, and photosynthesis and respiration gas exchanges of the plant (shoot and root) and rhizosphere compartments, we were able to demonstrate several interrelationships occurring among plant organs during a rehydration event following a drought period either above- or below-ground.

The resumption of root metabolic activity and post-rehydration photosynthesis is almost immediate (a few hours and less than 24 hours, respectively), showing how adapted the vine is to tolerate water stress. On the contrary, beech a mesophilic plant not adapted to arid climates (Fotelli et al., 2001), has been shown to take a few weeks for photosynthesis to recover to pre-stress conditions (Hagedorn et al. 2016), Furthermore, the presence in grapeveines of the fruit sink with considerable strength, triggered a photosynthetic and respiratory energy demand (Fatichi et al., 2014; Körner et al., 2015).

The water regime strongly influenced the partitioning of C towards the different sinks. Water stress caused a greater allocation of the newly photosynthesized carbonaceous resources to the berry (about double compared to WW controls), which are stored in a stable manner. On the other hand, the C allocated belowground over 30 days is mostly consumed. The plant in recovery diverts the same percentage of labelled C to the berry as the plants in water stress, although in absolute amounts its photosynthesis is about double that under water stress (it is comparable or even higher than photosynthesis in WW control plants). Therefore, the total C allocated to the berry is about 50% higher in recovery than in the irrigated control. These physiological mechanisms are at the basis of what is often experienced in irrigated fleshy fruit crops, where it has been previously shown that occasional irrigation events are more effective in determining sugar-related production, rather than maintaining a constant satisfactory water state (Chaves et al., 2010). Moreover, the rain fed areas with viticultural vocation present microclimatic situations of summer aridity with only occasional rains (Charrier et al., 2018).

Through a daily respired / photosynthesized C balance we show that during the ripening of the berry (30 days post *veraison*) 57% of the C assimilated in the irrigated condition is respired. In the same period, the

accumulation of neo-photosynthates is about 28%, showing that plant photosynthesis can support C accumulation in sinks without affecting plant reserves accumulated pre-*veraison*, as showed Rossouw et al. (2017) in irrigated grapevines. On the contrary, upon water stress 83% of the daily C assimilated is respired; since 43% of neo-photosynthesized C is stored in a stable manner, we conclude that the plant should affect C radical reserves accumulated before *veraison* to support the respiration rate. After rehydration in REC pants, 54% of the daily C assimilated of the post-*veraison* month is respired, similarly to what happened in WW controls; about 43% of neo-photosynthesized C is stored in a stable manner (especially in berries), much more than under WW condition. However, the increase in A was able to support the requests of the sinks, without affecting the reserves, as was the case in WS. During WS, the lack of turgor acting as major limitation to growth (Hernandez-Santana et al., 2021) forced plants to affect C reserves, adding evidence to the sink limitation hypothesis to photosynthesis (Fatichi et al., 2014). The highest proportion of photosynthates was partitioned into fruits (berries) and it was in WS plants, almost double than under WW condition, as indicated by figure 5 (for fruits: daily C needs / daily C available: 27/176=15% in WW plants, 24/81=29% in WS plants and 45/188=23% in REC ones). From a wider point of view, this indicates why fruits are usually seen as stronger sinks than other organs or even how fruit growth is generally seen as less sensitive to water stress than vegetative growth.

Molecular evidences supporting the model

Delivery of labelled ^{13}C to the different sinks was observed in parallel with the expression of genes involved in carbohydrate metabolism. Genes encoding proteins that regulate the delivery of sucrose to the sinks and which catalyze the hydrolysis of the sucrose discharged to trigger respiration or carbon storage have been analysed. SuSy is an enzyme with a central role in the source-sink coordination, it catalyses the breakdown of sucrose in sink tissues to keep the concentration and pressure gradient operational in the phloem (Gessler, 2021). *SuSy* gene resulted expressed mainly in roots. In rehydrated roots, thanks to the availability of new photo-assimilated resources and the recovery of root respiration, the molecular machinery quickly adjusted to that of WW plants, whereas WS root showed a lower level of *SuSy* expression, probably to compensate the lack of assimilation. Interestingly, *cwINV* gene expression resulted significantly higher in WS root in respect to WW and REC roots, ensuring an alternative route of sucrose breakdown and the maintaining of the root sink strength also in water stress condition, as confirmed by the ^{13}C partitioning analysis. The relative impacts of SuSy and invertase on C allocation appears to be dependent on tissue, species, developmental stage and season (Dominguez *et al.*, 2021). Moreover, poplar RNAi transgenic lines for *SuSy* showed increased invertase

activity, suggesting a partial compensation of the two enzymes in the sucrose cleavage activity, phenomenon that we can retrieve in our data also, looking at the complementary expression of *SuSy* and *cwINV* transcripts in the WW, WS and REC roots. The understanding of the reason why the grapevine root during water stress leans toward the preferential expression of the invertase requires further experiments. It is known that both pathways degrade sucrose but the products of their reactions differ considerably; the literature suggests that whereas SuSy could be involved in increased biomass (Gessler, 2021; Xu *et al.*, 2012), invertases could have a greater ability to stimulate specific sugar sensors (Ruan *et al.*, 2010; Ruan, 2012). The involvement of the water stressed root in the sucrose signalling was confirmed by the overexpression of the *threalose-6-phospate phosphatase* (TPP) transcript, catalysing the second step of threalose synthesis. Trehalose accumulation confers high tolerance levels to different abiotic stresses (Garg *et al.*, 2002) and, together with the precursor Threalose-6-phosphate, play key roles in the control of carbon allocation and of stress responses in plants (Morabito *et al.*, 2021). We could speculate that through the sugar signalling WS root orchestrated the maintaining of the sink strength despite the unfavorable conditions for C allocation. Hexoses produced from sucrose cleavage were not used for starch synthesis in WS root, as suggested by the low expression of *VvSTA* and the high expression of the *HT3*, confirming the mobilization of hexoses. On the contrary, the REC root started the starch synthesis quickly adjusting to the WW condition.

Sugar Will Eventually be Exported Transporters (SWEETs) 10 is a plasma membrane sucrose transporter of clade III SWEETs, deputated to the phloem unloading (Savoi *et al.*, 2021; Eom *et al.*, 2015). It is one of the two transcripts in our experiment expressed at high level in the berry. Although the main driver of sucrose unloading in the berry was the developmental stage (*veraison*), as suggested from the high *SWEET10* expression level over all the time course, a slight treatment effect could be noticed. Thanks to the photosynthesis and assimilation recovery, the REC plant was able to maximise the C allocation in the fruit. Interestingly, since *SWEET10* transcript level remained low in the REC root tissue, we can suggest that the prompt increase of root respiration after rehydration was not accompanied by an increase of the unloading rate of sucrose in root, differently from what happens in non-fruit trees (Hagedorn *et al.*, 2016). In grapevine, when the fruit is present, our experiment suggests that the root becomes a secondary sink. The unloading of sucrose was guaranteed by the *SWEET10* expression also in WS berries, although to a minor extent probably because of the limited photosynthates available in stress condition diverted also toward the root, as confirmed by *SWEET10* expression increasing in this tissue in respect to WW and REC plants. Finally, the analysis of the *vacuolar hexose transporter HT6* expression level, the second gene highly expressed in berry, pointed out that this transporter allowed the hexoses accumulation in the vacuole, so

that the sink strength can be maintained to attract more C (as Susy does in root). Moreover, the storage of sucrose in the vacuole was driven also by the *vacuolar invertase GIN2*. In general, the berry metabolism appeared to be stopped as confirmed by the general low expression level of carbohydrate metabolism-related genes analyzed, with the exception of the genes described above that are key modulators for hexose and sucrose accumulation and cell expansion (Ruan *et al.*, 2010) in the phenological stage of *veraison*. This molecular difference underlines what has been seen in our C distribution model between the root and fruit sinks, which shows how the allocated C amount remains constant in the REC fruit over 30 days, and there is no redistributive decrease trend, as in the root.

Possible implications of the research

Confirming the measurements of carbon fluxes and water potential levels that plants experienced during the experiment, the berries of the REC plants were found to be the heaviest and with the highest sugar concentration at DAR 30. In WS plants, the low growth levels of the berries that developed in a context of scarce water availability were not coupled with low levels of sugar concentration (expressed in degree Brix), found significantly not lower than in the WW berries, confirming what shown as carbon accumulation in figure 4b.
Our experimental design mimicked a peculiar *scenario*, optimized to observe how much and how root and fruit compete with each other, but not necessarily aligned with what would be other possible *scenarios* in the field. It couples with a field situation, where mainly until *veraison* grapevines perceive water deficiency, followed by rain fed in the subsequent phases of the productive cycle. In this *scenario*, an increase of C allocation in berries positively regulates berry quality not only in relation to the accumulation of primary metabolites *per se*, but also to the accumulation of secondary metabolites as glycosides in the cell vacuoles (Ferrandino and Lovisolo, 2014). Furthermore, C and sugar biosynthesis-transport related genes couple with the activation of the phenylalanine ammonia lyase (PAL), the key enzyme of the phenylpropanoid pathway (Pirie and Mullins, 1976).
However, in some viticultural areas pre-*veraison* water deficits could be less frequent than water deficits later in the ripening process. Scholasch and Rienth (2019) reviewed water deficit-mediated changes in vine and berry physiology, highlighting how this latter *scenario*, opposite to what described by our experimental setup, could increase berry quality. This because reducing water availability after *veraison* positively affects yield components, via both a reduction of berry volume (Zúñiga et al., 2018) and the activation of ABA-related biosynthetic pathways (Ferrandino and Lovisolo, 2014). As a specular confirmation, Intrigliolo et al. (2016) showed that a post-*veraison* irrigation results in a 26-30% yield increase

compared to rain fed vineyards that experienced a post-*veraison* water deficit.
In our work, the effects of the carbon distribution wave following rehydration coupled with the expected delivery of phloem-water. The genotype we used ('Barbera' on '420A') should mitigate the effects of a distinctly aniso-hydric response to water stress of the scion through the use of a rootstock that is not tolerant to drought, and therefore not inclined to force lowering of the water potential during drought (Tramontini et al., 2013; Lavoie-Lamoureux et al., 2017). In cases of varieties showing an aniso-hydric behavior grafted on tolerant rootstocks (for example descendants of *Vitis rupestris* L.), rehydration could have even more significant effects on the distribution wave of photosynthates; this is because the ability to compensate for the mechanisms of lowering the water potential (among all the osmotic adjustment and the control of embolism repair, Lovisolo et al., 2008b) in stressful situations would allow these phenotypes a fast and active post-rehydration recovery (Lovisolo et al., 2010; Scholasch and Rienth, 2019). By contrast, we can speculate that rehydration could be less effective in scions showing iso-hydric response to water deficit and/or rootstocks sensitive to drought (for example descendants of *Vitis riparia* L.) (Lovisolo et al., 2008b).

Conclusions

Our results show how periods of water stress activate a molecular response in the plant C sinks to compensate for the reduction in photosynthetic C assimilation. In fruit crops, the fruits compete strongly with the root. This derives from an ancestral need to convey nutrients to the seed with a parallel need to make the fruits palatable to the herbivore for a seed dissemination that ensures the continuity of the progeny. Furthermore, the selection of the most productive phenotypes has made the fruit sink quantitatively competitive against the root sink, much more than what happens in forest plants, where the root completely orchestrates the response to stress. In the rehydration phases, the strength of the sink persists but is coupled with a photosynthetic recovery activated by the phloem downloading capacity directed towards the strongest C-requesting sinks. This is so effective that the assimilation values of the rehydrated plants exceed those of the irrigated plants. In these moments, the effects of maximum C assimilation and relative delivery to the requesting sink take place. They therefore represent the key moments in the life of the fleshy fruit plants, especially if they coincide with the ripening phase of the fruit, as in our experimental design.

Acknowledgements

The authors thank, Klaas De Backer, Samuele Bolassa, Corrado Domanda, Cristina Lerda, Emilio Dicembrini, Mauro Caviglione, Marco D'Oria for technical help during experiments. Financial support: CARBOSTRESS project – CRT - Cassa Risparmio Torino Foundation.

Author contributions

DLP, DSP, IP and CL conceptualized and wrote the original draft. DLP, DSP, LEA, AFi, IP carried out the experimental part under supervision from GG, DRA, AFe, LC, CL. GG, WC, AFe critically reviewed the draft. All authors read and approved the manuscript.

References

Caemmerer, S. von and Farquhar, G.D. (1981) Some relationships between the biochemistry of photosynthesis and the gas exchange of leaves. Planta, 153, 376–387.

Charrier, G., Delzon, S., Domec, J.-C., Zhang, L., Delmas, C.E.L., Merlin, I., Corso, D., King, A., Ojeda, H., Ollat, N., Prieto, J. A., Scholach, T., Skinner, P., van Leeuwen, C. and Gambetta, G. A. (2018) Drought will not leave your glass empty: Low risk of hydraulic failure revealed by long-term drought observations in world's top wine regions. Science Advances, 4, eaao6969.

Chaves, M.M., Zarrouk, O., Francisco, R., Costa, J.M., Santos, T., Regalado, A.P., Rodrigues, M.L. and Lopes, C.M. (2010) Grapevine under deficit irrigation: hints from physiological and molecular data. Ann Bot, 105, 661–676.

Chen, L.-Q., Qu, X.-Q., Hou, B.-H., Sosso, D., Osorio, S., Fernie, A.R. and Frommer, W.B. (2012) Sucrose efflux mediated by SWEET proteins as a key step for phloem transport. Science, 335, 207–211.

Chitarra, W., Perrone, I., Avanzato, C.G., Chitarra, W., Perrone, I., Avanzato, C. G., Minio, A., Boccacci, P., Santini, D., Gilardi, G., Siciliano, I., Gullino, M.L., Delledonne, M., Mannini, F. and Gambino, G. (2017) Grapevine Grafting: Scion Transcript Profiling and Defense-Related Metabolites Induced by Rootstocks. Frontiers in Plant Science, 8. Available at: https://www.frontiersin.org/article/10.3389/fpls.2017.00654 [Accessed June 13, 2022].

Dominguez, P.G., Donev, E., Derba-Maceluch, M., Bünder, A., Hedenström, M., Tomášková, I., Mellerowicz, E.J. and Niittylä, T. (2021) Sucrose synthase determines carbon allocation in developing wood and alters carbon flow at the whole tree level in aspen. New Phytologist, 229, 186–198.

Douthe, C., Medrano, H., Tortosa, I., Escalona, J.M., Hernández-Montes, E. and Pou, A. (2018) Whole-Plant Water Use in Field Grown Grapevine: Seasonal and Environmental Effects on Water and Carbon Balance. Frontiers in Plant Science, 9. Available at: https://www.frontiersin.org/article/10.3389/fpls.2018.01540 [Accessed June 13, 2022].

Eom, J.-S., Chen, L.-Q., Sosso, D., Julius, B.T., Lin, I.W., Qu, X.-Q., Braun, D.M. and Frommer, W.B. (2015) SWEETs, transporters for intracellular and intercellular sugar translocation. Curr Opin Plant Biol, 25, 53–62.

Epron, D., Bahn, M., Derrien, D., Lattanzi, F. A., Pumpanen, J., Gessler, A., Högberg, P., Maillard, P., Dannoura, M., Gérant, D. and Buchmann, N. (2012) Pulse-labelling trees to study carbon

allocation dynamics: a review of methods, current knowledge and future prospects. Tree Physiol, 32, 776–798.
Faralli, M., Bontempo, L., Bianchedi, P. L., Moser, C., Bertamini, M., Lawson, T., Camin, F., Stefanini, M. and Varotto, C. (2022) Natural variation in stomatal dynamics drives divergence in heat stress tolerance and contributes to the seasonal intrinsic water-use efficiency in Vitis vinifera (subsp. sativa and sylvestris). J Exp Bot, 73, 3238-3250.
Fotelli, M.N., Geßler, A., Peuke, A.D. and Rennenberg, H. (2001) Drought affects the competitive interactions between Fagus sylvatica seedlings and an early successional species, Rubus fruticosus: responses of growth, water status and δ13C composition. New Phytologist, 151, 427–435.
Galmés, J., Medrano, H. and Flexas, J. (2007) Photosynthetic limitations in response to water stress and recovery in Mediterranean plants with different growth forms. New Phytologist, 175, 81–93.
Gambetta, G.A., Herrera, J.C., Dayer, S., Feng, Q., Hochberg, U. and Castellarin, S.D. (2020) The physiology of drought stress in grapevine: towards an integrative definition of drought tolerance. J Exp Bot, 71, 4658–4676.
Garg, A.K., Kim, J.-K., Owens, T.G., Ranwala, A.P., Choi, Y.D., Kochian, L.V. and Wu, R.J. (2002) Trehalose accumulation in rice plants confers high tolerance levels to different abiotic stresses. Proceedings of the National Academy of Sciences, 99, 15898–15903.
Gessler, A. (2021) Sucrose synthase – an enzyme with a central role in the source–sink coordination and carbon flow in trees. New Phytologist, 229, 8–10.
Hagedorn, F., Joseph, J., Peter, M., Luster, J., Pritsch, K., Geppert, U., Kerner, R., Molinier, V., Egli, S., Schaub, M., Liu, J. -F., Li, M., Sever, K., Weiler, M., Siegwolf, R. T. W., Gessler, A. and Arend M. (2016) Recovery of trees from drought depends on belowground sink control. Nature Plants, 2, 16111.
Hasibeder, R., Fuchslueger, L., Richter, A. and Bahn, M. (2015) Summer drought alters carbon allocation to roots and root respiration in mountain grassland. New Phytol, 205, 1117–1127.
Herrera, J.C., Calderan, A., Gambetta, G.A., Peterlunger, E., Forneck, A., Sivilotti, P., Cochard, H. and Hochberg, U. (2022) Stomatal responses in grapevine become increasingly more tolerant to low water potentials throughout the growing season. The Plant Journal, 109, 804–815.
Ho, L.C. (2003) Metabolism And Compartmentation Of Imported Sugars In Sink Organs In Relation To Sink Strength. Annual Review of Plant Physiology and Plant Molecular Biology, 39, 355–378.

Keller, I., Rodrigues, C.M., Neuhaus, H.E. and Pommerrenig, B. (2021) Improved resource allocation and stabilization of yield under abiotic stress. J Plant Physiol, 257, 153336.

Knoblauch, M., Knoblauch, J., Mullendore, D.L., Savage, J.A., Babst, B.A., Beecher, S.D., Dodgen, A.C., Jensen, K.H. and Holbrook, N.M. (2016) Testing the Münch hypothesis of long distance phloem transport in plants C. S. Hardtke, ed. eLife, 5, e15341.

Lavoie-Lamoureux, A., Sacco, D., Risse, P.-A. and Lovisolo, C. (2017) Factors influencing stomatal conductance in response to water availability in grapevine: a meta-analysis. Physiol Plant, 159, 468–482.

Lemoine, R., La Camera, S., Atanassova, R., Dédaldéchamp, F., Allario, T., Pourtau, N., Bonnemain, J. -L., Laloi, M. Coutos-Thévenot, P., Maurousset, L, Faucher, M., Girousse, C., Lemonnier, P., Parrilla, J. and Durand, M. (2013) Source-to-sink transport of sugar and regulation by environmental factors. Frontiers in Plant Science, 4. Available at: https://www.frontiersin.org/article/10.3389/fpls.2013.00272 [Accessed June 13, 2022].

Lovisolo, C., Perrone, I., Carra, A., Ferrandino, A., Flexas, J., Medrano, H. and Schubert, A. (2010) Drought-induced changes in development and function of grapevine (Vitis spp.) organs and in their hydraulic and non-hydraulic interactions at the whole-plant level: a physiological and molecular update. Functional Plant Biol., 37, 98–116.

Morabito, C., Secchi, F. and Schubert, A. (2021) Grapevine TPS (trehalose-6-phosphate synthase) family genes are differentially regulated during development, upon sugar treatment and drought stress. Plant Physiol Biochem, 164, 54–62.

Pastenes, C., Villalobos, L., Ríos, N., Reyes, F., Turgeon, R. and Franck, N. (2014) Carbon partitioning to berries in water stressed grapevines: The role of active transport in leaves and fruits. Environmental and Experimental Botany, 107, 154–166.

Perrone, I., Pagliarani, C., Lovisolo, C., Chitarra, W., Roman, F. and Schubert, A. (2012) Recovery from water stress affects grape leaf petiole transcriptome. Planta, 235, 1383–1396.

Ripoll, J., Urban, L., Staudt, M., Lopez-Lauri, F., Bidel, L.P.R. and Bertin, N. (2014) Water shortage and quality of fleshy fruits--making the most of the unavoidable. J Exp Bot, 65, 4097–4117.

Rodrigues, J., Inzé, D., Nelissen, H. and Saibo, N.J.M. (2019) Source–Sink Regulation in Crops under Water Deficit. Trends in Plant Science, 0. Available at: https://www.cell.com/trends/plant-science/abstract/S1360-1385(19)30101-3 [Accessed June 15, 2019].

Rodriguez-Dominguez, C.M., Forner, A., Martorell, S., Choat, B., Lopez, R., Peters, J. M. R., Pfautsch, S., Mayr, S., Carins-Murphy, M.R.,

McAdam, S. A. M., Richardson, F., Diaz-Espejo, A., Hernandez-Santana, V., Menezes-Silva, P. E., Torres-Ruiz, J. M., Batz T. A. and Sack L. (2022) Leaf water potential measurements using the pressure chamber: Synthetic testing of assumptions towards best practices for precision and accuracy. Plant, Cell & Environment, 45, 2037–2061.

Rossouw, G.C., Smith, J.P., Barril, C., Deloire, A. and Holzapfel, B.P. (2017) Carbohydrate distribution during berry ripening of potted grapevines: Impact of water availability and leaf-to-fruit ratio. Scientia Horticulturae, 216, 215–225.

Ruan, Y.-L. (2012) Signaling role of sucrose metabolism in development. Mol Plant, 5, 763–765.

Ruan, Y.-L., Jin, Y., Yang, Y.-J., Li, G.-J. and Boyer, J.S. (2010) Sugar input, metabolism, and signaling mediated by invertase: roles in development, yield potential, and response to drought and heat. Mol Plant, 3, 942–955.

Ryan, M.G., Oren, R. and Waring, R.H. (2018) Fruiting and sink competition. Tree Physiology, 38, 1261–1266.

Savoi, S., Torregrosa, L. and Romieu, C. (2021) Transcripts switched off at the stop of phloem unloading highlight the energy efficiency of sugar import in the ripening V. vinifera fruit. Hortic Res, 8, 1–15.

Vilonen, L., Ross, M. and Smith, M.D. (2022) What happens after drought ends: synthesizing terms and definitions. New Phytologist, n/a. Available at: https://onlinelibrary.wiley.com/doi/abs/10.1111/nph.18137 [Accessed June 13, 2022].

Vitali, M., Tamagnone, M., Iacona, T.L. and Lovisolo, C. (2013) Measurement of grapevine canopy leaf area by using an ultrasonic-based method. OENO One, 47, 183–189.

Wardlaw, I.F. (1990) Tansley Review No. 27 The control of carbon partitioning in plants. New Phytologist, 116, 341–381.

Xu, C., Yin, X., Lv, Y., Wu, C., Zhang, Y. and Song, T. (2012) A near-null magnetic field affects cryptochrome-related hypocotyl growth and flowering in Arabidopsis. Adv. Space Res., 49, 834–840.

Table 1. Gas exchange integral at DAR 1. Daily integrals of: whole-canopy assimilation (A), respiration of the whole-canopy during dark hours (R_{cd}), belowground respiration (R_{bg}), total respiration (R_{tot} = R_{bg} + R_{cd}) at DAR 1. Values are means ± SE (*n*=4). Statistical analysis of data was performed using the one-way analysis of variance (ANOVA) followed by a *post hoc* Tukey's test. Letters denote statistically significant variations ($p < 0.05$).

	Daily A	Daily R_{bg}	Daily R_{cd}	Daily R_{tot}	R_{tot}/A
	mmol CO_2	mmol CO_2	mmol CO_2	mmol CO_2	%
IRR	176 ± 14 a	92 ± 10 a	9 ± 1 a	101 ± 9 a	57 ± 2 b
WS	81 ± 10 b	59 ± 5 b	8 ± 1 a	67 ± 6 b	83 ± 4 a
REC	188 ± 33 a	90 ± 2 a	9 ± 1 a	100 ± 2 a	54 ± 8 b

Table 2. Weight of the berry (g), production of grapes per plant (kg), number of berries per plant (#), degree Brix (°Brix), total acidity as tartaric acid (g L^{-1}) measured on DAR 30. Values are means ± SE (*n*=4). Statistical analysis of data was performed using the one-way analysis of variance (ANOVA) followed by a *post hoc* Tukey's test. Letters denote statistically significant variations ($p < 0.05$).

	Weight of the berry	Production of grapes per plant	Number of berries per plant	°Brix	Total acidity as tartaric acid
	g	kg			g L-1
WW	1.80 ± 0.14 b	0.34 ± 0.02 b	192 ± 15 a	24.5 ± 0.46 b	8.00 ± 0.35 a
WS	1.53 ± 0.09 c	0.29 ± 0.05 c	192 ± 33 a	23.8 ± 0.63 b	6.65 ± 0.66 a
REC	2.27 ± 0.04 a	0.47 ± 0.04 a	205 ± 36 a	25.6 ± 0.36 a	7.25 ± 0.43 a

Figure legend

Figure 1. Whole-plant gas exchange analysis. (a) transpiration, E and (b) net photosynthesis, A. From DAR -5 to DAR -1 data of WW (black squares, n=4) and WS (white circles, n=8) plants before the rehydration event are represented; from DAR 0 to DAR 7 data of WW (n=4), WS (n=4) and REC (grey triangles, n=4) plants after rehydration are plotted. Dotted vertical lines before and after DAR 0 show re-hydration and 13CO2 pulse-labelling. Statistical analysis of data was performed using the one-way analysis of variance (ANOVA) followed by a post hoc Tukey's test. Letters in the table denote statistically significant variations ($p < 0.05$).

Figure 2. Whole-plant gas exchange analysis. Belowground respiration (Rbg). Symbols, replicates (n) and statistical analysis as in Figure 1.

Figure 3. 13C partitioning of neo-photosynthates after a re-hydration event. Partitioning of assimilated labelled 13CO2 during feeding event at DAR 1. (a), (b), (c), (d) represent % of labelled 13C at DAR 1, 2, 3, 6, 15, 30 respectively in leaf, berry, root and whole plant. Values are means ± SE (n=3). Statistical analysis of data was performed using the one-way analysis of variance (ANOVA) followed by a post hoc Tukey's test. Letters in the table denote statistically significant variations ($p < 0.05$).

Figure 4. Carbon accumulation. Amounts of carbon allocations in different sinks obtained by multiplying the residual 13C percent found in the different pools at DAR 1, 2, 3, 6, 15 and 30 with the integrated daily A of DAR 1 (the 13C pulse day) in the leaf canopy (a), in all berries (b), and in the whole root (c). Values are means ± SE (n=3). Statistical analysis of data was performed using the one-way analysis of variance (ANOVA) followed by a post hoc Tukey's test. Letters in the table denote statistically significant variations ($p < 0.05$).

Figure 5. Model of C allocation to different C pools. The model is the combination of data from gas exchange analysis with data from pulse-chasing C isotope analysis. In blue, yellow and grey we showed the amount of neo-photosynthates that will be permanently stocked respectively in root, berries and leaf C pools. In orange and green, daily Rtot and daily A is reported.

Figure 6. Transcripts of key genes of sugar metabolism. Relative expression level of sucrose synthase (VvSusy), cell wall invertase (VvcwINV), threalose-6-phosphate phosphatase (VvTPP), starch synthase (VvSTA), hexose transporter 3 (VvHT3), Sugar Will Eventually be Exported Transporter 10 (VvSWEET10), hexose transporter 6 (VvHT6) and vacuolar invertase 2 (VvGIN2) genes in leaf, root and berry tissues sampled from WW, WS and REC plants at DAR 4, as determined by qRT-

PCR signals normalized to actin (VvACT) and ubiquitin (VvUBI) transcripts. Data are presented as the mean ±SE of three biological and technical replicates. Gene IDs and oligonucleotides used for each gene are indicated in the Table S1. Different lowercase letters above the bars indicate significant differences according to a post hoc Tukey's test ($p \leq 0.05$).

Figure 7. Imposition and maintenance of water deficit levels. Relative soil humidity measured gravimetrically, and midday leaf water potential measured by pressure chamber technique on detached leaves. Values are means

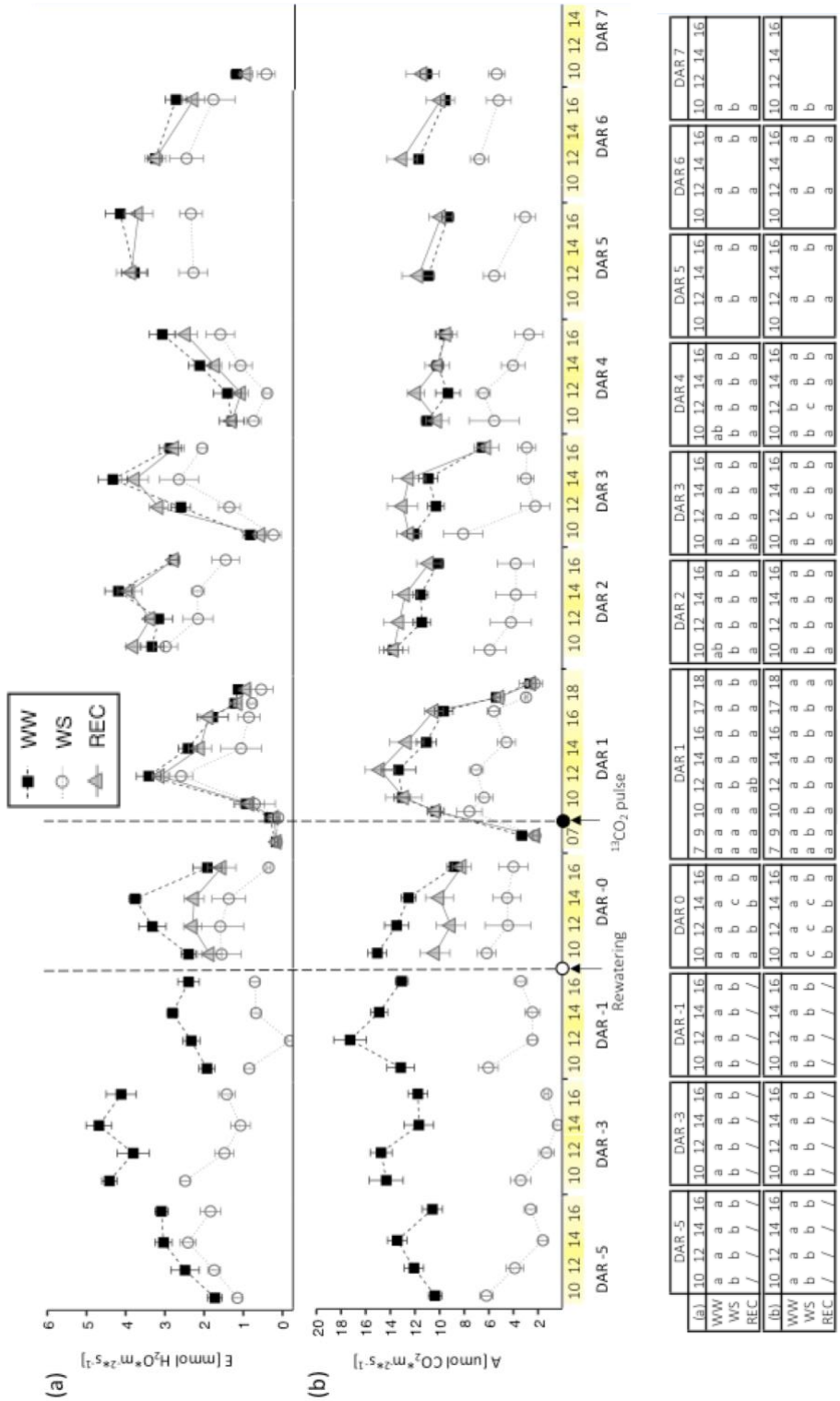

Figure 1. Whole-plant gas exchange analysis.

	DAR -5				DAR -3				DAR -1				DAR 0				DAR 1				DAR 2				DAR 3				DAR 4				DAR 5				DAR 6			
	04	10	16	22	04	10	16	22	04	10	16	22	04	10	16	22	04	10	16	22	04	10	16	22	04	10	16	22	04	10	16	22	04	10	16	22	04	10	16	22
WW	a	a	a	a	a	a	a	a	a	a	a	a	a	a	a	a	a	a	a	a	a	a	a	a	a	a	a	a	a	a	a	a	a	a	a	a	a	a	a	a
WS	b	b	b	b	b	b	b	b	b	b	b	b	b	b	b	b	b	b	b	b	b	b	b	b	b	b	b	b	b	b	b	b	a	b	a	a	b	b	b	b
REC	/	/	/	/	/	/	/	/	/	/	/	/	/	/	/	/	a	a	a	a	a	a	a	a	a	a	a	a	a	a	a	a	a	a	a	a	a	a	a	a

Figure 2. Whole-plant gas exchange analysis.

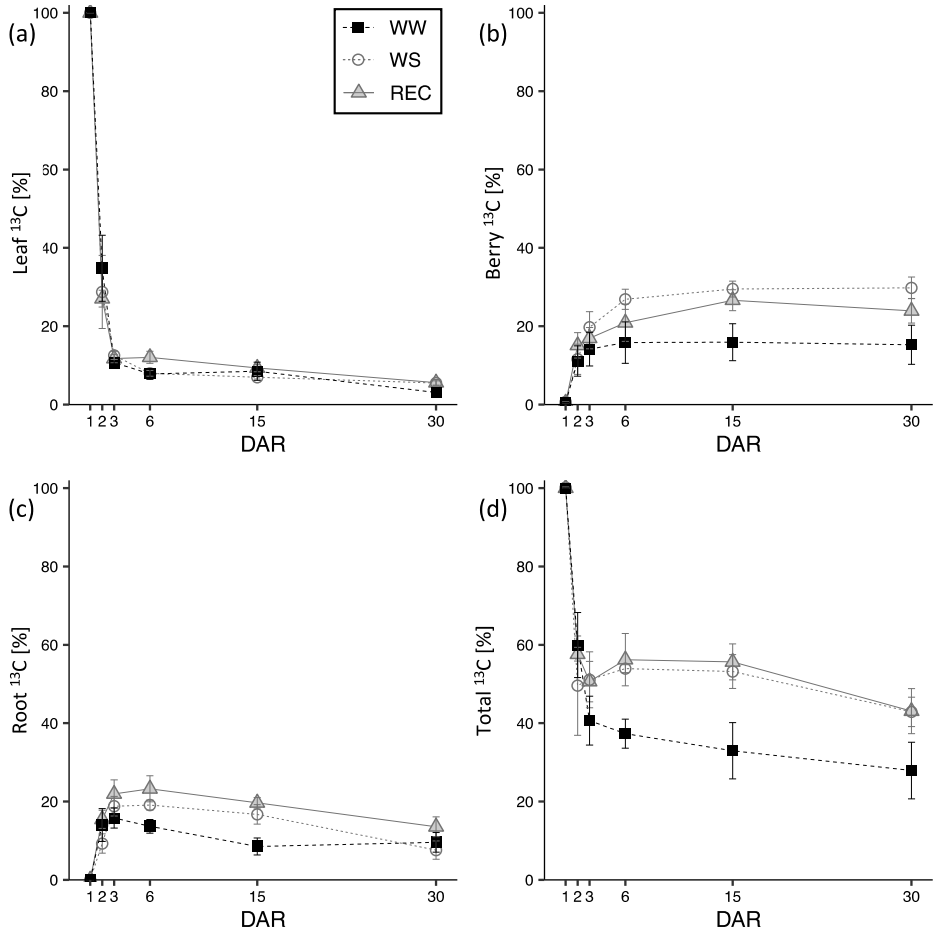

(a)	1	2	3	6	15	30
WW	a	a	a	b	a	a
WS	a	a	a	b	a	a
REC	a	a	a	a	a	a

(b)	1	2	3	6	15	30
WW	a	a	a	b	b	b
WS	a	a	a	a	a	a
REC	a	a	a	a	a	ab

(c)	1	2	3	6	15	30
WW	a	a	a	b	b	a
WS	a	a	a	a	a	a
REC	a	a	a	a	a	a

(d)	1	2	3	6	15	30
WW	a	a	a	b	b	b
WS	a	a	a	a	a	a
REC	a	a	a	a	a	a

Figure 3. ^{13}C partitioning of neo-photosynthates after a re-hydration event. Partitioning of assimilated labelled $^{13}CO_2$ during feeding event at DAR 1.

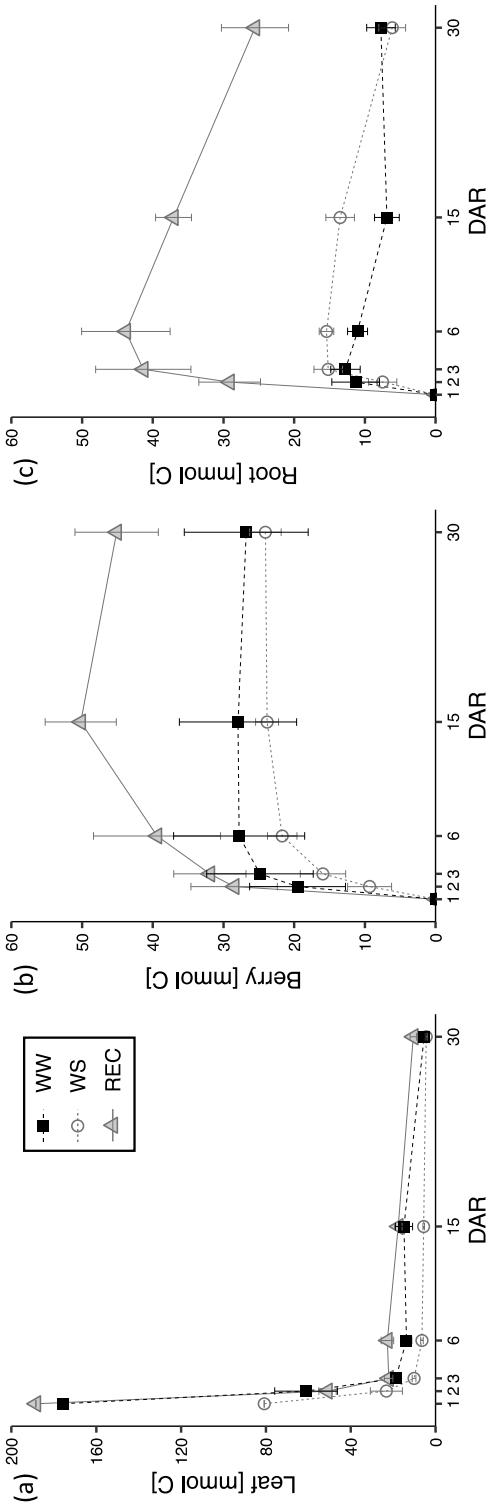

(a)	1	2	3	6	15	30
WW	a	a	a	a	a	a
WS	b	b	b	c	b	a
REC	a	a	a	b	a	a

(b)	1	2	3	6	15	30
WW	a	ab	ab	ab	b	b
WS	a	b	b	b	b	b
REC	a	a	ab	a	a	a

(c)	1	2	3	6	15	30
WW	a	b	b	c	c	b
WS	a	b	b	b	b	b
REC	a	a	a	a	a	a

Figure 4. Carbon accumulation.

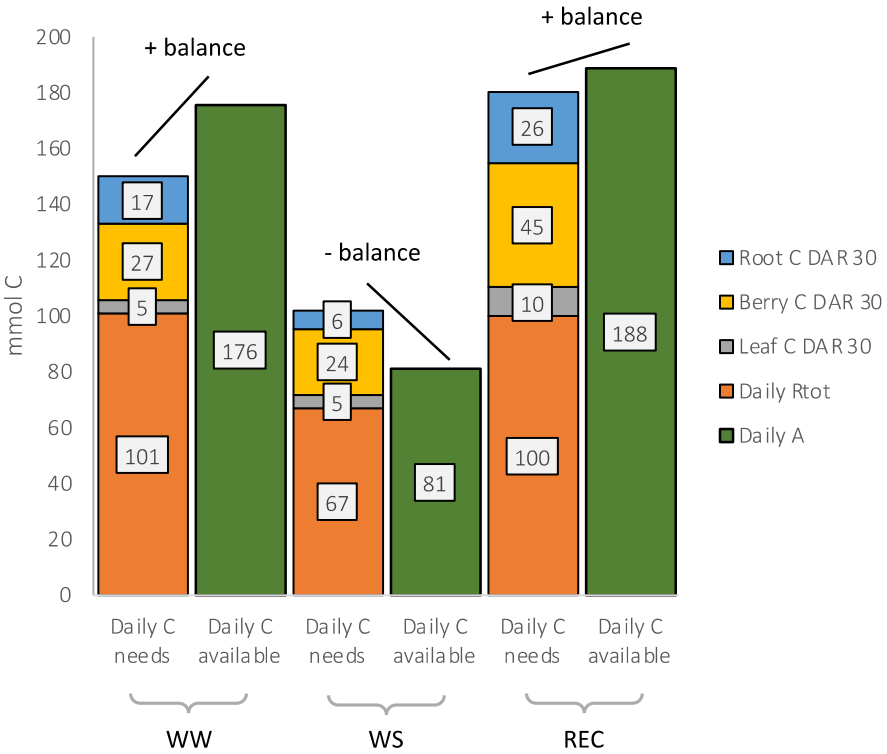

Figure 5. Model of C allocation to different C pools.

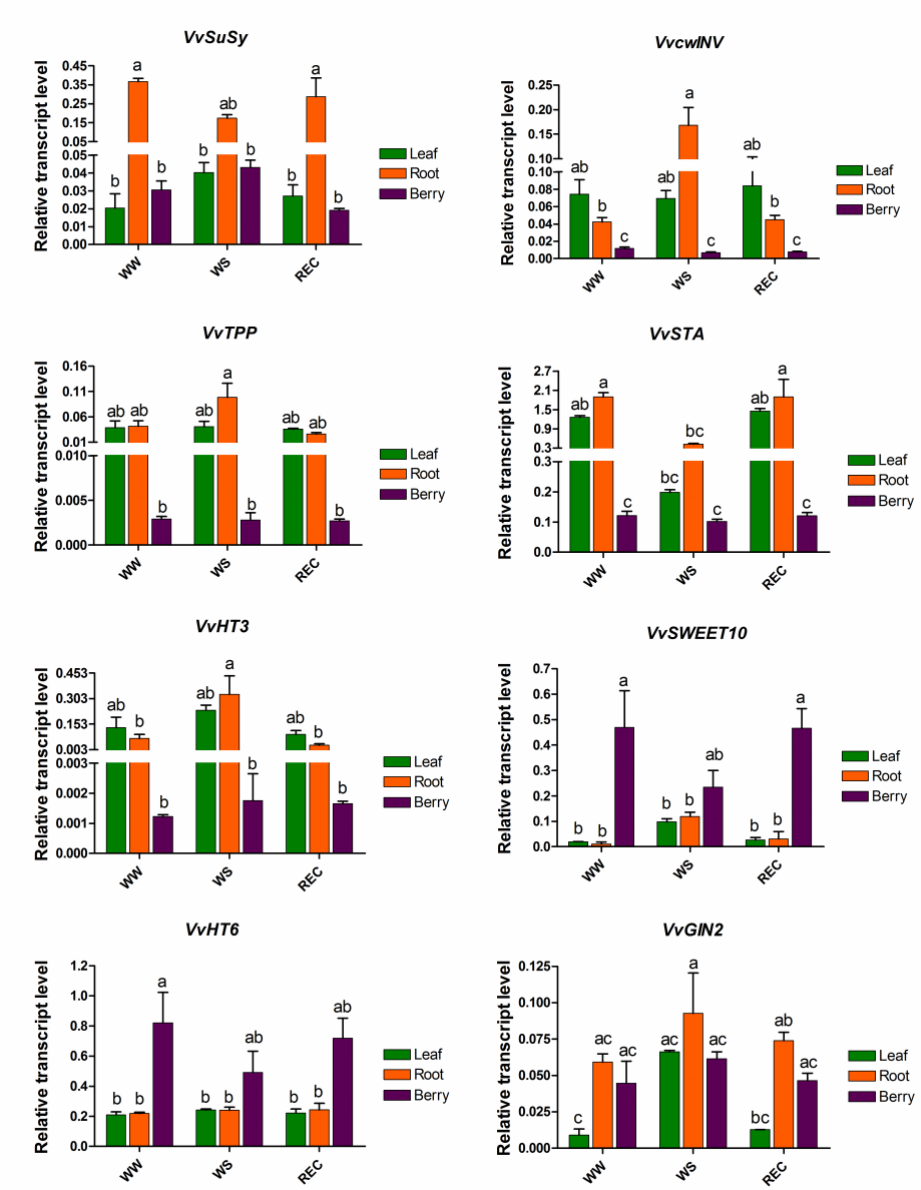

Figure 6. Transcripts of key genes of sugar metabolism.

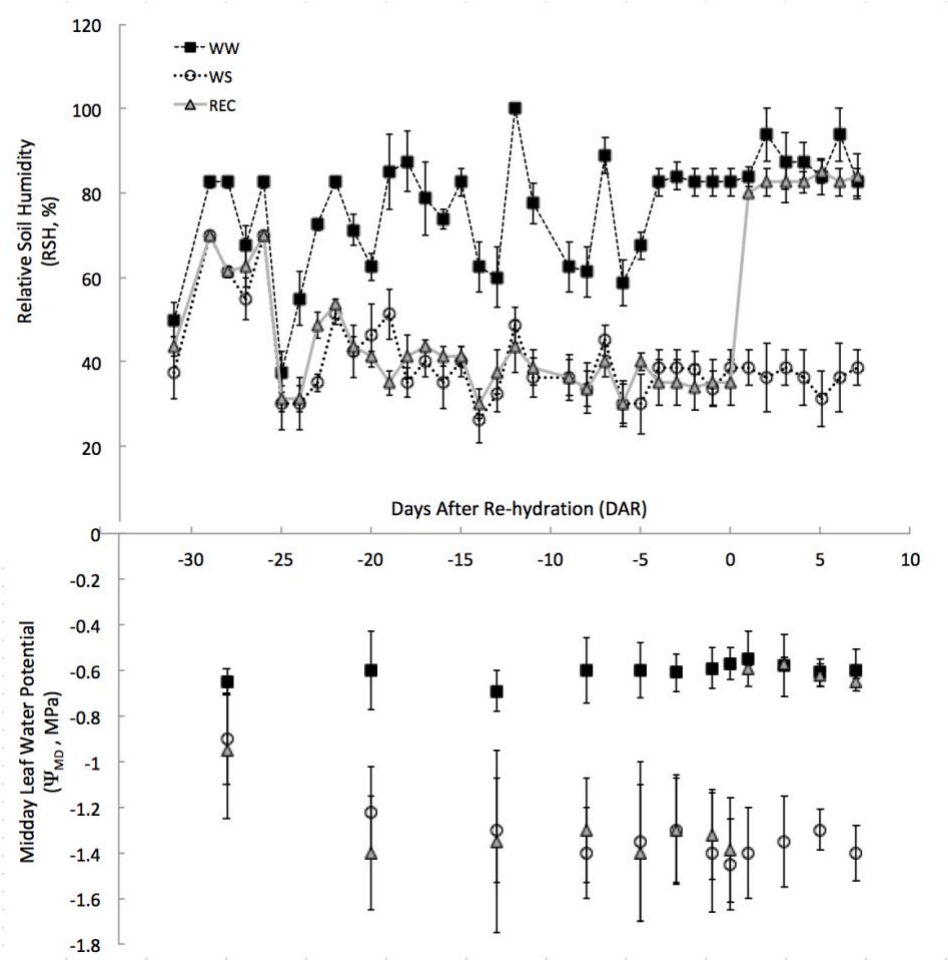

Figure 7. Imposition and maintenance of water deficit levels.

Supplementary materials

Target (Gene ID)	*Gene abbreviation*	Gene Description	Primer	Primer sequences 5'-3'	References
VIT_11s0016g00470	*VvSuSy*	Sucrose synthase	Forward	TGTTAAGGCTCCTGGATTTCAATTA	Prezelj et al., 2016
			Reverse	AGCCAAATCTTGGCAAGCA	
VIT_09s0002g02320	*VvcwINV*	Cell wall apoplastic invertase	Forward	AGGAGGTGGAAAGGTTTGCATA	Ferrero et al., 2018
			Reverse	TGGGCTTCACCGTCAATAGC	
VIT_00s0304g00080	*VvTPP*	Trehalose-6-phosphate phosphatase	Forward	TCCATCCCAGGAGCAAGTGT	Gambino et al., 2012
			Reverse	CACAGCGGTAATGCACACAGAGA	
VIT_02s0025g02790	*VvSTA*	Starch synthase	Forward	GGCGACTCTGACTGCTTCTCA	Gambino et al., 2012
			Reverse	CCTGGGTGCCGTTGACAT	
VIT_11s0149g00050	*VvHT3*	Hexose transporter 3	Forward	AGTACGACAACCAAGGGCTACAG	Gambino et al., 2012
			Reverse	GAGGTCAAGCCCGCAAGATA	
VIT_17s0000g00830	*VvSWEET10*	Sugar Will Eventually be Exported Transporter	Forward	TATCTGCGGATTCGGTTCCA	Prezelj et al., 2016
			Reverse	ACGCTTAGCGAGAACACGAGAC	
VIT_18s0122g00850	*VvHT6*	Hexose transporter 6	Forward	TTCTTGAAGGTGCCCGAGAC	Pagliarani et al., 2019
			Reverse	AGTAACCTGCCTTGCTCCAAC	
VIT_02s0154g00090	*VvGIN2*	Vacuolar invertase 2	Forward	CCAACCAAGGCGATCTATG	Prezelj et al., 2016
			Reverse	TTGAGGCAGTGATGCTGG	
VIT_04s0044g00580	*VvACT*	Actin	Forward	TCCGTTCTCAGAGATCAACAA	Gambino et al., 2012
			Reverse	ACTCTCTCATCTCAAGATATTCTATGG	
VIT_16s0098g01190	*VvUBI*	Ubiquitin	Forward	TCTGAGGCTTCGTGGTGGTA	Gambino et al., 2012
			Reverse	AGGCGTGCATAACATTTGCG	

Supplementary Table 1. List of the oligonucleotides used in this study.

Figure S1. $^{13}CO_2$ pulse of 9 grapevine plants under climate-controlled condition at DAR 1 in the labelling chamber. 1) Electrical panel for temperature and humidity control, 2) nine grapevines in plastic pots equipped with connection pipes and fittings for balloon setup, 3) External PC connected to the IRGA for labelling chamber CO_2 concentration monitoring, 4) injection system explained in the white panel 5) artificial LED light for natural light integration.

Figure S2. Transcripts of key genes of sugar metabolism. Relative expression level of (a) sucrose synthase (*VvSusy*), cell wall invertase (*VvcwINV*), threalose-6-phosphate phosphatase (*VvTPP*), starch synthase (*VvSTA*), and (b) hexose transporter 3 (*VvHT3*), Sugar Will Eventually be Exported Transporter 10 (*VvSWEET10*), hexose transporter 6 (*VvHT6*) and vacuolar invertase 2 (*VvGIN2*) genes in leaf, root and berry tissues sampled from WW, WS and REC plants at DAR 0 and DAR1, as determined by qRT-PCR signals normalized to actin (*VvACT*) and ubiquitin (*VvUBI*) transcripts. Data are presented as the mean ±SE of three biological and technical replicates. Gene IDs and oligonucleotides used for each gene are indicated in the Table S1. Different lowercase letters above the bars indicate significant differences according to a *post hoc* Tukey's test ($p \leq 0.05$).

Figure S2. Multi-chamber system for continuous gas exchange analysis. (a) schematic representation of multi-chamber system: 1) PE balloon, 2) Custom made metallic pot, 3) centrifuge fan, 4) hot-wire anemometer, 5) T junction for balloon air inlet, 6) diaphragm pump, 7) manifold with solenoid valves, 8) IRGA, 9) 12V DC fan. (b) Multi-chamber system during measurements. In the upper panel a 12-multi-chamber platform.

Figure S4. Linear correlation between leaf area (LA) and leaf diameter^2 (d^2) and linear correlation between leaf dry weight (DW) and d^2. Linear correlation between leaf area (LA) and leaf diameter^2 (d^2) and linear correlation between leaf dry weight (DW) and d^2.of *Vitis vinifera cv* Barbera grafted onto *Vitis riparia* × *Vitis berlandieri* 420A rootstocks.

Figure S5. Environmental check during the whole-plant gas exchange analysis. (a) air temperature, T; (b) photosynthetic photon flux density, PPFD; (c) air relative humidity, RH.

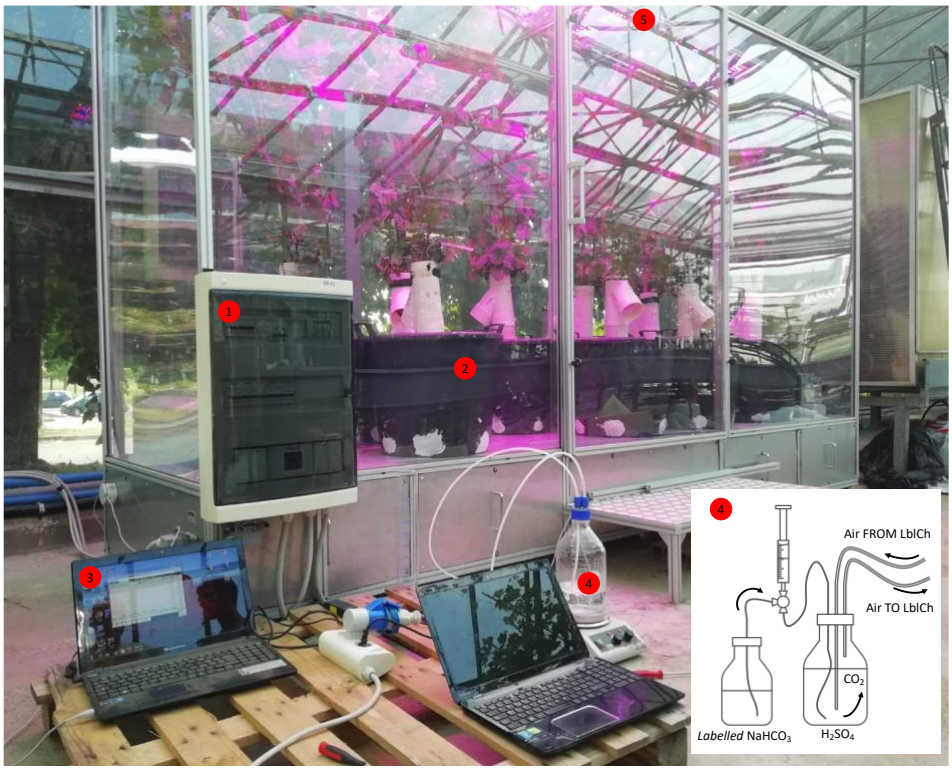

Figure S1. $^{13}CO_2$ pulse of 9 grapevine plants under climate-controlled condition at DAR 1 in the labelling chamber.

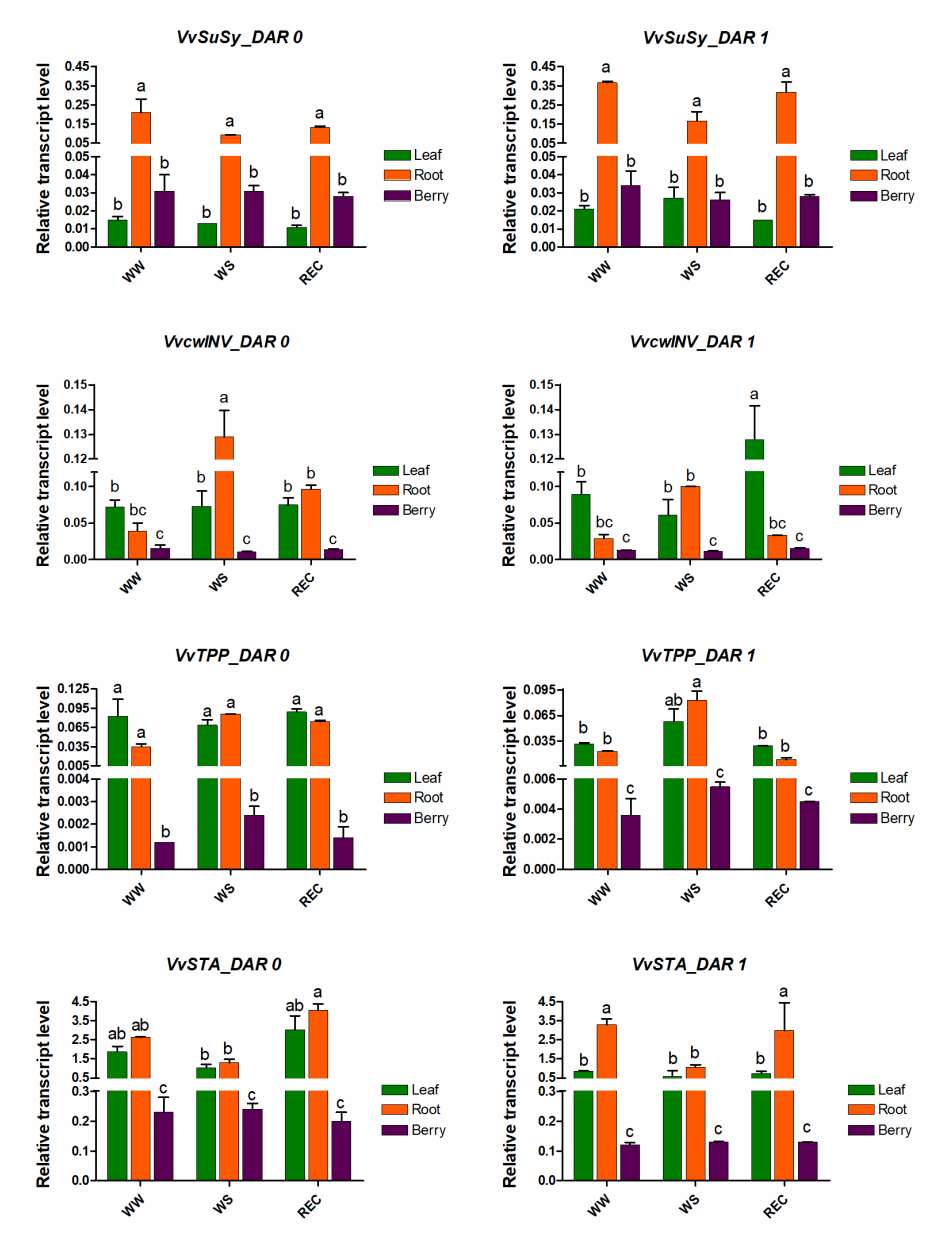

Figure S2A. Transcripts of key genes of sugar metabolism.

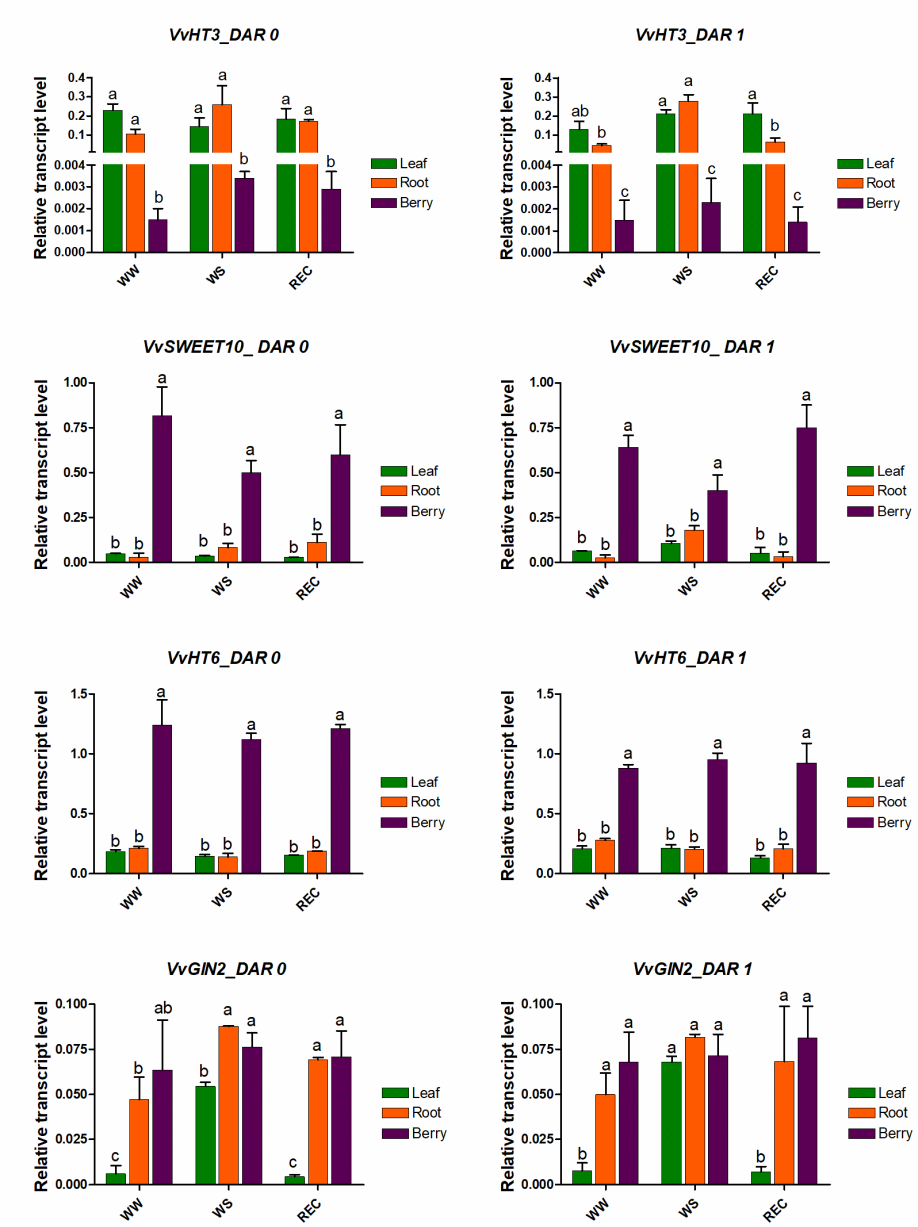

Figure S2B. Transcripts of key genes of sugar metabolism..

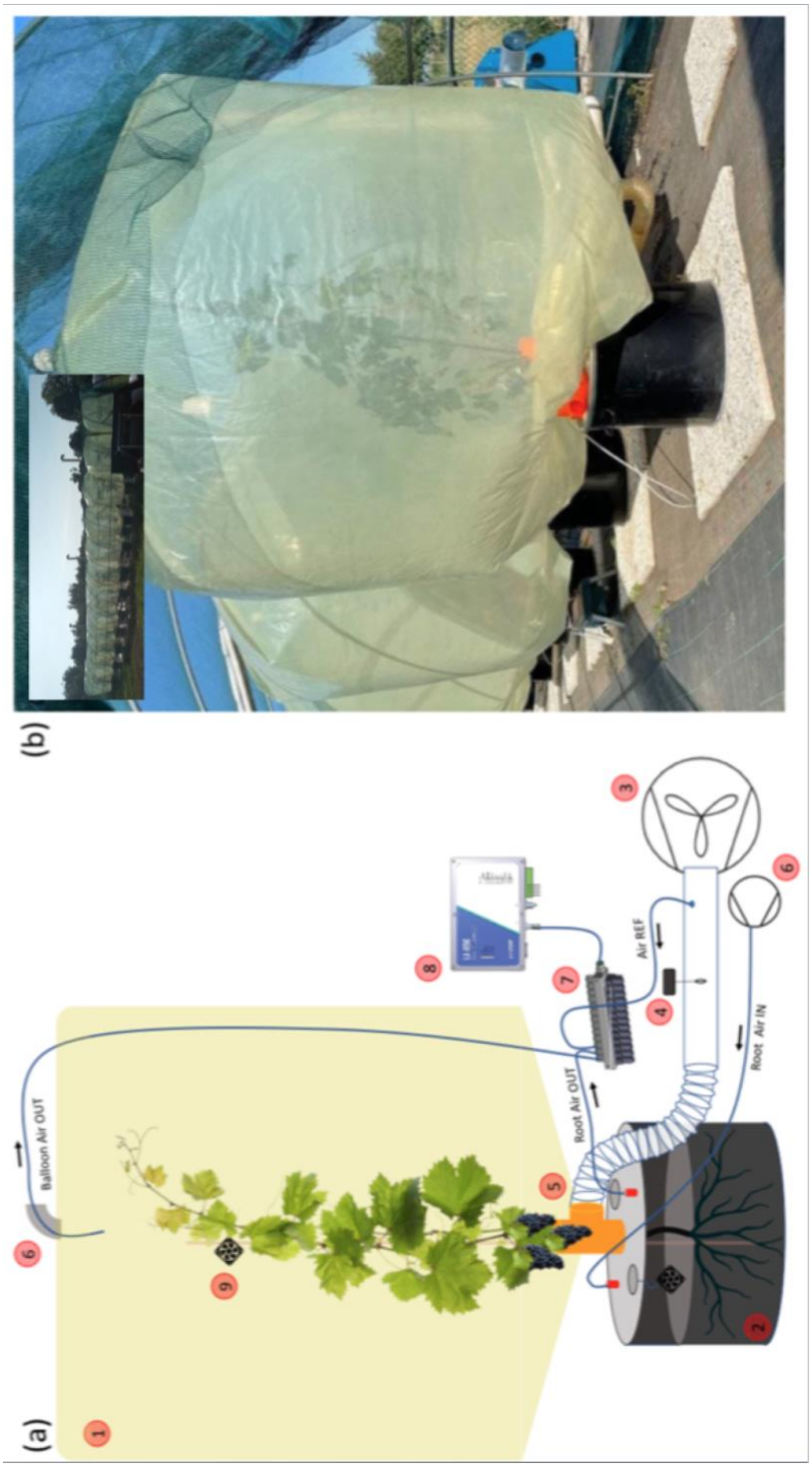

Figure S3. Multi-chamber system for continuous gas exchange analysis.

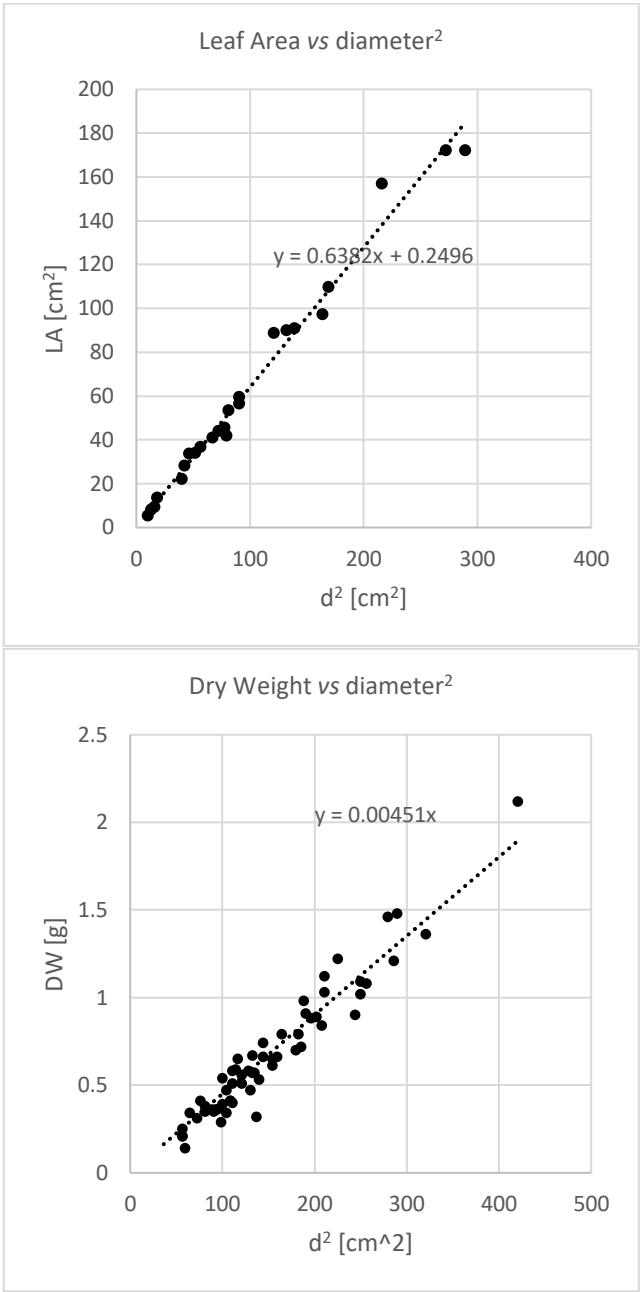

Figure S4. Linear correlation between leaf area (LA) and leaf diameter^2 (d^2) and linear correlation between leaf dry weight (DW) and d^2.

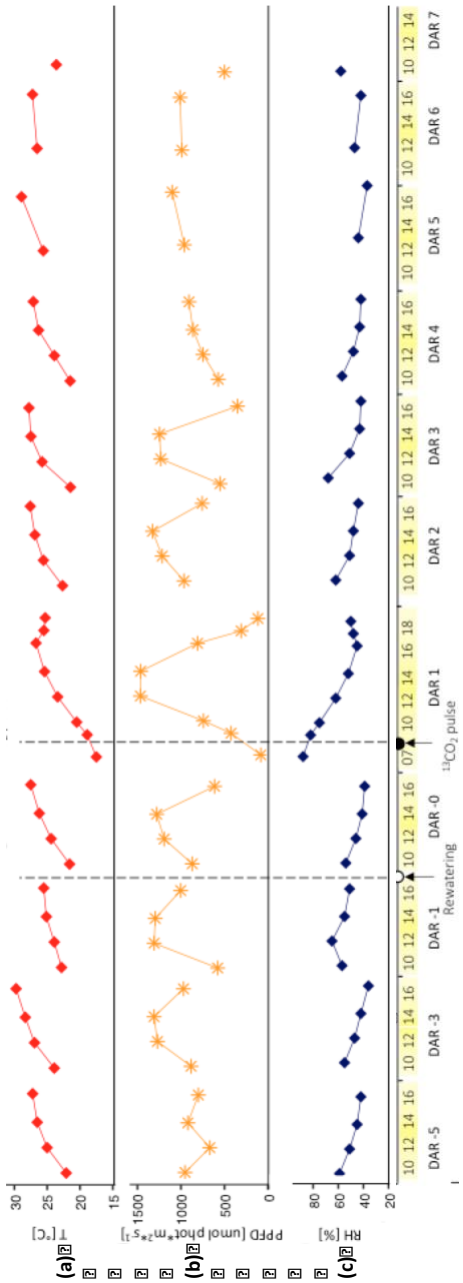

Figure S5. Environmental check during the whole-plant gas exchange analysis.

4. General conclusions

What general conclusions, peculiar to each result of my thesis and / or transversal to them, can be added to the broad scientific discussion of factors limiting carbon assimilation in plants?

4.1. Limitation of carboxylation rate related to soil water availability and atmospheric evaporative demand

- In the rehydration phases after drought, the strength of the sink persists but is coupled with a photosynthetic recovery activated by the phloem downloading capacity directed towards the strongest C-requesting sinks.
- The assimilation values of the rehydrated plants exceed those of the irrigated plants. In these moments, the effects of maximum C assimilation and relative delivery to the requesting sink take place.

4.2. Electron transport rate limitations related to intensity and quality of light

- Red and blue (RB) light maximizes photosynthetic activity, but this advantage does not lead to greater biomass accumulation, which is greater in plants under red, green and blue (RGB) and further under full spectrum (FS) light.
- Plants subjected to the RB light regime incorporate less carbon than what has been assimilated due to higher level of respiration / assimilation. RB leaves have a smaller PSII antenna size and the cyclic electron transport around PSI is higher, implying a lower NADPH / ATP ratio. Exposure to RB light affects plant overall metabolic biosynthetic pathways at the expense of growth, while RGB and especially FS light, by not triggering this adaptation, are more suited to constant low light indoor growing conditions.
- The plants subjected to the RB light regime invest less carbon in the distension of the leaf blade, i.e. the leaf thickens instead of spreading out.
- The plants subjected to the RB light regime invest proportionally little in the leaf in relation to the root.
- The plants subjected to the RB light regime have the highest daily integral of photosynthesis per leaf area unit, but, as the specific leaf area is low and the investment in foliar compared to root carbon is low they incorporate little carbon in relation to what has been assimilated.
- This last situation happens since the leaf at night respires more and since the respiration of the whole-root is maximum: under RB light, plants have unbalanced carbon allocation towards the root rather than towards the leaves.

- The RB spectrum at low light intensity determines a growth adaptation, which is normally induced upon acclimation to high light conditions.
- The greater energy demand in the leaf of RB plants is also highlighted by a greater recruitment of cyclic photosynthesis.
- FS (and RGB) plants, on the other hand, do not trigger this photoprotective adaptation and their growth advantage lies in adopting a growth strategy that conforms to growing indoor light conditions (Robson et al., 2022).

4.3. Limitation concerning plant triose phosphate utilization capacity

- Periods of water stress activate a molecular response in the plant C sinks to compensate for the reduction in photosynthetic C assimilation.
- In fruit crops, the fruits compete strongly with the root. The selection of the most productive phenotypes has made the fruit sink quantitatively competitive against the root sink, much more than what happens in forest plants, where the root completely orchestrates the response to stress.
- Maximizing C assimilation and delivery in REC plants leads to a high amount of newly fixed C already two days after rehydration in root, and two days later in the berries, in line with the expression of genes responsible for sugar metabolism.
- In rehydrated plants, the increase in C assimilation is able to support the requests of the sinks during fruit ripening, without affecting the reserves, as in the case of water-stressed plants.
- The rehydration phases represent the key moments in the life of the fleshy fruit plants, especially if they coincide with the ripening phase of the fruit, as in our experimental design.
- These mechanisms clarify what is experienced in fruit crops, when occasional rain or irrigation events are more effective in determining sugar delivery toward fruits, rather than constant and satisfactory water availabilities.

Ringraziamenti

Poter scrivere queste righe è uno dei piaceri più grossi che provo nel terminare il mio percorso di dottorato.
Per quanto uno anneghi ogni frase con dei "grazie" è difficile esprimere interamente la gratitudine che si ha nei confronti di alcune persone.
Io voglio dedicare questa tesi di dottorato al mio tutor, il Professor Claudio Lovisolo, che mi ha guidato in questi 4 anni tanto nel percorso scientifico quanto nel percorso umano.
Quando ho iniziato a lavorare con Claudio non ci conoscevamo affatto, io non sapevo nulla di lui e lui aveva raccolto giusto qualche informazione su di me. Una volta deciso di intraprendere assieme il mio percorso di dottorato il Professore mi ha comunicato in una frase quello che sarebbe stato da li in avanti il nostro rapporto: "il nostro gruppo di ricerca sarà composto da me e te, io sarò qui al tuo servizio affinché tu possa compiere un percorso di dottorato di qualità". Ciò è stato.
Dico con certezza che con qualsiasi altro tutor possibile il mio percorso di dottorato si sarebbe interrotto poco dopo l'inizio, la mia esperienza di dottorato è stata burrascosa ma Claudio è sempre riuscito a farmi trovare la motivazione per portare a termine ciò che avevo iniziato.

Sento il dovere di aggiungere alcune righe per poter raccontare a tutti coloro che leggeranno la mia tesi i meriti di Claudio come "insegnante".
Claudio mi ha trasmesso subito la ricetta per lavorare con passione, competenza e serenità, in questa ricetta l'ingrediente centrale è il benessere emotivo e lui si è adoperato affinché questo ingrediente mi fosse sempre disponibile.
So per certo che Claudio ritenga che la responsabilità principale del suo lavoro è quella di mettere a disposizione la propria esperienza e conoscenza affinché i suoi studenti possano maturare e emanciparsi come scienziati, come lavoratori e come persone. Claudio non pone freni alla libertà dei propri studenti, non vuole fotocopie di sé ma ragazzi autonomi e capaci di andare incontro alle proprie passioni.
Questo suo profondo senso di responsabilità e il suo modo di metterlo in pratica ha portato a un simpatico equivoco nel primo periodo sotto la sua guida, che per la prima volta qui gli comunico: mi recavo regolarmente nel suo ufficio proponendo svariate idee sul progetto, da lui sentivo pronunciare solo "si", "va bene, "fai pure". Mi ha detto talmente tanti si che a un certo punto ho iniziato a pensare: "boh, probabilmente Claudio

non capisce niente scientificamente, non è possibile che mi dica sempre si, ogni tanto dirò qualche stupidaggine per la quale mi dovrebbe dire no. E poi, non ha qualche idea migliore della mia? Non ha degli argomenti che preferisce a quelli che propongo io?". Solo qualche mese dopo mi è stato tutto chiaro.

Dopo Claudio voglio ringraziare il Professor Matteo Ballottari, il Professor Davide Ricauda, il Professor Daniel Said Pullicino, il Dottor Giorgio Gambino e la Dottoresa Irene Perrone che sono stati pienamente disponibili nelle collaborazioni che abbiamo intrapreso e al pari di loro voglio ringraziare tutti i componenti dei loro gruppi di ricerca con cui ho interagito per ottenere i risultati qui presentati. Ringrazio i miei colleghi con i quali ho condiviso il tempo lavorativo, le esperienze, le competenze e l'emotività. Ringrazio i tesisti che mi hanno dato un aiuto concreto in molte attività. Ringrazio la mia famiglia che mi ha dato l'appoggio per decidere di intraprendere il mio dottorato in piena serenità, ci tengo a sottolineare come mia mamma debba essere da me ringraziata anche sul piano scientifico poiché ha accudito le mie lattughe e tabacchi durante il lockdown. Infine ringrazio tutti coloro che mi sono stati vicini durante questo lungo percorso.